SSC-382

REEXAMINATION OF DESIGN CRITERIA FOR STIFFENED PLATE PANELS
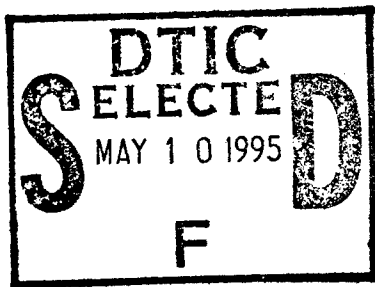
DTIC
SELECTED
MAY 1 0 1995
F

19950508 143

SHIP STRUCTURE COMMITTEE

1995

SHIP STRUCTURE COMMITTEE

The SHIP STRUCTURE COMMITTEE is constituted to prosecute a research program to improve the hull structures of ships and other marine structures by an extension of knowledge pertaining to design, materials, and methods of construction.

RADM J. C. Card, USCG (Chairman)
Chief, Office of Marine Safety, Security
  and Environmental Protection
U. S. Coast Guard

Mr. Thomas H. Peirce
Marine Research and Development
  Coordinator
Transportation Development Center
Transport Canada

Mr. Edwin B. Schimler
Associate Administrator for Ship–
  building and Technology Development
Maritime Administration

Dr. Donald Liu
Senior Vice President
American Bureau of Shipping

Mr. Edward Comstock
Director, Naval Architecture
  Group (SEA 03H)
Naval Sea Systems Command

Mr. Thomas W. Allen
Engineering Officer (N7)
Military Sealift Command

Mr. Warren Nethercote
Head, Hydronautics Section
Defence Research Establishment–Atlantic

EXECUTIVE DIRECTOR

CDR Stephen E. Sharpe, USCG
U. S. Coast Guard

CONTRACTING OFFICER TECHNICAL REPRESENTATIVE

Mr. William J. Siekierka
Naval Sea Systems Command

SHIP STRUCTURE SUBCOMMITTEE

The SHIP STRUCTURE SUBCOMMITTEE acts for the Ship Structure Committee on technical matters by providing technical coordination for determinating the goals and objectives of the program and by evaluating and interpreting the results in terms of structural design, construction, and operation.

MILITARY SEALIFT COMMAND

Mr. Robert E. Van Jones (Chairman)
Mr. Rickard A. Anderson
Mr. Michael W. Touma
Mr. Jeffrey E. Beach

MARITIME ADMINISTRATION

Mr. Frederick Seibold
Mr. Richard P. Voelker
Mr. Chao H. Lin
Dr. Walter M. Maclean

U. S. COAST GUARD

CAPT G. D. Marsh
CAPT W. E. Colburn, Jr.
Mr. Rubin Scheinberg
Mr. H. Paul Cojeen

AMERICAN BUREAU OF SHIPPING

Mr. Stephen G. Arntson
Mr. John F. Conlon
Mr. Phillip G. Rynn
Mr. William Hanzelek

NAVAL SEA SYSTEMS COMMAND

Mr. W. Thomas Packard
Mr. Charles L. Null
Mr. Edward Kadala
Mr. Allen H. Engle

TRANSPORT CANADA

Mr. John Grinstead
Mr. Ian Bayly
Mr. David L. Stocks
Mr. Peter Timonin

DEFENCE RESEARCH ESTABLISHMENT ATLANTIC

Dr. Neil Pegg
LCDR Stephen Gibson
Dr. Roger Hollingshead
Mr. John Porter

SHIP STRUCTURE SUBCOMMITTEE LIAISON MEMBERS

U. S. COAST GUARD ACADEMY

LCDR Bruce R. Mustain

U. S. MERCHANT MARINE ACADEMY

Dr. C. B. Kim

U. S. NAVAL ACADEMY

Dr. Ramswar Bhattacharyya

CANADA CENTRE FOR MINERALS AND ENERGY TECHNOLOGIES

Dr. William R. Tyson

SOCIETY OF NAVAL ARCHITECTS AND MARINE ENGINEERS

Dr. William Sandberg

U. S. TECHNICAL ADIVSORY GROUP TO THE INTERNATIONAL STANDARDS ORGANIZATION

CAPT Charles Piersall

NATIONAL ACADEMY OF SCIENCES – MARINE BOARD

Dr. Robert Sielski

NATIONAL ACADEMY OF SCIENCES – COMMITTEE ON MARINE STRUCTURES

Mr. Peter M. Palermo

WELDING RESEARCH COUNCIL

Dr. Martin Prager

AMERICAN IRON AND STEEL INSTITUTE

Mr. Alexander D. Wilson

OFFICE OF NAVAL RESEARCH

Dr. Yapa D. S. Rajapaske

STUDENT MEMBER

Mr. Trevor Butler
Memorial University of Newfoundland

**Ship
Structure
Committee**

An Interagency Advisory Committee

March 24, 1995

REEXAMINATION OF DESIGN CRITERIA FOR STIFFENED PLATE PANELS

The emphasis on reducing vessel weight in the recent generation of ships has lead to increased usage of high strength steels to allow for thinner scantlings. These designs provided panels of equivalent overall strength but with less inherent rigidity. This, in turn, has resulted in unanticipated failures at the intersections of transverse and longitudinal stiffeners with the plating. These failures demonstrated the need to rethink some of the assumptions currently used in the design process.

This project analyzed the total stresses at the panel to stiffening system interface. After using conventional design procedures for a panel section, finite element models of the panel were subjected to various anticipated panel loads and the resulting stresses were analyzed. The report concludes with a discussion of the effect of the less stiff panel structures on failures and adjustments which should be considered in the design procedures. Recommendations for future research are given.

J. C. CARD
Rear Admiral, U.S. Coast Guard
Chairman, Ship Structure Committee

1. Report No. SSC-382	2. Government Accession No. PB95-188181	3. Recipient's Catalog No.

4. Title and Subtitle "Re-Examination of Design Criteria for Stiffened Plate Panels"	5. Report Date June 1994
	6. Performing Organization Code

7. Author's) Dhruba J. Ghose and Natale S. Nappi	8. Performing Organization Report No. "SR-1350"

9. Performing Organization Name and Address Designers & Planners, Inc. 2120 Washington Blvd., Suite 200 Arlington, VA 22204	10. Work Unit No. (TRAIS)
	11. Contract or Grant No. DTCG23-92-R-E01030

12. Sponsoring Agency Name and Address Ship Structure Committee U.S. Coast Guard 2100 Second Street, S.W. Washington, D.C. 20593	13. Type of Report and Period Covered FINAL
	14. Sponsoring Agency Code G-M

15. Supplementary Notes

Sponsored by the Ship Structure Committee and its member agencies.

16. Abstract

Current ship structural design criteria for stiffened plate panels is based upon a strength of materials approach using either linear plate or beam theory. This approach neglects the effects of vertical shear (normal to the plate surface), membrane and torsional stress components induced by the flexibility of the panel's supporting structure. Recent trends towards the use of higher strength materials have resulted in the design of grillage structures which are more flexible and therefore increase the vertical shear, membrane and torsional stress components in the plate panel. This report presents the results of a study undertaken to determine the effect of the stiffness characteristics of the supporting members of the grillage structure on the plate panel stress. Grillage scantlings were developed using first principals based approach and then analyzed using finite element techniques to take into account the flexibility of the grillage stiffeners and to quantify the effects of vertical shear, membrane and torsional stress components.

17. Key Words Finite Elements, Stiffened Plates, Stiffeners, Grillage, Design Criteria, Shear Stress, Normal Stress, Hull Structure	18. Distribution Statement Available from: National Technical Information Service Springfield, VA 22161

19. Security Classif. (of this report) Unclassified	20. Security Classif. (of this page) Unclassified	21. No. of Pages 112	22. Price $27.00 Paper $12.50 Micro

Form DOT F 1700.7 (8-72)   Reproduction of completed page authorized

NIST

METRIC CONVERSION CARD

Approximate Conversions to Metric Measures

Symbol	When You Know	Multiply by	To Find	Symbol
LENGTH				
in	inches	2.5	centimeters	cm
ft	feet	30	centimeters	cm
yd	yards	0.9	meters	m
mi	miles	1.6	kilometers	km
AREA				
in²	square inches	6.5	square centimeters	cm²
ft²	square feet	0.09	square meters	m²
yd²	square yards	0.8	square meters	m²
mi²	square miles	2.6	square kilometers	km²
	acres	0.4	hectares	ha
MASS (weight)				
oz	ounces	28	grams	g
lb	pounds	0.45	kilograms	kg
	short tons (2000 lb)	0.9	metric ton	t
VOLUME				
tsp	teaspoons	5	milliliters	mL
Tbsp	tablespoons	15	milliliters	mL
in³	cubic inches	16	milliliters	mL
fl oz	fluid ounces	30	milliliters	mL
c	cups	0.24	liters	L
pt	pints	0.47	liters	L
qt	quarts	0.95	liters	L
gal	gallons	3.8	liters	L
ft³	cubic feet	0.03	cubic meters	m³
yd³	cubic yards	0.76	cubic meters	m³
TEMPERATURE (exact)				
°F	degrees Fahrenheit	subtract 32, multiply by 5/9	degrees Celsius	°C

Approximate Conversions from Metric Measures

Symbol	When You Know	Multiply by	To Find	Symbol
LENGTH				
mm	millimeters	0.04	inches	in
cm	centimeters	0.4	inches	in
m	meters	3.3	feet	ft
m	meters	1.1	yards	yd
km	kilometers	0.6	miles	mi
AREA				
cm²	square centimeters	0.16	square inches	in²
m²	square meters	1.2	square yards	yd²
km²	square kilometers	0.4	square miles	mi²
ha	hectares (10,000 m²)	2.5	acres	
MASS (weight)				
g	grams	0.035	ounces	oz
kg	kilograms	2.2	pounds	lb
t	metric ton (1,000 kg)	1.1	short tons	
VOLUME				
mL	milliliters	0.03	fluid ounces	fl oz
mL	milliliters	0.06	cubic inches	in³
L	liters	2.1	pints	pt
L	liters	1.06	quarts	qt
L	liters	0.26	gallons	gal
m³	cubic meters	35	cubic feet	ft³
m³	cubic meters	1.3	cubic yards	yd³
TEMPERATURE (exact)				
°C	degrees Celsius	multiply by 9/5, add 32	degrees Fahrenheit	°F

Temperature:

°C	-40	-20	0	20	37	60	80	100
°F	-40	0	32	80	98.6	160	212	

water freezes — body temperature — water boils

Table of Contents

List of Tables

List of Figures

Nomenclature

b = breadth of the panel, m

b_e = effective width of plating, m

t = thickness of the panel, mm

C = Constant depending on the plate material and location on the ship

H = Head of sea water, feet

K = Factor depending on the aspect ratio of the panel

E = Young's Modulus, N/mm^2

σ_Y = Yield Stress, N/mm^2

A = Total cross-sectional area of the beam, cm^2

A_{SH} = Shear area, cm^2

A_y = Shear area along 'y' axis, cm^2

A_z = Shear area along 'z' axis, cm^2

I = Moment of Inertia, cm^4

I_y = Moment of Inertia about 'y' axis, cm^4

I_z = Moment of Inertia about 'z' axis, cm^4

y_p = distance of neutral axis from plating, cm

y_f = distance of neutral axis from stiffener flange, cm

SM_p = Sectional Modulus to the plating, cm^3

SM_f = Sectional Modulus to the stiffener flange, cm^3

J = St. Venant's Torsional Constant, cm^4

r = radius of gyration, cm

F_{ULT} = Ultimate Strength of the plating, N/mm^2

F_{CR} = Critical Buckling stress due to axial compression, N/mm^2

F_{BCR} = Critical Buckling stress due to bending, N/mm^2

F_{SCR} = Critical Buckling stress due to shear, N/mm^2

σ_{xx} = Normal Stress in longitudinal direction, $N/mm2$

σ_{yy} = Normal Stress in transverse direction, N/mm^2

σ_{zz} = Normal Stress in vertical direction, N/mm^2

σ_{xy} = In-plane shear Stress, N/mm^2

σ_{xz} = Vertical shear Stress, N/mm^2

σ_{yz} = Vertical shear Stress, N/mm^2

vm = Von Mises Stress, N/mm^2

$\Delta_{(x,y)}$ = Initial Deformation at x and y, mm

L = Length of Beam, m

s = stiffener spacing, m

d_w = web depth, mm

t_w = web thickness, mm

b_f = flange width, mm

t_f = flange thickness, mm

p = normal pressure, N/mm^2

IL = moment of inertia of the stiffened plate in the
     longitudinal direction

IT = moment of inertia of the stiffened plate in the
     transverse direction

iL = moment of inertia of the stiffened plate per longitudinal

iT = moment of inertia of the stiffened plate per transverse

(A/B) (iT/iL)$^{0.25}$ = Virtual Aspect Ratio. (Measure of stiffness
of cross stiffened panels)

1.0 INTRODUCTION

1.1 Background

Due to the emphasis on increasing ship lengths and reducing structural weight to increase cargo capacity, there has been an increase in the use of high strength steels on commercial vessels, especially tankers. Recently, tankers constructed of high strength steel have experienced damage to their side shell and bottom structures. This damage is characterized by the initiation of cracks in plating at the intersection of transverses and longitudinal stiffeners.

The use of high strength materials has resulted in the design of grillage structures that are lighter and more flexible. But, even though the material's strength is greater, its stiffness is the same. Therefore, reducing the area of the stiffener increases its flexibility. The result of this increased flexibility is an increase in secondary stresses due to the increased deflection of supporting structure.

The stiffened plate panel, which is intended to provide watertightness and contribute to a major portion of hull girder longitudinal and transverse strength, must be designed to withstand primary stresses due to hull girder bending, secondary stresses due to bending from local loading of the plate-stiffener combination and tertiary stresses due to bending of the plate panel itself from local lateral loads. Current design criteria for plate panels of grillage structure are based upon a strength of materials approach using either linear plate or beam theory. Acceptance is based upon comparing calculated stresses with allowable stress levels (yielding or buckling). For high strength steel,

certification bodies (i.e. regulatory bodies and U.S. Navy) have allowed higher levels for both primary and secondary design stresses, which in turn means larger values of actual cyclic as well as static stresses. Vertical shear (normal to the plate panel), membrane and torsional stress components are not accounted for in the selection of the plate panel scantlings when using a strength of materials approach.

Based upon this, it is assumed that the damage found in stiffened plate panels is due to stress levels which either exceed the yield stress of the material or induce fatigue failure. In practice, fatigue failure is avoided through quality control of welds, careful design of connection details and limiting the allowable stress levels. The design of plates based upon first principals approach does not take into consideration the stresses induced by the flexibility of its supporting structure. Therefore, the emphasis of this study will be on determining the added stresses in plate panels due to increased flexibility of grillage structure.

1.2 Objective

The objective of this task was to evaluate the combined effects of vertical shear (normal to the plate panel), membrane stress and torsion on the total stress of a stiffened plate panel as a result of the effects of the overall grillage response. Specifically, the impact of the error introduced by ignoring grillage behavior, such as the effects of vertical shear and membrane stresses, was determined. In order to quantify the additional stresses induced by grillage behavior on stiffened plate panels, a series of finite element model were developed and parametric studies performed varying key

2

design parameters for a typical grillage structure designed to current industry recognized practice. For this task, the U.S. Navy design practice was chosen since it is based upon a first principals approach versus emprically based design equations.

1.3 Approach

The purpose of this study was to determine the effect of the stiffness characteristics of the supporting members. of grillage structures on the plate panel stress. The first step of this process was to design a grillage using strength of materials - first principals based approach. Grillage scantlings designed were then analyzed using FEM techniques to take into account the flexibility of the grillage stiffeners and to quantify stress componenets.

Six grillage designs were developed, three of Ordinary Strength Steel and three of High Strength Steel. The designs represent the bottom structure between transverse bulkheads fore and aft and longitudinal girders on either side. The overall length of the grillage and the plate panel aspect ratios were kept constant, and the breadth of the grillage was varied to modify the stiffness characteristics.

Finite element analysis of the grillages were performed to determine the stress components and variation of stress through out the grillage structure. Two sensitivity studies were performed to determine simplifications that would allow for results that are within the acceptable level of accuracy and the hardware resources and computational time available. First the optimum mesh size was determined. Second, a comparison of the results of a grillage model using plate elements to represent both plates and stiffeners to a grillage

model using plate elements to represent plates and beam elements to represent stiffeners was accomplished. Finite element models of the six grillages developed made use of the results of these simplifications. In order to quantify the stress components, the following types of models were developed:

Plate Models - used as the base model for comparison.

Brick Models - used to quantify the vertical shear stress component

Plate Model with initial deflection - used to quantify the membrane effect.

2.0 DESIGN OF STIFFENED-PLATE STRUCTURE

Current U.S. Navy structural design practices [1,2,3][1] were used to calculate the scantlings for six (6) stiffened panel structures. These stiffened panels are comprised of 3 OSS and 3 HSS systems. The overall length, A, of the grillage was maintained at 15.24 m (50 ft), while the overall breadth, B, was varied, e.g. 10.06 m (33 ft), 6.4 m (21 ft), and 2.74 m (9 ft). The resulting geometrical grillage aspect ratio are 1.52, 2.38, and 5.56. The plate panel aspect raio remained the same, namely 3.05 m x 0.9 m (10' x 3'), for all six systems.

The panel was loaded with an uniform lateral pressure of 0.107 N/mm^2 (15.56 lb/in^2), which is equivalent to a head of sea water of 9.14 m (30 ft). The plate panel thickness was selected using Navy formula [2] of:

$$\frac{b}{t} \leq \frac{C}{K \cdot \sqrt{H}}$$

Where H is the head of sea water, in feet. C is a constant which is a function of plate material and its location on the ship. The C values takes into account the acceptable deformation of the structure. C values have been established for the following locations:

    a.   Topside Plating

    b.   Lower shell and tank boundaries

    c.   Boundaries for the control of flooding.

---

[1] References in section 6.0

5

And K is a factor that takes into consideration the aspect ratio of the panel, b/a>0.5 (i.e., short panels).

For these studies, C was taken as 350 for OSS plating and 400 for HSS plating which corresponds to topside structure where the minimum amount of deformation (no permanent set) is allowed for and hence would result in a conservative design. The resulting plate thicknesses were 15.88 mm (0.6250") and 14.29 mm (0.5625") for OSS and HSS respectively.

The longitudinal beam stiffeners were designed as continuous beams over non-deflecting supports, while the transverse girders were designed as clamped beams. The following steps were used to develop these designs:

1. Calculate plating thickness, t, for normal loads due to a uniform pressure from a head of sea water using the equation above.

2. Determine the effective width of plating, b_e, based on shear lag approach (post-buckling response),

$$b_e = 2t\sqrt{\frac{E}{\sigma_y}}$$

3. Select a beam size (i.e., a tee beam attached to the plate).

6

4. Determine plate/beam section properties, including the cross sectional area, A; shear area, A_{SH}; moment of inertia, I; distance of the neutral axis from the plating, y_P; distance of the neutral axis from the stiffener flange, y_f; sectional modulus to the plating, SM_P; sectional modulus to the stiffener flange, SM_f; and radius of gyration, r.

5. Determine the secondary bending moments and shear forces.

6. Determine the shear stress at the supports and the secondary bending stresses at two locations; one at the support and the other at the mid span of the beam. At each location, compute bending stresses at the plate and at the flange of the stiffener.

7. Check plating for ultimate strength (F_{ULT}).

8. Check plating for buckling under in-plane compression, bending and shear, (F_{CR}, F_{BCR}, F_{SCR}).

9. Check composite plate-tee beam for yielding in tension/compression due to bending.

10. Check composite plate-tee beam for maximum web shear stress.

11. Check tee stiffener for Tripping.

12. Check tee stiffener flange for local buckling.

13. Check tee stiffener web for local buckling.

The results of the above design procedures have been summarized in Tables 2.1 and 2.2 for OSS and HSS grillage designs respectively. These scantlings were used to develop the FEM models described in section 3.0. The symbols used in the first column of tables 2.1 and 2.2 are listed below:

'A' = dimension of the stiffened panel in the long direction

'B' = dimension of the stiffened panel in the short direction

'a' = dimension of the unsupported span of plating in the long direction

'b' = dimension of the unsupported span of plating in the short direction

'p' = uniform lateral pressure

't' = plate thickness

'IL' = moment of inertia of the stiffened plate in the longitudinal direction

'IT' = moment of inertia of the stiffened plate in the transverse direction

'iL' = moment of inertia of the stiffened plate per longitudinal

'iT' = moment of inertia of the stiffened plate per transverse

'(A/B)(iT/iL)^0.25' = Virtual Aspect Ratio. (Measure of stiffness of cross stiffened panels)

The virtual aspect ratio, $(A/B)(i_T/i_L)^{0.25}$, is derived from the fact that the stiffness of an unstiffened gross panel, of constant thickness, is usually a function of the length to breadth ratio (i.e A/B). This ratio is commonly refered to as

the panel aspect ratio. Therefore A/B would represent the ratio of the stiffness in one direction to the other direction. If the panel is supported by mutually perpendicular intersecting beams, whose stiffnesses are different, then the ratio of the gross panel stiffness would have to be modified to account for the stiffness provided by the moment of inertia of those beams. When this is accomplished the quantity called "virtual aspect ratio" is used. Hence, the virtual aspect ratio is equal to $(A/B)(i_T/i_L)^{0.25}$, assuming that the Young's Modulus, E, is the same in both directions.

Detail calculations for one grillage, are provided in Appendix 1.0 to illustrate the process used. It should be noted that the original calculations were performed using the English system, therefore the plate thickness selected in the appendix is not a standard metric plate size.

TABLE 2.1 - DIMENSIONS AND SCANTLINGS OF OSS GRILLAGE

Model No.	1	2	3
A (m)	15.24	15.24	15.24
B (m)	10.06	6.40	2.74
a (m)	3.05	3.05	3.05
b (m)	0.91	0.91	0.91
t (mm)	15.88	15.88	15.88
Long'l Size	WT 205x140x23	WT 205x140x23	WT 205x140x23
Trans Size	914x457x15.9/28.6 T	W-T 690x250x123.5	W-T 410X180X53
p (N/mm^2)	0.107	0.107	0.107
IL (cm^4)	6984.36	6984.36	6984.36
IT (cm^4)	717,041.14	255,524.21	48,157.93
ASL (cm^2)	14.06	14.06	14.06
AST (cm^2)	149.68	100.65	39.87
iL=IL/b (cm^4/cm)	76.36	76.36	76.36
iT=IT/a (cm^4/cm)	2,352.53	838.36	157.97
A/B	1.52	2.38	5.56
(A/B)(iT/iL)^1/4	3.57	4.33	6.66

TABLE 2.2 – DIMENSIONS AND SCANTLINGS OF HSS GRILLAGE

Model No.	1	2	3
A (m)	15.24	15.24	15.24
B (m)	10.06	6.40	2.74
a (m)	3.05	3.05	3.05
b (m)	0.91	0.91	0.91
t (mm)	14.3	14.3	14.3
Long'l Size	WT 180x130x19.5	WT 180x130x19.5	WT 180x130x19.5
Trans Size	W-T 920x305x167.5	W-T 610x230x101	W-T 410x175x38
p (N/mm^2)	0.107	0.107	0.107
IL (cm^4)	4,578.55	4,578.55	4,578.55
IT (cm^4)	444,701.66	156,461.39	34,630.45
ASL (cm^2)	11.48	11.48	11.48
AST (cm^2)	144.58	80.77	30.19
iL=IL/b (cm^4/cm)	49.98	49.98	49.98
iT=IT/a (cm^4/cm)	1,458.94	513.41	113.56
A/B	1.52	2.38	5.56
(A/B)(iT/iL)^1/4	3.52	4.26	6.82

11

3.0 FINITE ELEMENT MODELS OF STIFFENED PLATE STRUCTURE

3.1 Introduction

This section discusses the finite element analysis of the stiffened-plate structures designed in section 2.0. The P.C. based finite element software ALGOR was used to analyze the plate and brick models using linear elastic theory. The VAX based NASTRAN software was used to analyze the brick model with an initial deformation. All analyses in this study were originally performed using english units. The final results presented in this document are in metric units, therefore standard metric sizes were not selected. For each of the six configurations designed in section 2.0, two models were developed, one using plate elements and the other using brick elements. Additional models were developed to; determine optimum mesh size, study the effect of using offset beams, study the response of single panels under uniform load with clamped boundary conditions and study the effect of initial deformation of the plating. The procedures adopted for each of these studies are described in detail below.

3.2 Determination of Mesh Size.

It is a well known fact that the results of a finite element analysis are predicated by the mesh size adopted in the analysis. For accurate results finer mesh sizes are desirable. But at times the price to be paid in terms of hardware resources and computational time is too enormous to justify such refinements. Therefore, to ascertain mesh sizes which would yield results within established limits of

accuracy without straining available computer resources, a study was undertaken to determine the optimum mesh size.

The usual procedure is to study the convergence of finite element results obtained using various mesh sizes to available theoretical results. For a single unstiffened panel that is part of a grillage, the edge fixity will depend upon its location within the grillage and the stiffness of its supporting structure. Currently, theoretical solutions of stiffened-plate structures under normal pressure loads with various edge fixities are not available. Hence, the convergence study was performed using one single unsupported panel with fully fixed end conditions for which theoretical results exist.

Performing a convergence study on a single panel has two advantages. First, the results of a finite element analysis of a panel under uniform pressure could be compared to available theoretical solutions of rectangular plates with all edges fixed under uniform pressure. Second, using a single panel of unsupported plating for the mesh size determination, enormously reduces the size of the model.

The single panel chosen for the mesh size determination was the unsupported span of plating, 3.05m x 0.91m (10'x3'), from the stiffened-plate structure designed in section 2.0. The plating thickness used was as determined in section 2.0 for OSS steel panels, which is 15.88mm (0.625"). The plating was subjected to the same lateral pressure of 0.107 N/mm^2 (15.56 psi) as used in section 2.0 and clamped on all sides. For this configuration, five models using plate elements were developed having uniform square meshes. The element sizes for the models were as follows: 304.8mm (12"), 152.4mm (6"),

13

76.2mm (3"), 38.1mm (1.5"), and 19.05mm (0.75"). The displacement and the two normal stresses, σ_{xx} and σ_{yy} , were compared with theoretical results given in Reference [4] based on elastic small deflection theory. These results are summarised in Table 3.1 which also contains the in-plane shear, τ_{xy}, Von-Mises and the maximum principal stresses. For illustrative purpose, the time and the memory required to run each model are also included in the table. In Figure 3.1, results from Table 3.1 are plotted as percentage differences between the finite element analysis and theory. As expected, with a finer mesh, the results converge to the theoretical values. For element sizes less than 152.4mm (6"), displacement converge exactly to the theoretical value while for element

sizes less than 76.2mm (3"), stresses are within 10% of the theoretical values. Each refinement produces results closer to theory, but the amount of time and storage space (memory) required increases. While model 5, with a mesh size of 19.05mm (0.75") produces results which are almost within 2.5% of the theoretical result, it takes 75 times longer and about 70 times more memory than model 3 having a mesh size of 76.2mm (3"). Hence, for the present study models having element sizes of 76.2mm (3") square were chosen.

3.3 Modeling of Longitudinals and Transverses.

Full 3-dimensional models of cross stiffened panels using plate elements to model the plating as well as the longitudinals and transverses are complex. As mentioned in section 2.0, when designing stiffened-plate structure, the longitudinals and transverses have been checked explicitly for their various modes of failure. Therefore for the

14

TABLE 3.1. OPTIMUM MESH SIZE DETERMINATION USING PLATE ELEMENTS

Model	1	2	3	4	5	Elas. Small Defl.
Element Size (mm x mm)	304.8 x 304.8	152.4 x 152.4	76.2 x 76.2	38.1 x 38.1	19.05 x 19.05	
Displ.(mm) (% Diff)	2.04 -20.82	2.59 0.45	2.59 0.45	2.59 0.45	2.59 0.45	2.57
σ_{xx}(N/mm^2) (% Diff)	51 -58.13	97 -19.86	109 -10.29	115 -5.12	118 -2.41	121
σ_{yy}(N/mm^2) (% Diff)	119 -33.17	149 -16.40	164 -7.99	171 -3.78	175 -1.68	178
τ_{xy}(N/mm^2)	18	24	22	23	23	
vm (N/mm^2)	119	149	164	171	175	
max. prin. (N/mm^2)	119	149	164	171	175	
time(min)	0.23	0.42	1.51	11.03	117.28	
memory (Mb)	0.024	0.095	1.001	8.8	71.3	

s_{xx} = Normal Stress in 'x' direction
s_{yy} = Normal Stress in 'y' direction
t_{xy} = In-plane Shear Stress
vm   = von mises Stress
max.prin. = maximum principal Stress
Note : % Differences are with respect to Elastic Small Deflection Theory

15
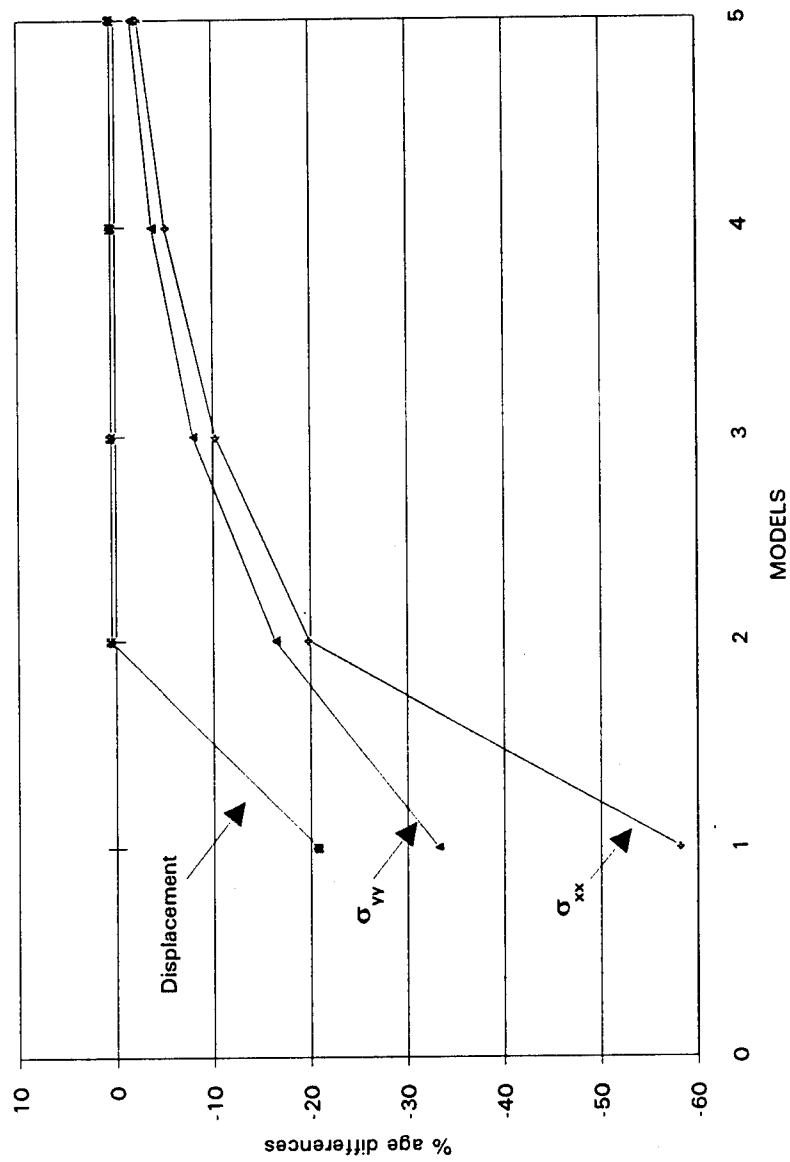
FIGURE 3.1   Mesh Size Determination using Plate Elements

16

present study, the area of interest was the behavior of the plating in a cross stiffened structure under normal loads. To economise on the size of the models and still maintain accuracy, the longitudinal and transverse stiffeners were modeled using beam elements. Since FEM grids combine elements at their neutral axis, the beam elements were offset from the plating by an amount equal to the distance of their neutral axis from the plating. Sectional properties used to represent the stiffeners include total cross-sectional area (A), the shear areas (A_y and A_z), moment of inertias about the strong and weak axes of bending (I_y and I_z) and the St. Venant's torsional constant (J). The properties were obtained by treating the longitudinals and transverses as stand alone beams with no effective plating.

To validate the use of offset beams to represent the longitudinal and transverse stiffeners, two finite element models were developed. In one, the stiffeners were modeled using discrete plate elements, in the other offset beam elements were used. For this comparative study, the second ordinary strength steel (OSS) stiffened-plate model, 15.24m x 6.4m (50' X 21'), designed in section 2.0 was used. For the model in which the stiffeners were represented by discrete plate elements, the webs of the longitudinals were two elements deep and those of the transverses were four elements deep. The flanges of both the longitudinals and transverses were two elements wide. In both models, the plating was represented by 152.4mm (6") square elements. Due to symmetry in loading and boundary conditions, only a quarter of the structure was modeled. Results of the comparison are shown in Table 3.2. In addition to displacement, Table 3.2 also contains the computational time taken and the memory required for analyzing each of the models. Table 3.2 indicates that

17

TABLE 3.2.   COMPARISON OF   STIFFENER MODELS USING PLATES AND OFFSET
BEAMS.   (PLATING MODELED USING PLATE ELEMENTS)

MODEL	STIFFENERS AS PLATES	STIFFENERS AS BEAMS	% DIFFERENCE
Displacement (mm)	9.73	9.99	2.69
σ_{xx} (N/mm^2)	140.53	139.85	-0.48
σ_{yy} (N/mm^2)	190.34	192.92	1.36
τ_{xy} (N/mm^2)	54.28	55.55	2.34
v.mises (N/mm^2)	169.31	171.87	1.51
Time (min)	21	4	-81.00
Memory (Mb)	25	6	-76.00

σ_{xx} = Normal Stress in 'x' direction

σ_{yy} = Normal Stress in 'y' direction

τ_{xy} = In-plane Shear Stress

v.mises   = von mises Stress

Note : % Differences are with respect to the model in which the
stiffeners are modeled using plates.

while the differences in the displacements and stresses between the two models are less than 3%, the saving in time and storage (memory) is as high as 75%.

3.4 Modeling of Plating using Plate Elements

Six stiffened-plate structures, three made of ordinary strength steel (OSS) and three of high strength steel (HSS) were designed in section 2.0. To study the effect of deflection of the supports (longitudinals and transverses) on the plate panels of a stiffened-plate structure, linear elastic finite element models were developed for each of the above six structures using 76.2mm (3") square plate elements to model the plating and offset beams to represent the longitudinals and the transverses. The beam elements used to model the stiffeners were offset at the connection points to the plating by an amount equal to the distance of the neutral axis of the stiffeners from the bottom of the plate surface.
  The thicknesses of the plating used were 15.88mm (0.625") for the OSS models and 14.29mm (0.563") for the HSS. The sectional area properties for the longitudinals and transverses used for the six models are summarised in Table 3.3 and 3.4. For all six models, Young's modulus, E, of 206,850 N/mm^2 (30 X 10^6 psi) and Poisson's ratio of 0.3 were used as material constants, an uniform pressure load of 0.107 N/mm^2 (15.56 psi) was applied normal to the plane of the plating, in the direction of the stiffeners. Due to symmetry of the structure and the load, only a quarter of the structure was modeled.   These stiffened-plate models represent bottom structures between transverse bulkheads on the forward and aft ends and longitudinal girders on either

TABLE 3.3. SECTIONAL PROPERTIES OF LONGITUDINALS AND TRANSVERSES (OSS)

	MODEL 1		MODEL 2		MODEL 3	
	LONGL.	TRANSV.	LONGL.	TRANSV.	LONGL.	TRANSV.
A (cm^2)	29.006	271.270	29.006	157.322	29.006	67.058
$A_y(cm^2)$	14.090	145.161	14.090	100.322	14.090	39.864
$A_z(cm^2)$	14.916	126.109	14.916	57.000	14.916	27.193
$I_y(cm^4)$	258.65	22,787.01	258.65	3,310.95	258.65	775.23
$I_z(cm^4)$	1,136.35	233,612.22	1,136.35	80,869.90	1,136.35	12,041.53
$J(cm^4)$	8.70	473.71	8.70	180.10	8.70	36.42
Y_{na} (cm)	14.983	66.309	14.983	46.772	14.983	28.699

A = Total Area

A_y = Area along 'y' axis

A_z = Area along 'z' axis

I_y = Moment of Inertia about 'y' axis

I_z = Moment of Inertia about 'z' axis

J = St.Venant's Torsional Constant

Y_{na} = Distance of the neutral axis from the plating

TABLE 3.4.   SECTIONAL PROPERTIES OF LONGITUDINALS AND TRANSVERSES (HSS)

	MODEL 1		MODEL 2		MODEL 3	
	LONGL.	TRANSV.	LONGL.	TRANSV.	LONGL.	TRANSV.
$A \ (cm^2)$	24.387	214.445	24.387	129.387	24.387	48.761
$A_y (cm^2)$	11.452	145.671	11.452	81.458	11.452	30.187
$A_z (cm^2)$	12.935	68.774	12.935	47.929	12.935	18.574
$I_y (cm^4)$	185.76	5,622.25	185.76	2,255.60	185.76	510.76
$I_z (cm^4)$	718.50	192,408.89	718.50	52,509.55	718.50	8,499.36
$J (cm^4)$	6.66	259.02	6.66	128.45	6.66	13.19
$Y_{na} \ (cm)$	13.246	59.731	13.246	41.849	13.246	27.607

A   = Total Area

A_y = Area along 'y' axis

A_z = Area along 'z' axis

I_y = Moment of Inertia about 'y' axis

I_z = Moment of Inertia about 'z' axis

J   = St.Venant's Torsional Constant

Y_{na} = Distance of neutral axis from plating

side. For the quarter models, two of the edges are fully fixed representing fixities at the transverse bulkhead and longitudinal girder. On the other two edges, symmetry boundary conditions are applied. A schematic of the structure is shown in Figure 3.2.

Figure 3.3, shows the actual finite element model of the first OSS plate-stiffened structure, 15.24m X 10.06m (50' X 33') designed in section 2.0. The other five models are similar except for their overall dimensions and scantlings.

3.5 Modeling of Plating using Brick Elements

To study the effect of vertical shear on the plate panels of a stiffened-plate structure, linear elastic finite element models were developed by substituting the plate elements used in the previous sub-section with 76.2mm (3") square brick elements to model the plating. One layer of brick elements was used through the thickness, therefore the thickness of the brick elements was the same as the thickness of the plating. The thicknesses of the plating used were 15.88mm (0.625") for the OSS models and 14.29mm (0.563") for the HSS model. As in the previous sub-section, offset beams were used to represent the longitudinal and the transverse stiffeners. The sectional area properties for the stiffeners, material properties, load and boundary conditions were the same as those used in the plate models, see Table 3.3 and 3.4.

3.6 Modeling of Plating with Initial Deformation

It has been observed that in stiffened-plate structures, due to the shrinkage of welds at the attachment of the
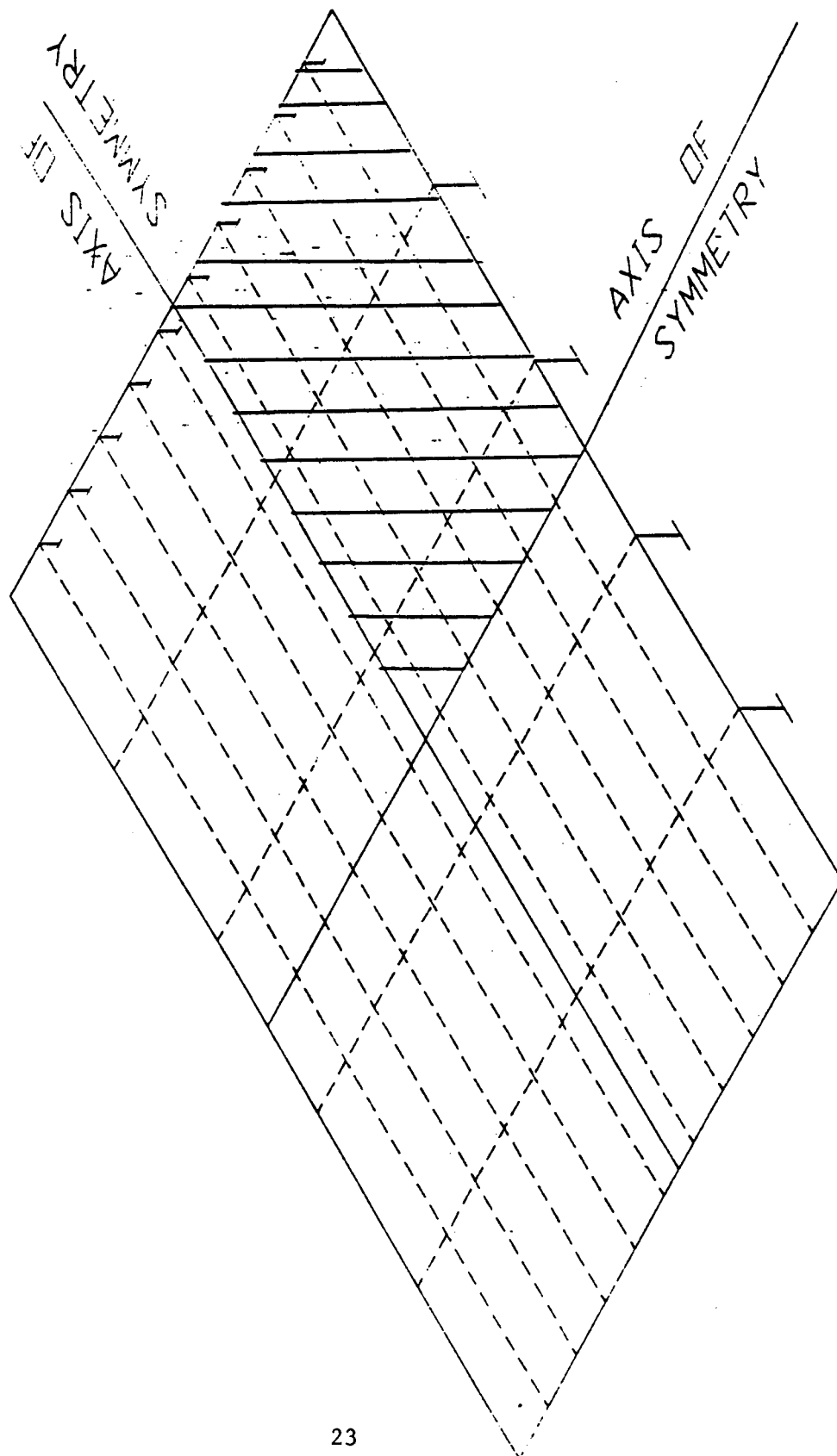
FIGURE 3.2   SCHEMATIC OF A QUARTER MODEL FOR F.E ANALYSIS

PLATING MODELED USING PLATE ELEMENTS (MODEL 1 : 50'x33'; OSS)

SYMMETRY B.C.

FIXED B.C.
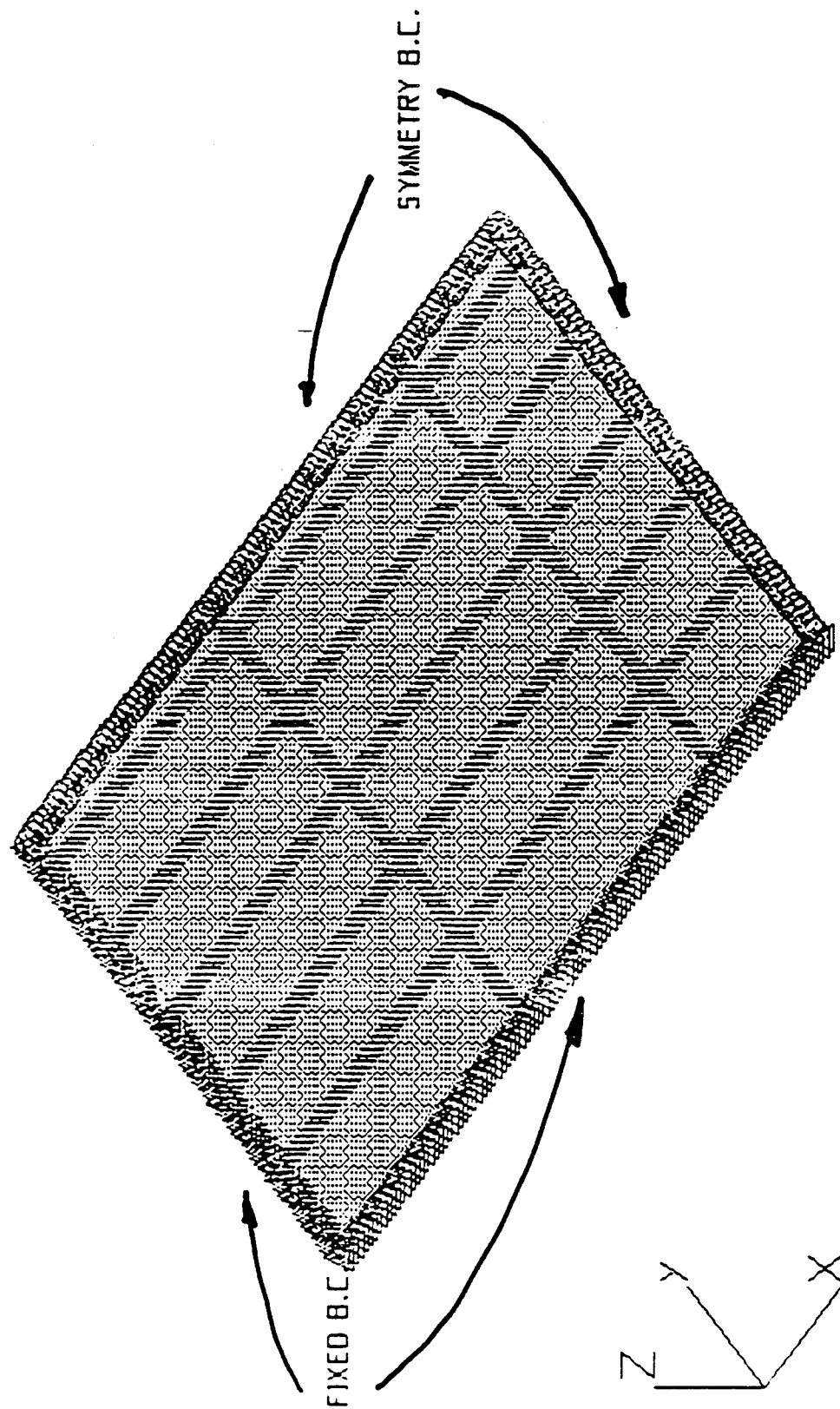
FIGURE 3.3   FINITE ELEMENT MODEL OF PLATE STIFFENED STRUCTURE

24

stiffeners to the plating, the unsupported span of the plating bounded by the stiffeners develops an initial deformation. As mentioned in [4] depending on the amount of initial deformation present in the plating and the degree to which the edges are restrained from pulling in, the plating under normal (lateral) loads, develops membrane tension. This membrane effect which, is absent when the plate is perfectly flat, produces a normal (or lateral) component of membrane tension which can carry a portion of the normal pressure load and hence can be beneficial. To study such membrane effects on stiffened-plate structure with deflecting supports (longitudinals and transverses), two finite element models of the third stiffened-plate structure 15.24m x 2.74m (50' X 9') designed in section 2.0 were developed. For both, the OSS and HSS models, brick elements were used to model the plating and as before offset beam elements were used to represent the stiffeners.

The initial deformation in the unsupported span of the plating between the stiffeners was defined by a double sine function as given below :

$$\Delta_{(x,y)} = t \, Sin\left(\frac{\pi x}{a}\right) Sin\left(\frac{\pi y}{b}\right)$$

where :

$\Delta_{(x,y)}$ = Initial deformation

t   = thickness of the plating

a,b = length and breadth of the unsupported span of plating

Using this expression the maximum deflection always occurs at the middle of the panel. The deflection value was chosen to be equal to one plate thickness. For this study, 38.1mm (1.5") square brick elements were used and as before their

25

thicknesses were the same as that of the plate. The same material constants, loading and boundary conditions were used as in sub-section 3.4 and 3.5.

4.0 RESULTS OF FINITE ELEMENT ANALYSIS

4.1 Comparison of Stresses using Plate Elements

Tables 4.1 and 4.2 summarize the results of the analysis performed using plate elements to represent plate panels of the six stiffened-plate models designed in section 2.0. The output includes maximum displacement, normal stresses σ_{xx} and σ_{yy}, in-plane shear stress τ_{xy}, and Von-Mises stress for the OSS and HSS models respectively. The normal stress, σ_{xx}, is in the longitudinal direction or the long direction of the structure while σ_{yy} is the normal stress in the transverse direction. The Von-Mises stress represents the Hecky - Von-Mises failure criteria and takes into account all the normal stress components as well as the the shear stresses. In the tables, locations of the maximum values of displacements and stresses are given in parenthesis below each quantity.

For comparison, the last column of Tables 4.1 and 4.2 (with the heading 'SP') contains results of a single panel with fully fixed edges. This single panel is the same as an unsupported panel of plating of models 1, 2, and 3. This panel has the same thickness as that of the stiffened-panel (15.88mm) (0.625") for OSS structures and 14.3mm (0.563") for HSS structures). This single panel represents a case where the longitudinals and transverses are excessively stiff and hence are undeflecting.

Figures 4.1 to 4.12 show the stress patterns of the normal, σ_{yy}, and the Von-Mises stresses for models 1, 2 and 3. Stress

27

TABLE 4.1. MAXIMUM DISPLACEMENT AND STRESSES AT THE BOTTOM SURFACE OF OSS MODELS
(USING PLATE ELEMENTS; t = 15.88 mm; $\sigma_y = 235$ N/mm^2)

	MODEL 1 (15.24x10.06)	MODEL 2 (15.24x6.40)	MODEL 3 (15.24x2.74)	S.P. (3.05x0.91)
Disp. (mm) (cm,cm)	14.45 (457,503)	10.42 (457,320)	7.44 (457,137)	2.59 (152,46)
σ_{xx} (N/mm^2) (cm,cm)	157.28 (0,137)	151.97 (0,137)	151.94 (610,137)	108.57 (0,46)
σ_{yy} (N/mm^2) (cm,cm)	241.70 (610,0.0)	209.13 (518,0.0)	195.92 (457,0.0)	163.76 (122,0.0)
τ_{xy} (N/mm^2) (cm,cm)	60.99 (587,107)	53.26 (587,99)	37.54 (587,99)	22.48 (23,15)
v.mises (N/mm^2) (cm,cm)	230.64 (610,0.0)	189.87 (610,0.0)	184.05 (457,0.0)	145.55 (122,0.0)

TABLE 4.2. MAXIMUM DISPLACEMENT AND STRESSES AT THE BOTTOM SURFACE OF HSS MODELS
(USING PLATE ELEMENTS; t = 14.29 mm; $\sigma_y = 350$ N/mm^2)

	MODEL 1 (15.24x10.06)	MODEL 2 (15.24x6.40)	MODEL 3 (15.24x2.74)	S.P. (3.05x0.91)
Disp. (mm) (cm,cm)	18.68 (457,503)	14.46 (457,320)	10.32 (457,137)	3.55 (152,46)
σ_{xx} (N/mm^2) (cm,cm)	192.31 (0,137)	187.65 (0,137)	188.01 (610,137)	134.03 (0,46)
σ_{yy} (N/mm^2) (cm,cm)	281.23 (610,0.0)	258.09 (518,0.0)	241.85 (457,0.0)	202.18 (122,0.0)
τ_{xy} (N/mm^2) (cm,cm)	73.54 (587,107)	67.07 (587,99)	46.51 (587,99)	27.76 (23,15)
v.mises (N/mm^2) (cm,cm)	250.50 (610,0.0)	232.66 (610,0.0)	227.43 (457,0.0)	179.70 (122,0.0)

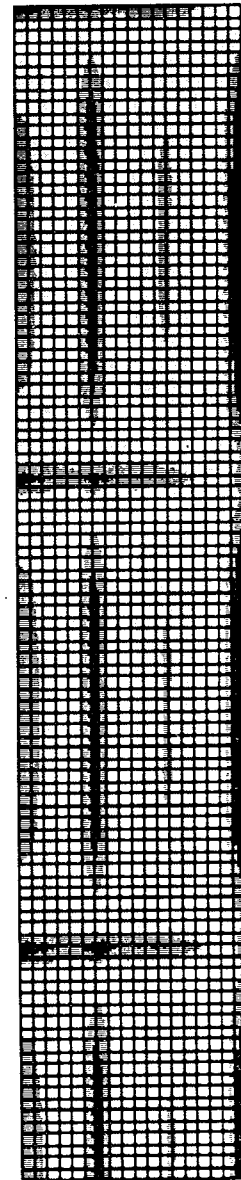| psi	N/mm²
33481	231
25138.5	173
16796	116
8453.5	58
111	1
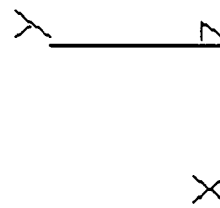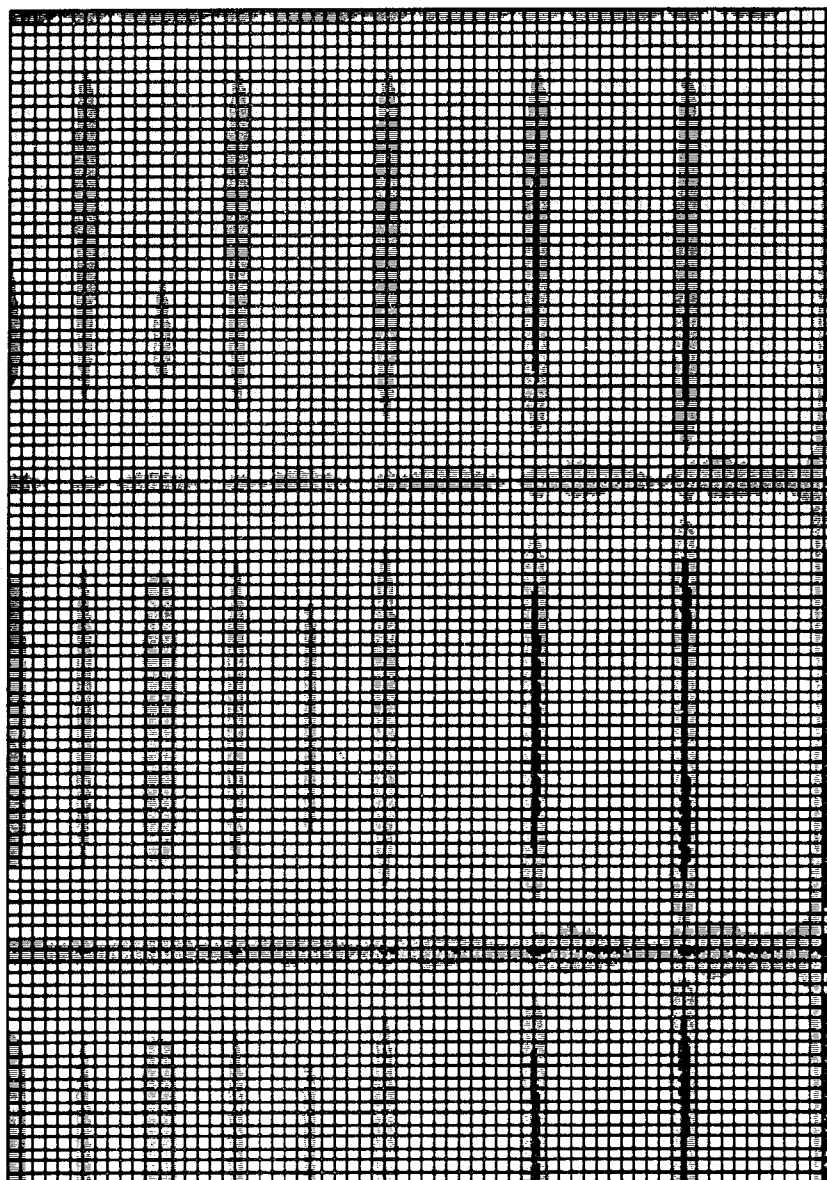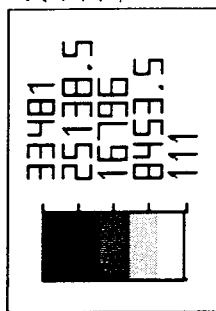
FIGURE 4.1   OSS PLATE MODEL 1; VON-MISES STRESS (VIEW FROM THE BOTTOM)
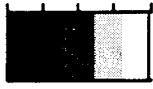
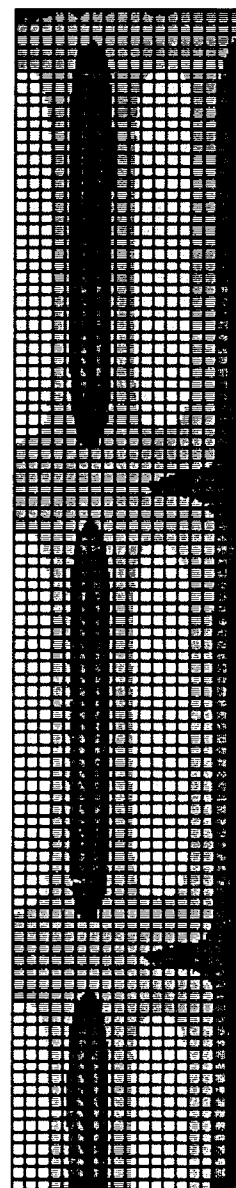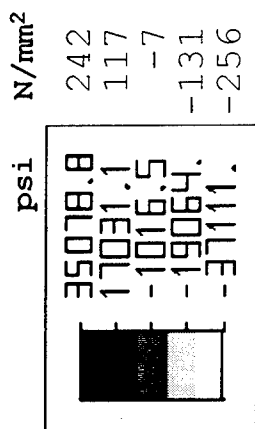| psi	N/mm²
37205.6	257
20872.9	144
4540.32	31
-11792.	-81
-28124.	-194
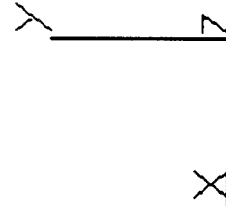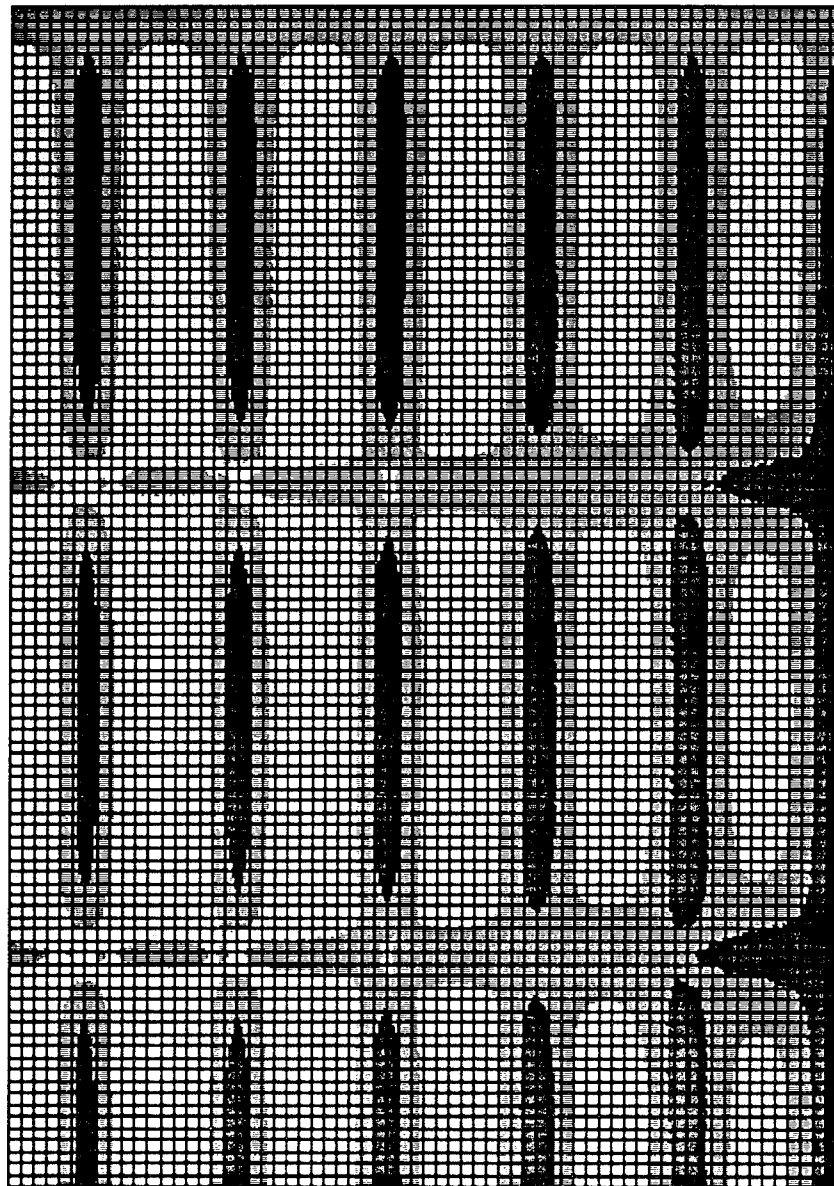
FIGURE 4.2   OSS PLATE MODEL 1; σ_{yy} STRESS (VIEW FROM THE BOTTOM)

psi	N/mm²
36348.8	251
27291.1	188
18233.4	126
9175.71	63
118	1
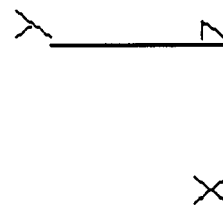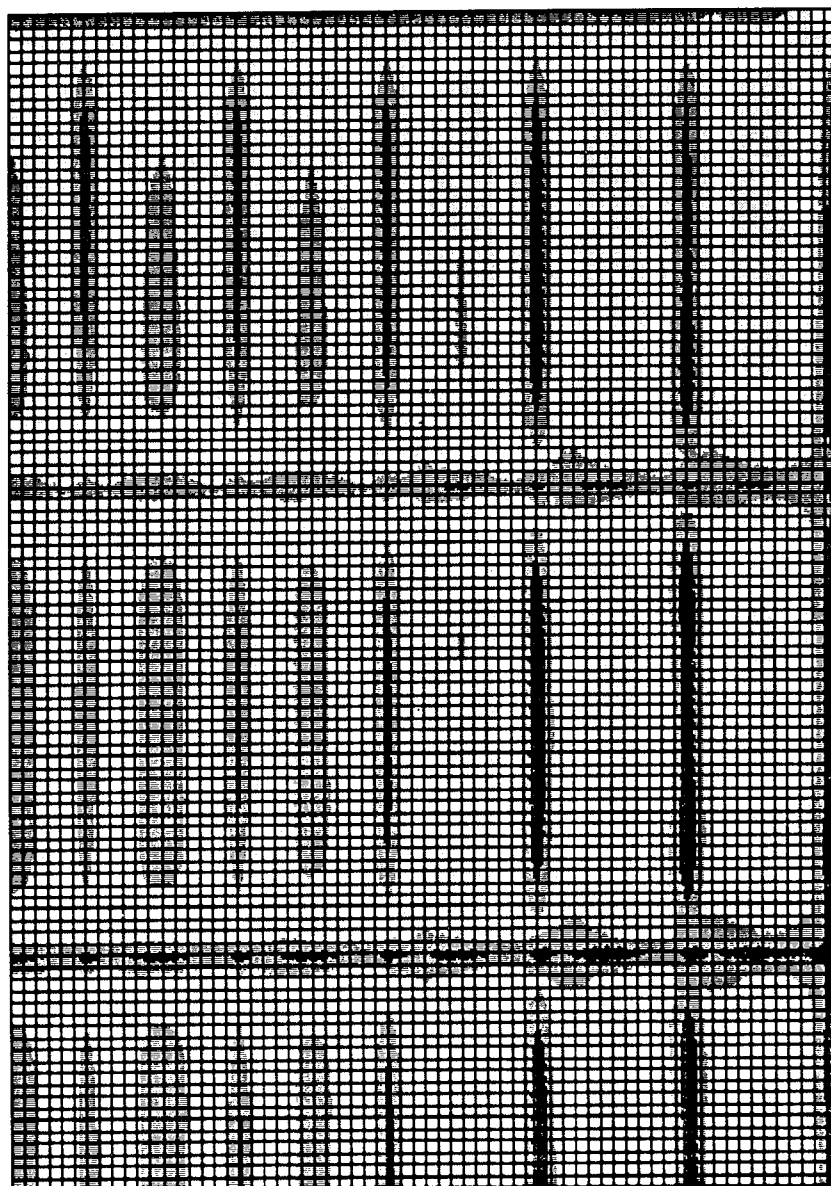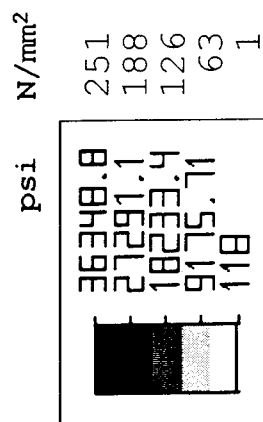
FIGURE 4.3 HSS PLATE MODEL 1; VON-MISES STRESS (VIEW FROM THE BOTTOM)

psi	N/mm²
40856.7	282
22078.2	152
3299.68	23
-15478.	-107
-34257.	-236
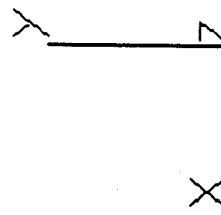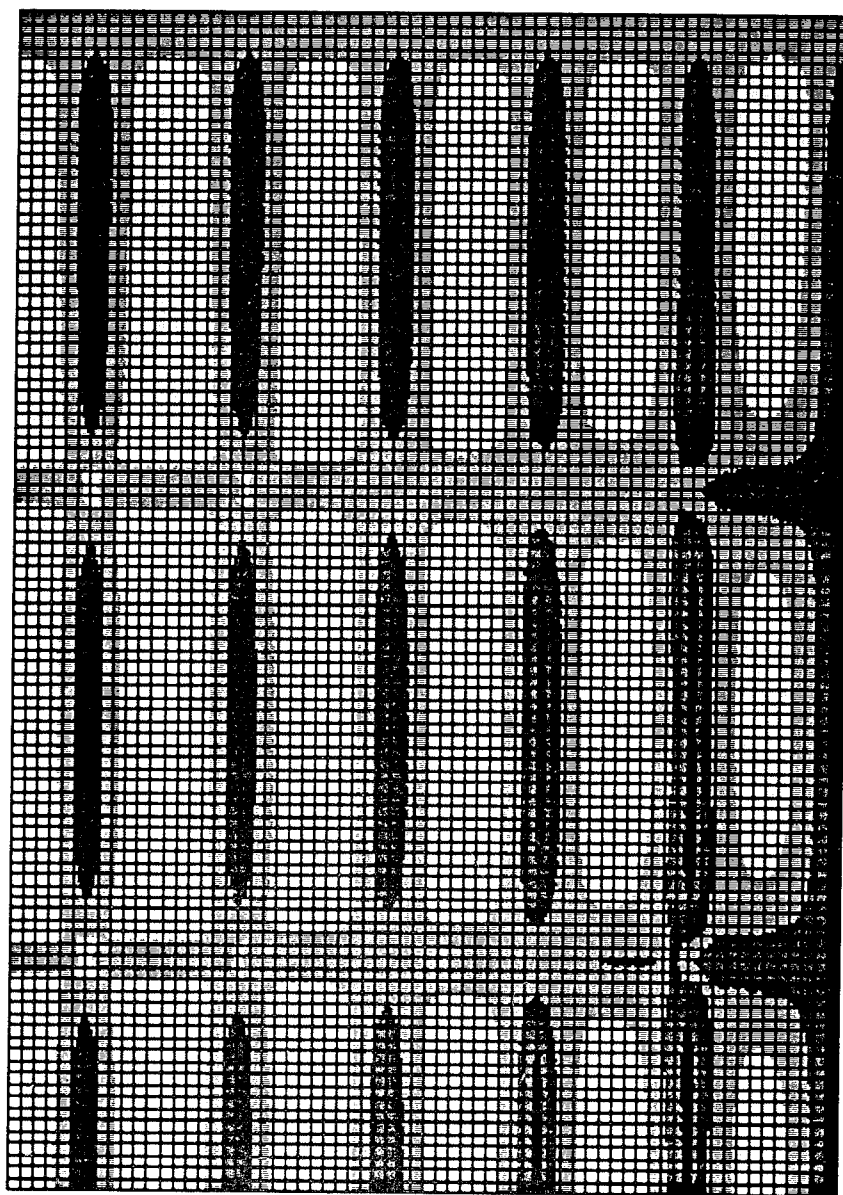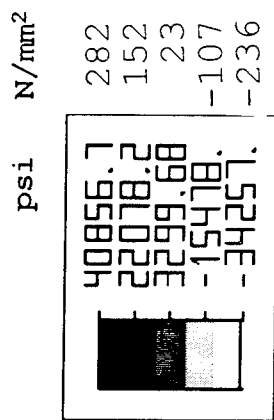
FIGURE 4.4   HSS PLATE MODEL 1; σ_{yy} STRESS (VIEW FROM THE BOTTOM)
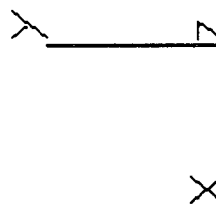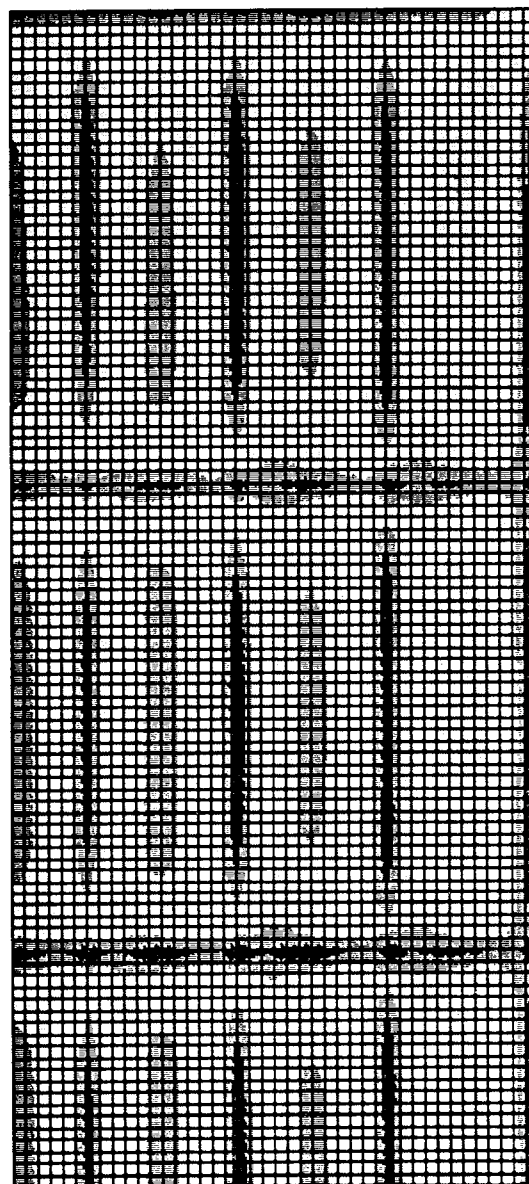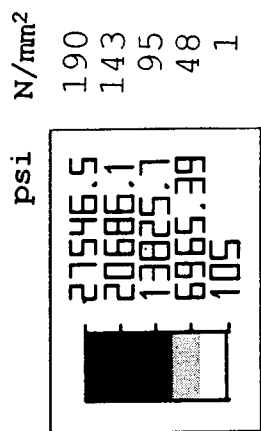
FIGURE 4.5 ÓSS PLATE MODEL 2; VON-MISES STRESS (VIEW FROM THE BOTTOM)

psi	N/mm²
30375.4	209
15580.5	107
785.584	5
-14009.	-97
-28804.	-199
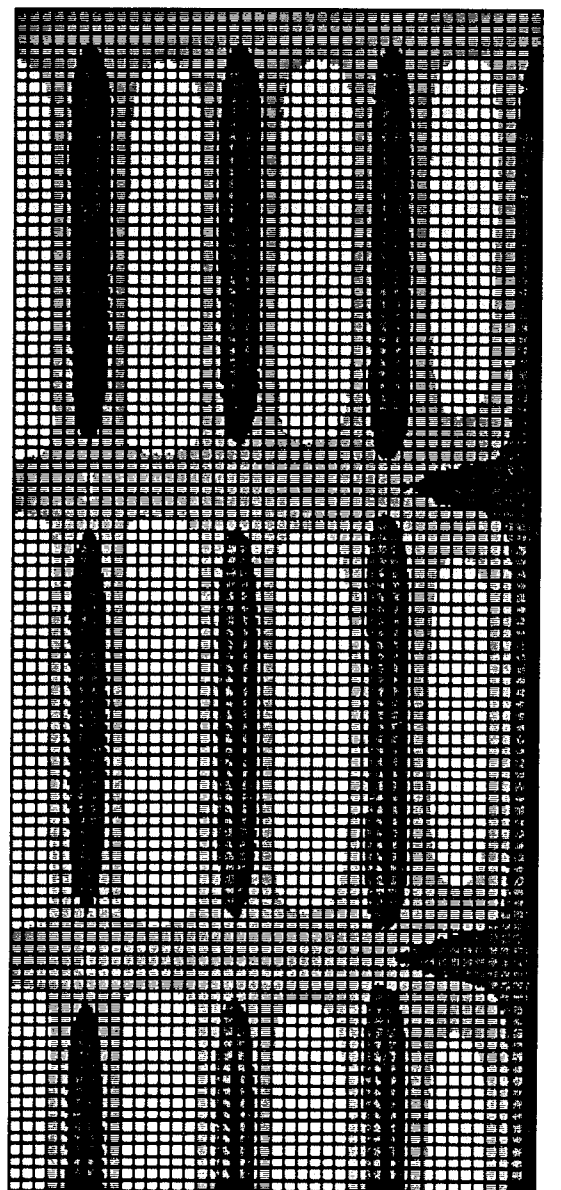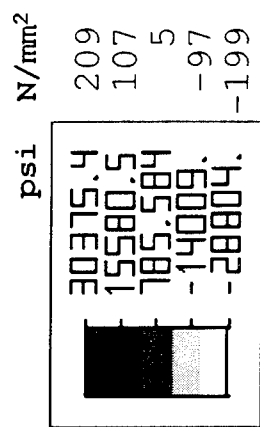
FIGURE 4.6   OSS PLATE MODEL 2; σ_{yy} STRESS   (VIEW FROM THE BOTTOM)

psi	N/mm^2
33754.8	233
25349.8	175
16944.9	117
8539.98	59
135.051	1
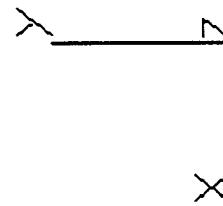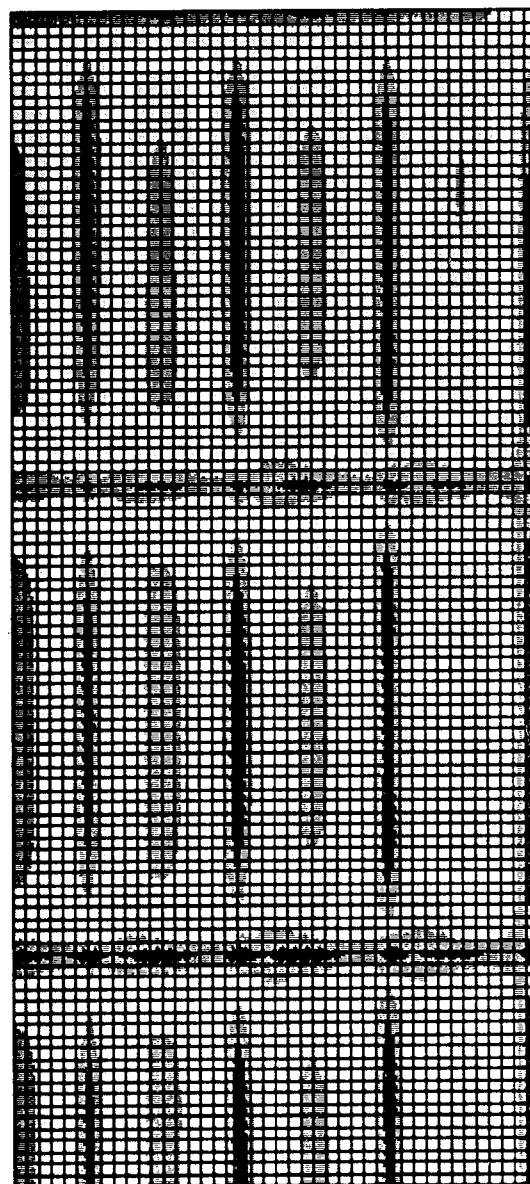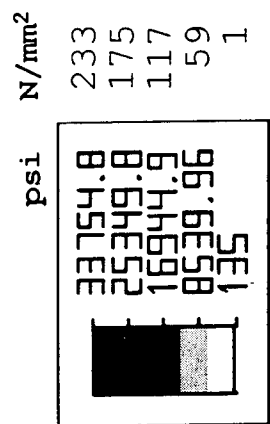
FIGURE 4.7 HSS PLATE MODEL 2; VON-MISES STRESS (VIEW FROM THE BOTTOM)
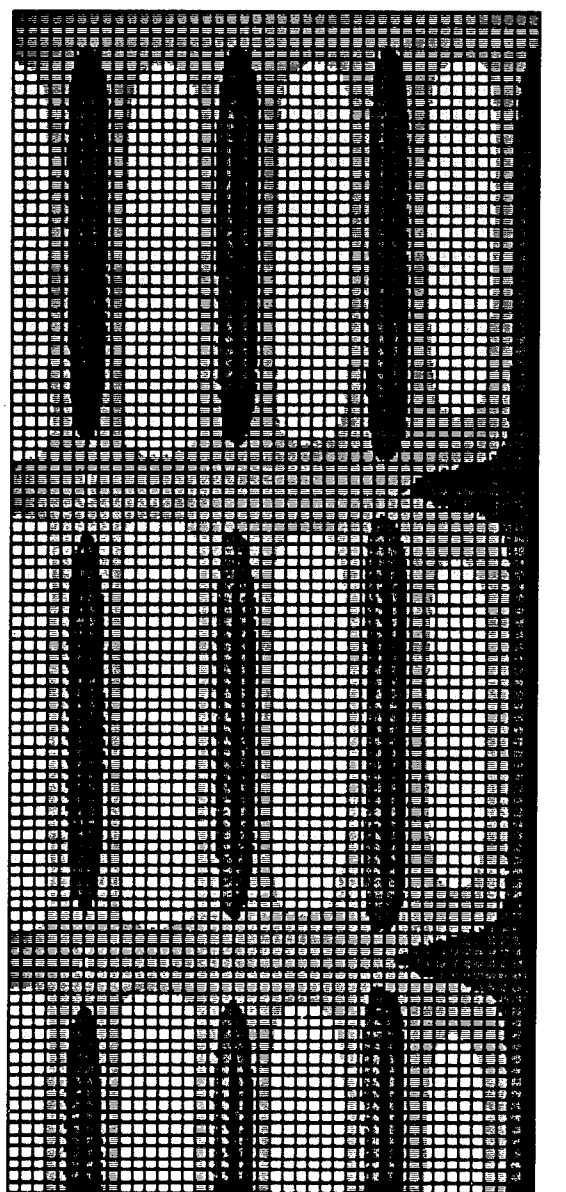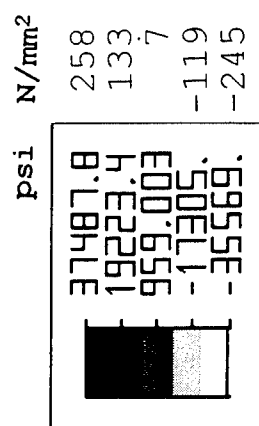
FIGURE 4.8   HSS PLATE MODEL 2; σ_{yy} STRESS (VIEW FROM THE BOTTOM)

psi	N/mm²
26692.6	184
20075.5	138
13458.3	93
6841.16	47
224	2
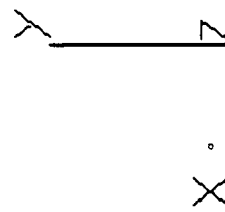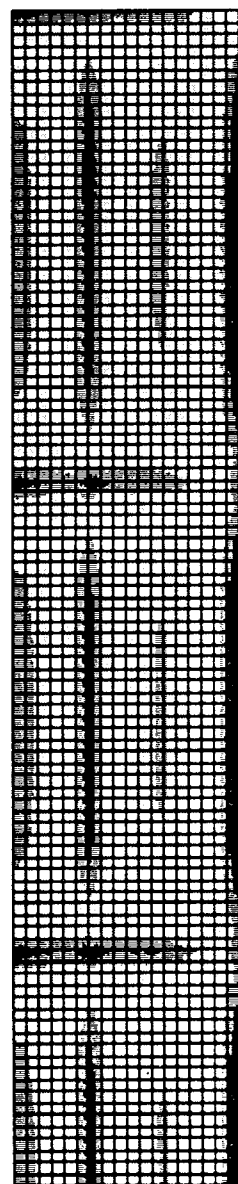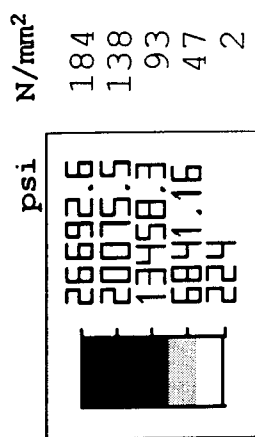
FIGURE 4.9 OSS PLATE MODEL 3; VON-MISES STRESS (VIEW FROM THE BOTTOM)

psi	N/mm²
28418.2	196
13805.7	95
-806.77	-6
-15419.	-106
.3E00E-	-207
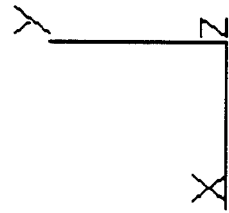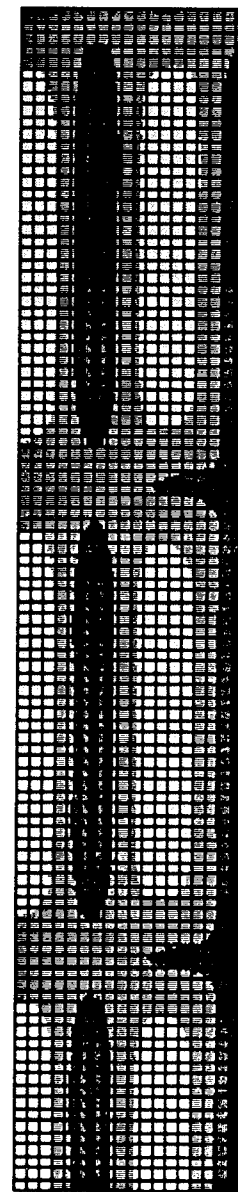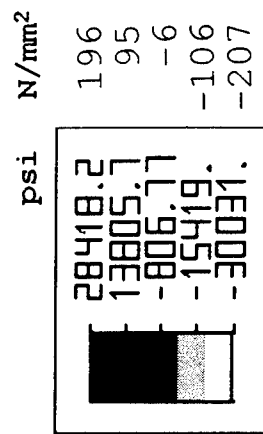
FIGURE 4.10 OSS PLATE MODEL 3; σ_{yy} STRESS (VIEW FROM THE BOTTOM)
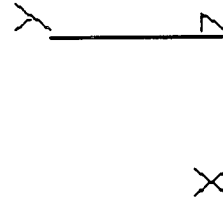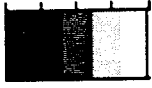
FIGURE 4.11 HSS PLATE MODEL 3; VON-MISES STRESS (VIEW FROM THE BOTTOM)

psi	N/mm²
32985.4	227
24819.3	171
16653.2	115
8487.10	59
321	2

psi	N/mm²
35078.8	242
17031.1	117
-1016.5	-7
-19064.	-131
-37111.	-256
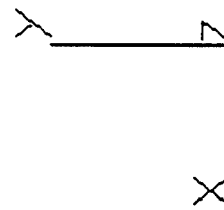
FIGURE 4.12 HSS PLATE MODEL 3; σ_{yy} STRESS (VIEW FROM THE BOTTOM)

patterns of the other two components, σ_{xx} and τ_{xy}, are not included since in all cases the magnitude of σ_{xx} is less than σ_{yy} and τ_{xy} is very small. As the figures indicate, the maximum stresses occur at the two fixed edges and along the intersection of the stiffeners with the plate. The two fixed edges are those which are closer to the right and top edges of the paper respectively. In each of the figures, the stress distribution has been represented by five ranges, values of which are shown at the top. The OSS and HSS models have the same stress patterns although their magnitudes are different due to the difference in plate thicknesses and grillage beam sizes.

Figures 4.13 and 4.14 provide a direct comparison of the stress components. The maximum values of four stress components, two normal stress components σ_{xx} and σ_{yy}, in-plane shear τ_{xy} and von-mises, are plotted with respect to the virtual aspect ratio defined in section 2.0. For comparison, the values of these stresses for the single panel model described above have also been plotted. For each value of virtual aspect ratio, the percentage differences in the stresses of the stiffened-plate and the single panel model are shown in the plots.

4.2 Comparison of Stresses using Brick Elements

Tables 4.3 and 4.4 provide maximum values of the normal stress σ_{zz} and vertical shear stresses τ_{yz}, τ_{xz} in addition to displacement, normal stresses σ_{xx} and σ_{yy}, in-plane shear

41
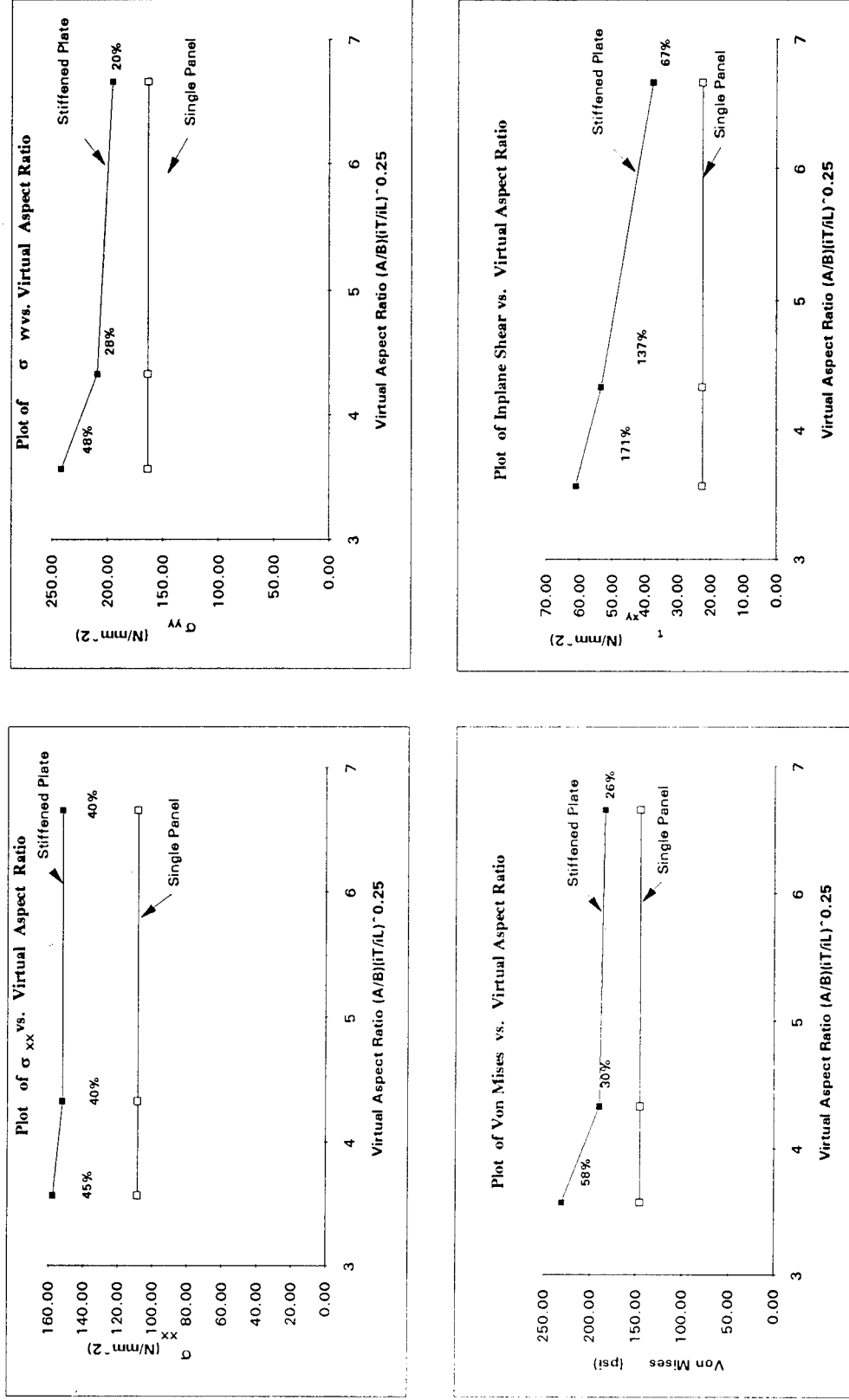
FIGURE 4.13   COMPARISION OF STRESSES IN OSS PLATE MODEL WITH SINGLE PANEL

42
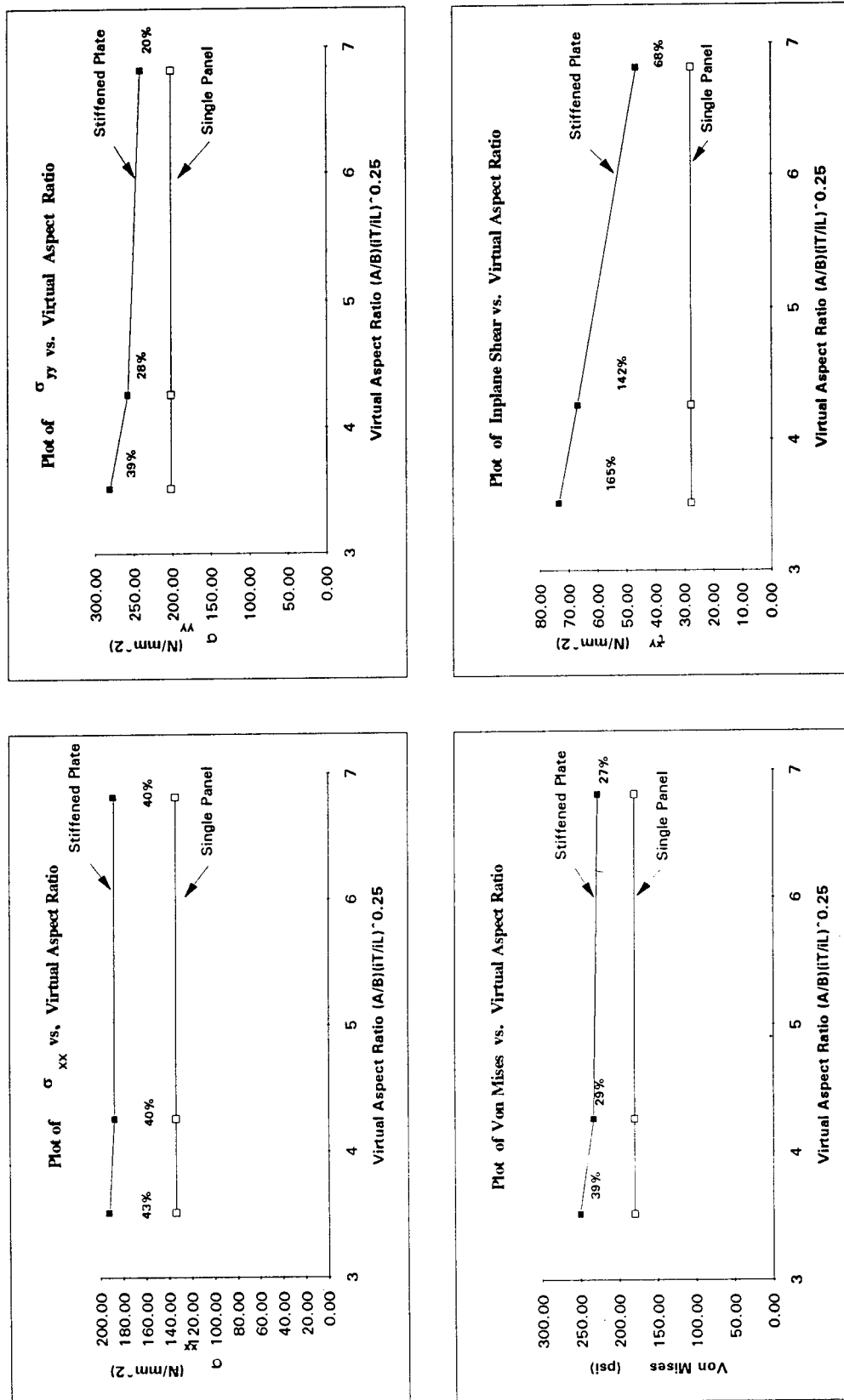
FIGURE 4.14   COMPARISION OF STRESSES IN HSS PLATE MODEL WITH SINGLE PANEL

43

TABLE 4.3. MAXIMUM DISPLACEMENT AND STRESSES OF OSS MODELS

(USING BRICK ELEMENTS; t = 15.88 mm; $\sigma_y = 235$ N/mm^2)

	MODEL 1 (15.24x10.06)	MODEL 2 (15.24x6.40)	MODEL 3 (15.24x2.74)
Disp. (mm) (cm,cm,cm)	14.12 (457,503,0.000)	10.14 (457,320,0.000)	7.27 (457,137,0.000)
σ_{xx} (N/mm^2) (cm,cm,cm)	140.44 (0,457,0.000)	130.32 (0,274,0.000)	130.15 (610,137,0.000)
σ_{yy} (N/mm^2) (cm,cm,cm)	255.51 (610,0,0.000)	204.55 (610,0,0.000)	164.11 (457,0,0.000)
σ_{zz} (N/mm^2) (cm,cm,cm)	87.45 (610,0,1.588)	68.94 (610,0,1.588)	39.26 (610,0,1.588)
τ_{xy} (N/mm^2) (cm,cm,cm)	63.03 (594,99,1.588)	54.50 (594,99,1.588)	36.70 (587,99,1.588)
τ_{yz} (N/mm^2) (cm,cm,cm)	29.31 (610,0,0.000)	23.59 (610,0,0.000)	15.71 (610,0,0.000)
τ_{xz} (N/mm^2) (cm,cm,cm)	16.58 (0,457,0.000)	14.96 (0,274,0.000)	13.11 (0,91,0.000)
v.mises (N/mm^2) (cm,cm,cm)	202.55 (610,8,0.000)	162.47 (610,8,0.000)	153.86 (457,0,1.588)

TABLE 4.4. MAXIMUM DISPLACEMENT AND STRESSES OF HSS MODELS

(USING PLATE ELEMENTS; $t = 14.29$ mm; $\sigma_y = 350$ N/mm^2)

	MODEL 1 (15.24x10.06)	MODEL 2 (15.24x6.40)	MODEL 3 (15.24x2.74)
Disp. (mm) (cm,cm,cm)	18.20 (457,503,0.000)	14.02 (457,320,0.000)	10.02 (457,137,0.000)
σ_{xx} (N/mm^2) (cm,cm,cm)	167.47 (0,457,0.000)	159.07 (0,274,0.000)	159.81 (610,137,0.000)
σ_{yy} (N/mm^2) (cm,cm,cm)	279.77 (610,0,0.000)	253.56 (610,0,0.000)	202.67 (457,0,0.000)
σ_{zz} (N/mm^2) (cm,cm,cm)	100.04 (610,0,1.430)	86.80 (610,0,1.430)	46.34 (610,0,1.430)
τ_{xy} (N/mm^2) (cm,cm,cm)	74.99 (594,99,1.430)	67.98 (594,99,1.430)	44.98 (587,99,1.430)
τ_{yz} (N/mm^2) (cm,cm,cm)	25.48 (610,0,0.000)	26.16 (610,0,0.000)	18.04 (610,0,0.000)
τ_{xz} (N/mm^2) (cm,cm,cm)	17.20 (0,457,0.000)	15.76 (0,274,0.000)	13.73 (0,91,0.000)
v.mises (N/mm^2) (cm,cm,cm)	228.49 (610,8,0.000)	203.92 (610,8,0.000)	190.14 (457,0.0,1.430)

stress τ_{xy}, and Von-Mises stress for the OSS and HSS models respectively. The normal stresses σ_{xx} and σ_{yy} are in the same direction as described in sub-section 4.1. The normal stress σ_{zz} acts vertically upwards. The two additional shear stresses τ_{xz} and τ_{yz} act vertically on the two faces perpendicular to the longitudinal and transverse directions of the panel. The Von-Mises stress represents the Hecky – Von- mises failure criteria and takes into account all the normal stress components as well as the shear stresses. As in the previous sub-section in the tables, locations of the maximum values of displacements and stresses are given in parenthesis below each quantity. Figures 4.15 to 4.38 show the stress patterns of the normal stress σ_{yy}, von-mises stress and the vertical shear stresses τ_{xz} and τ_{yz} for models 1, 2 and 3. As before, only σ_{yy}, whose magnitude is greater than the other two normal stresses, are shown. For all the models, maximum σ_{yy} and von mises occur at the two fixed edges and along the intersection of the plate with the stiffeners. The two fixed edges are those which are closer to the right and top edges of the paper respectively. Maximum vertical shear stress τ_{yz} occurs along the transverses while the maximum τ_{xz} occurs along the longitudinals. In each of the figures, the total stress distribution has been divided into five ranges, values of which are shown at the top. The OSS and HSS models have the same stress patterns although their magnitudes are different because of the difference in plate thicknesses and grillage beam sizes.

In Figures 4.39 and 4.40, the maximum values of four stress components, two normal stress components σ_{xx} and σ_{yy}, in-plane shear τ_{xy} and von-mises, are plotted with respect to the

46

psi	N/mm²
30000	207
22600	156
15200	105
7800	54
400	3
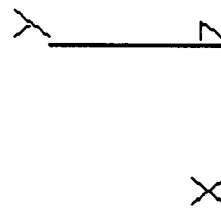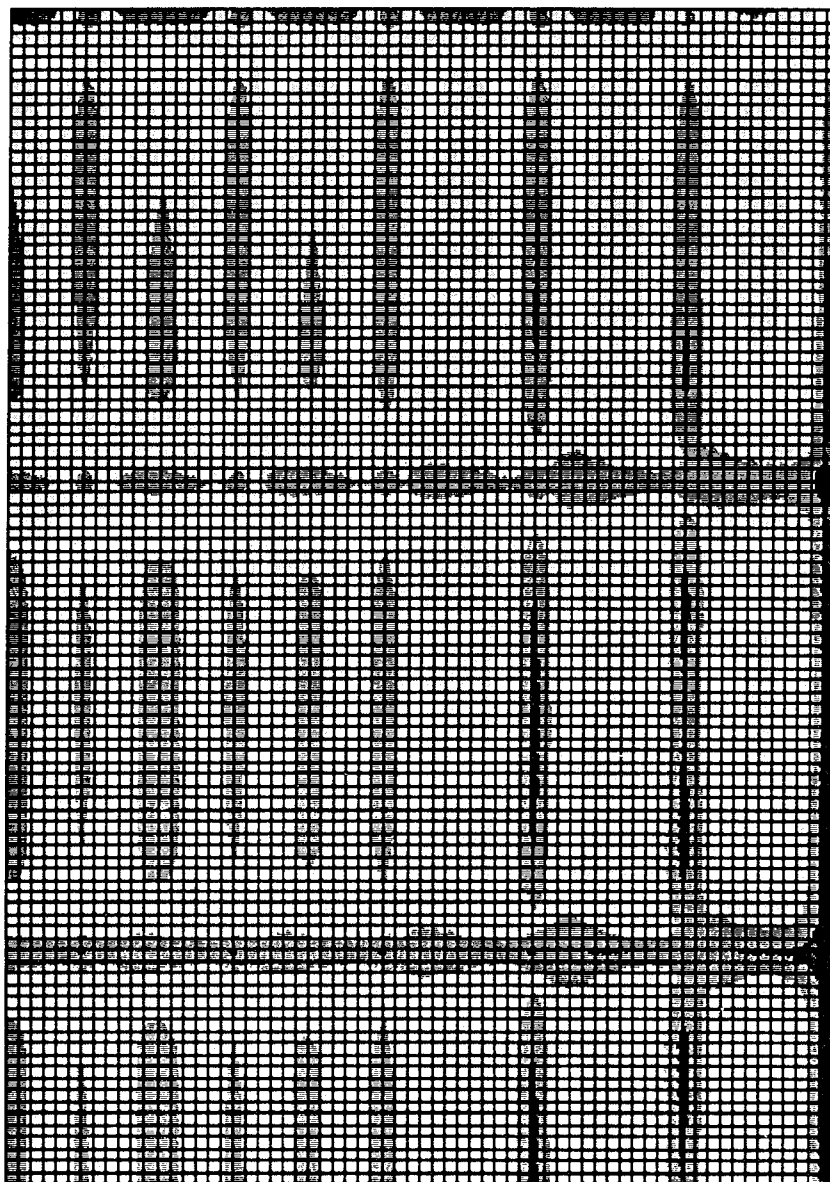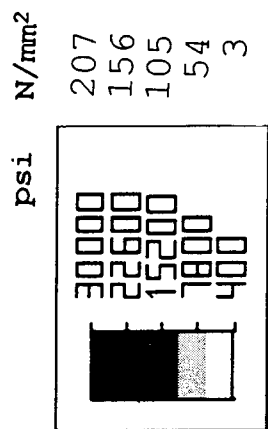
FIGURE 4.15 OSS BRICK MODEL 1; VON-MISES STRESS (VIEW FROM THE BOTTOM)
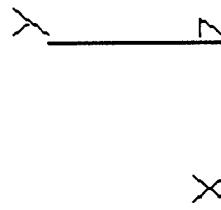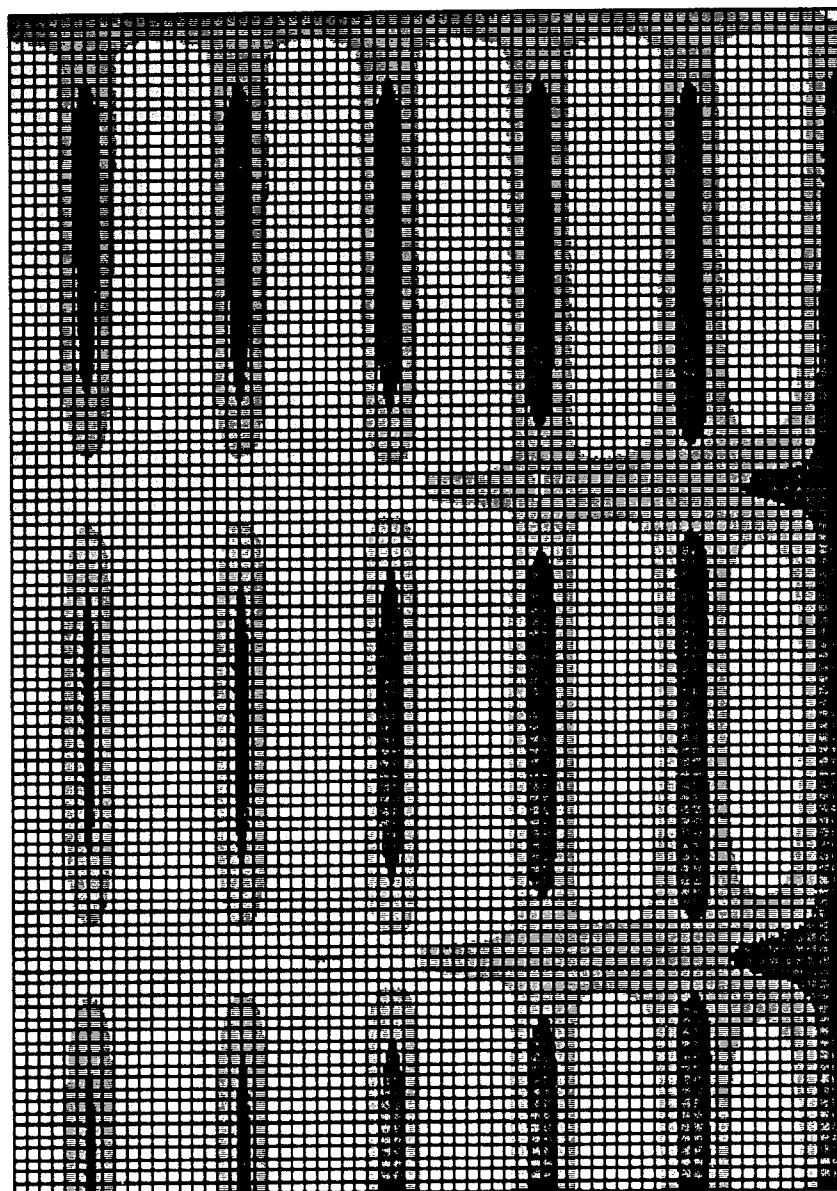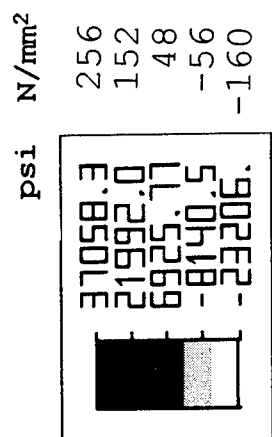
FIGURE 4.16 OSS BRICK MODEL 1; σ_{yy} STRESS (VIEW FROM THE BOTTOM)
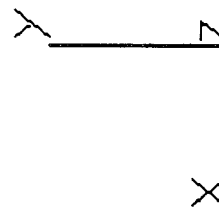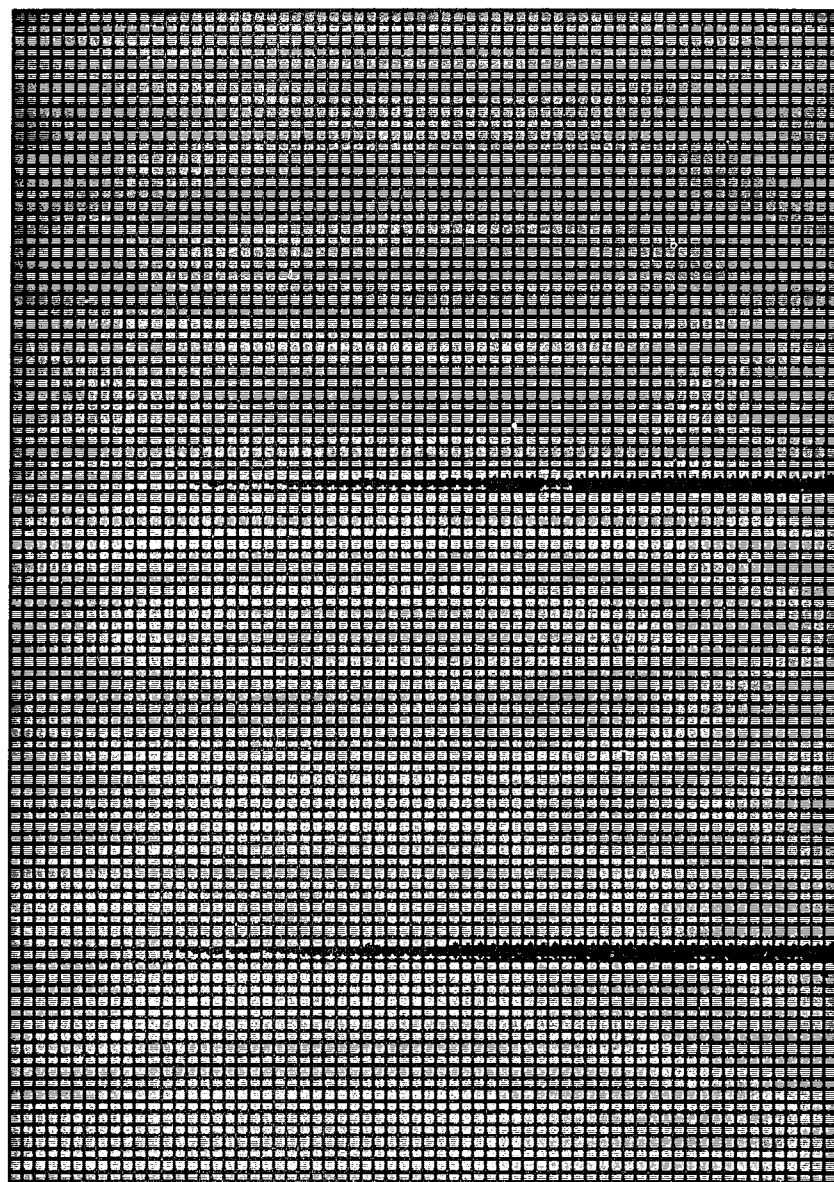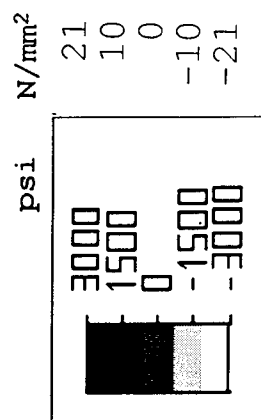
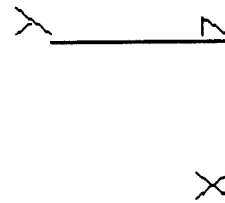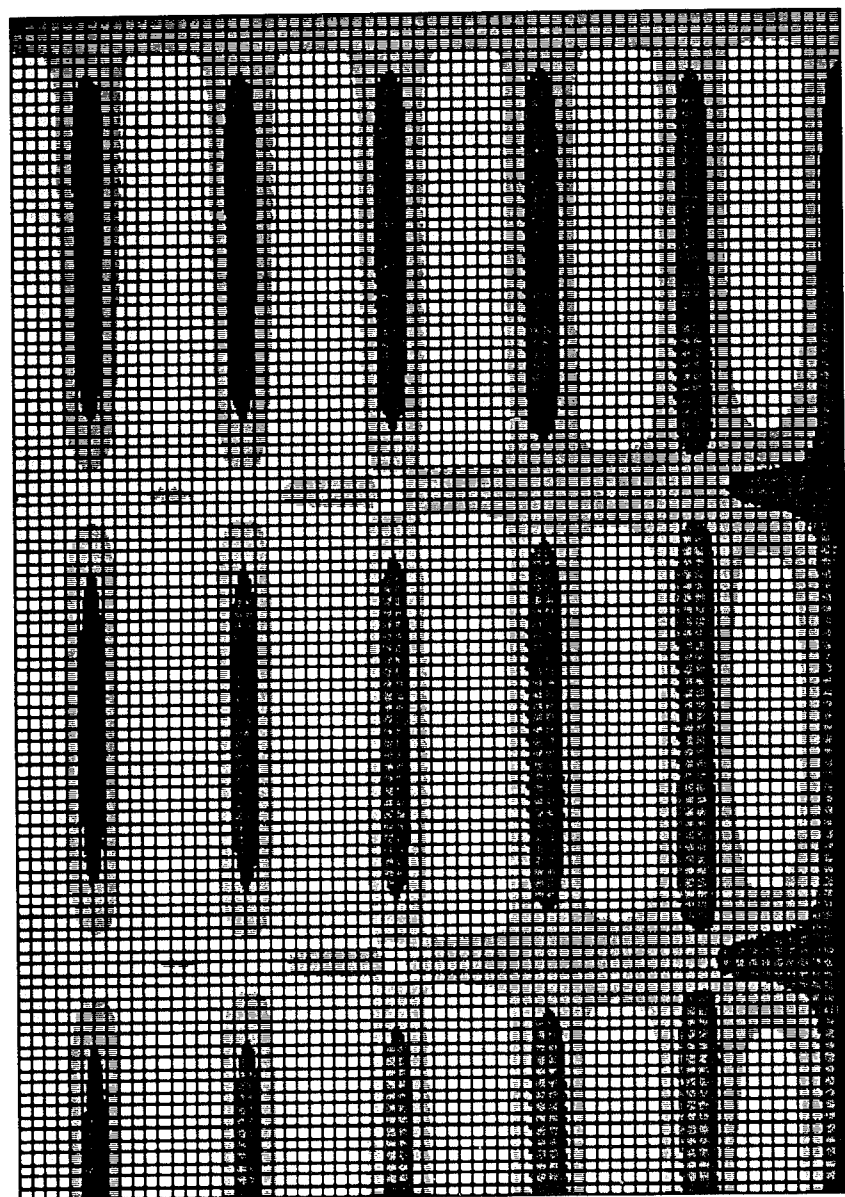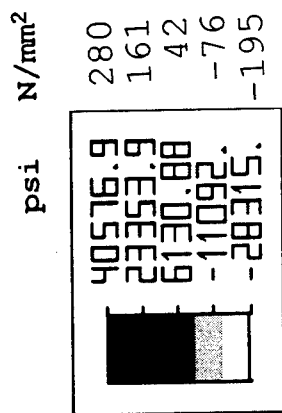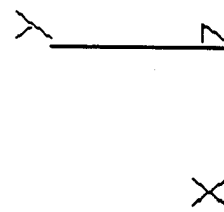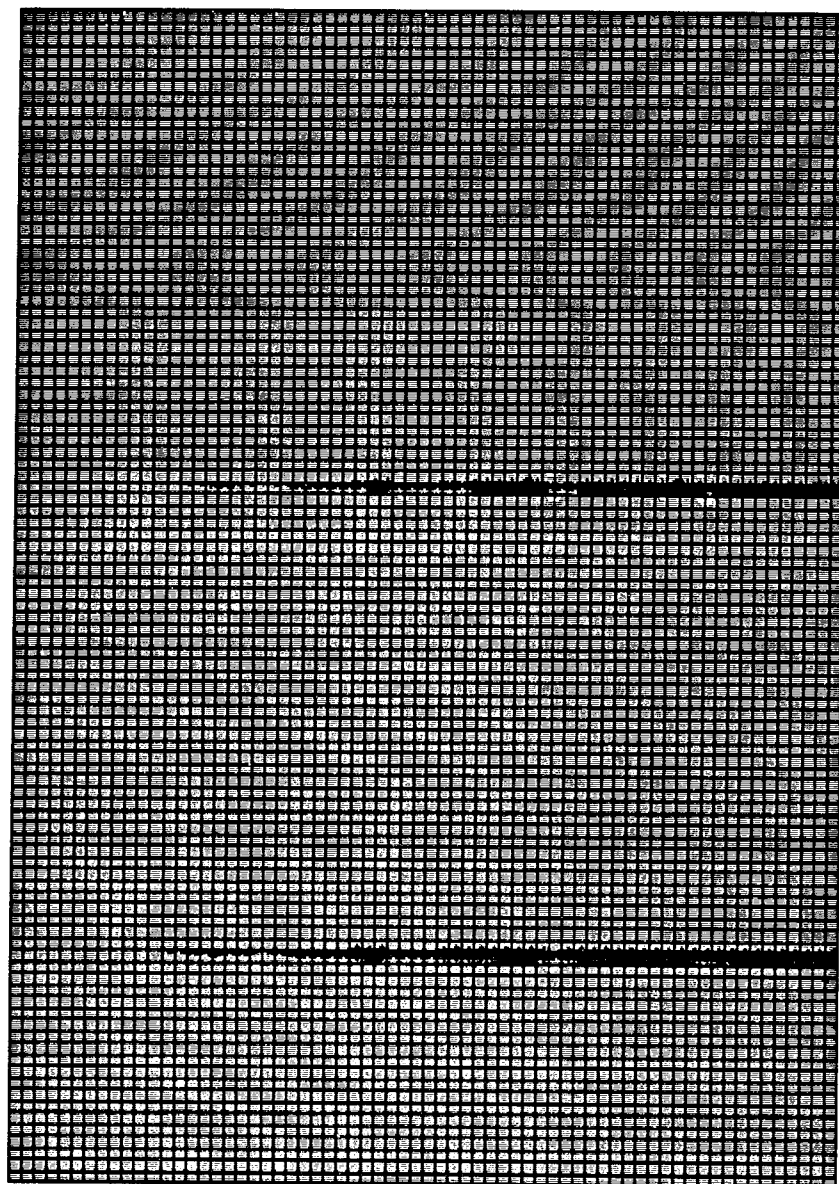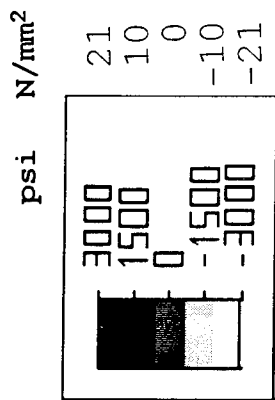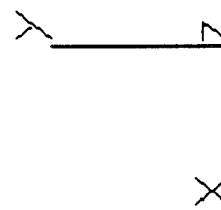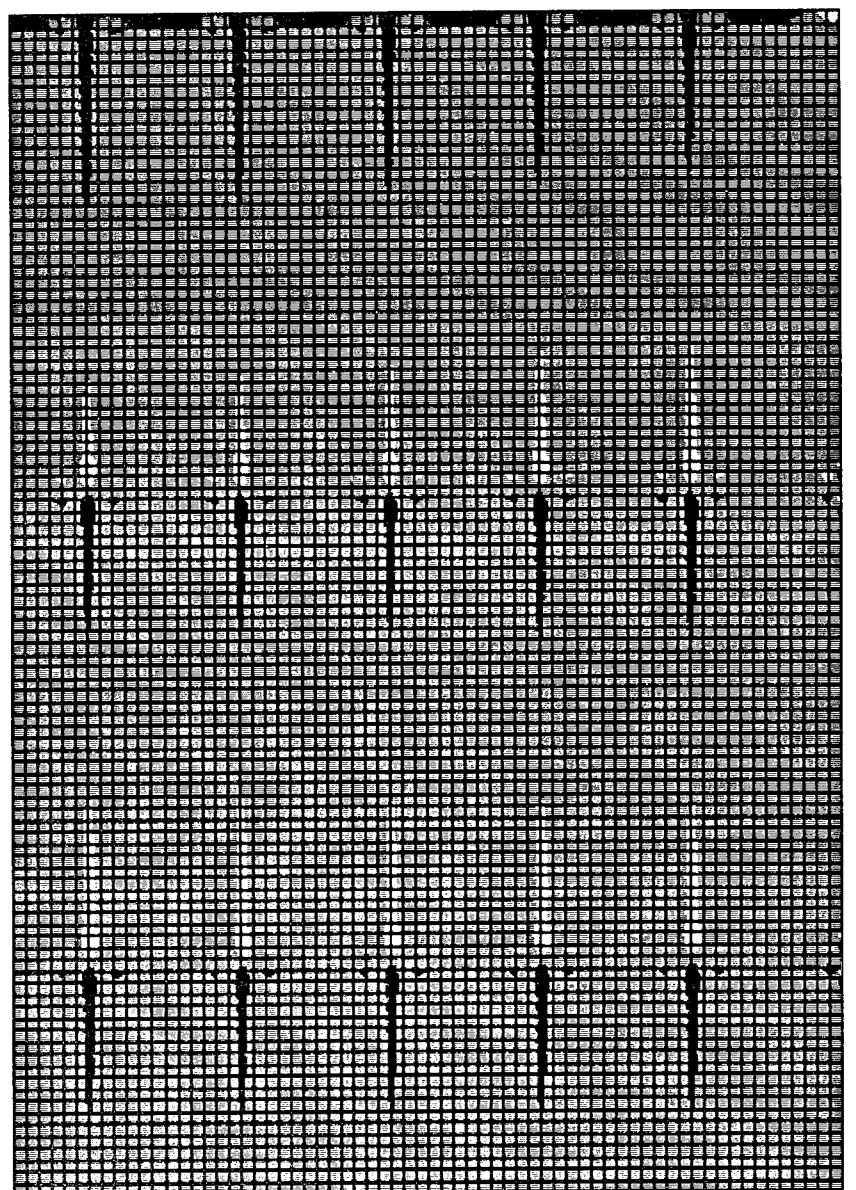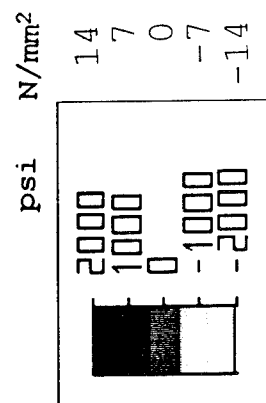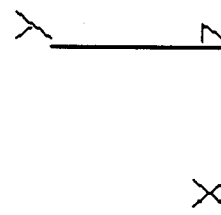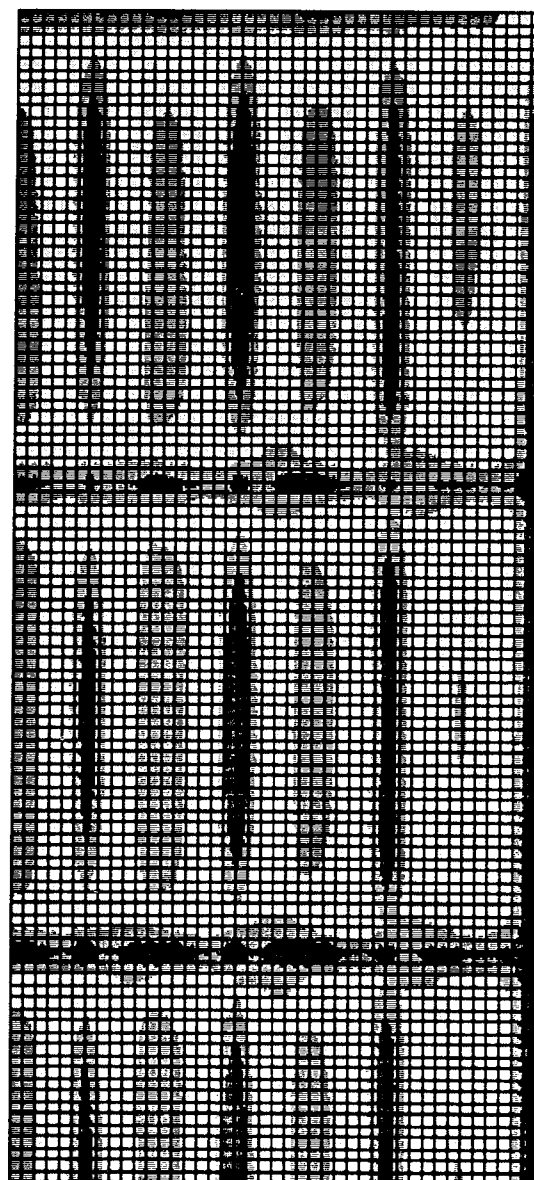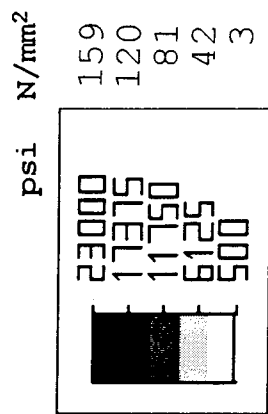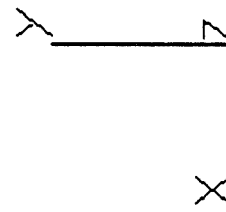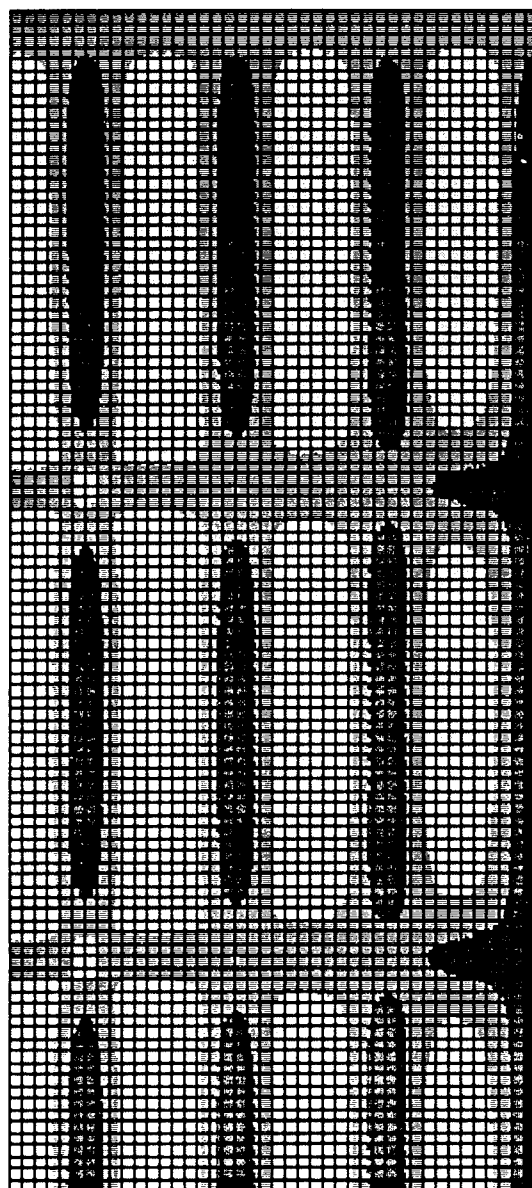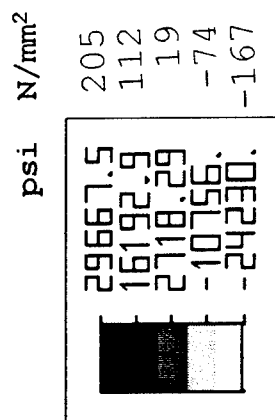FIGURE 4.17 OSS BRICK MODEL 1; τ_{yz} STRESS (VIEW FROM THE BOTTOM)
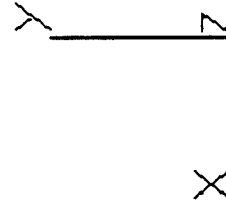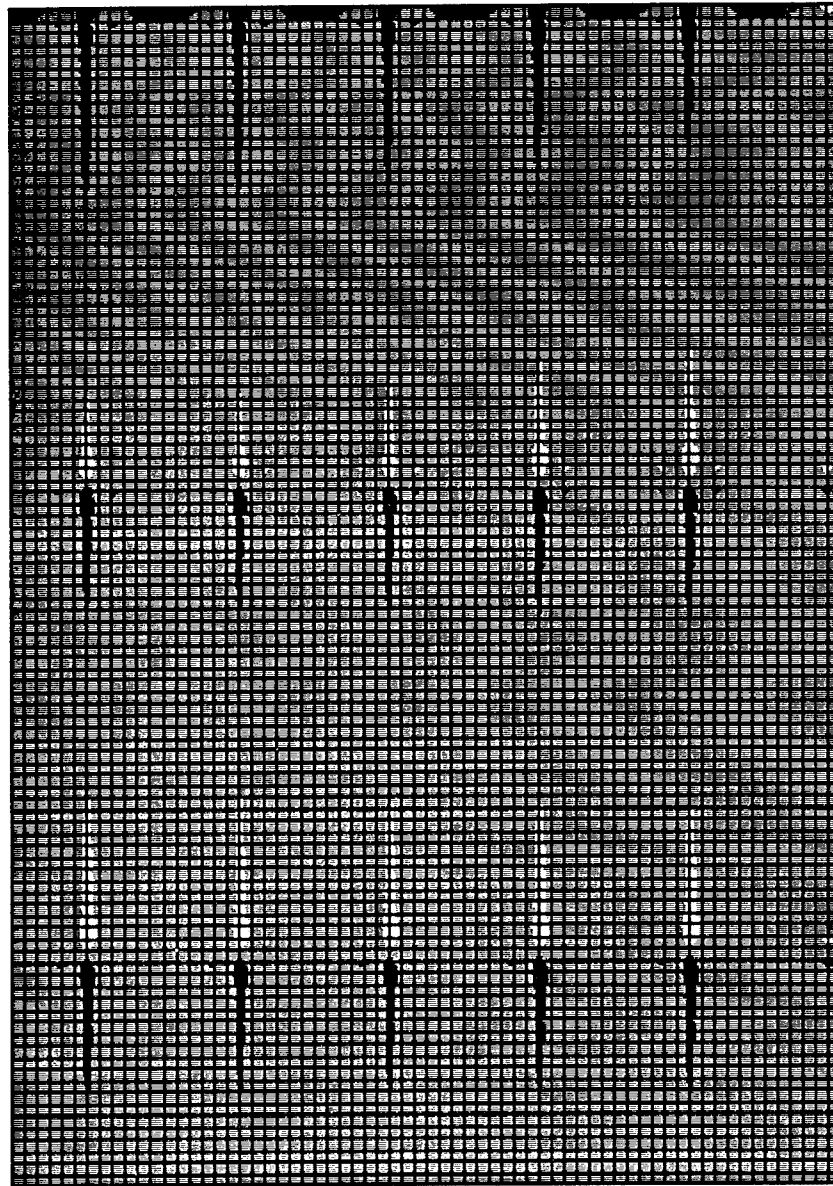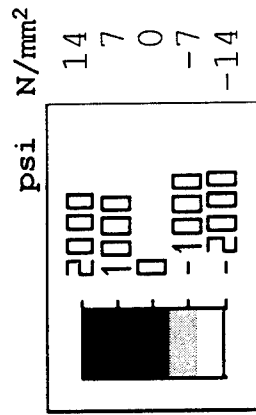
FIGURE 4.18 OSS BRICK MODEL 1; τ_{xz} STRESS (VIEW FROM THE BOTTOM)

psi	N/mm²
32000	221
24162.5	167
16325	113
8487.5	59
650	4
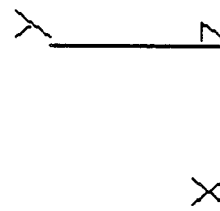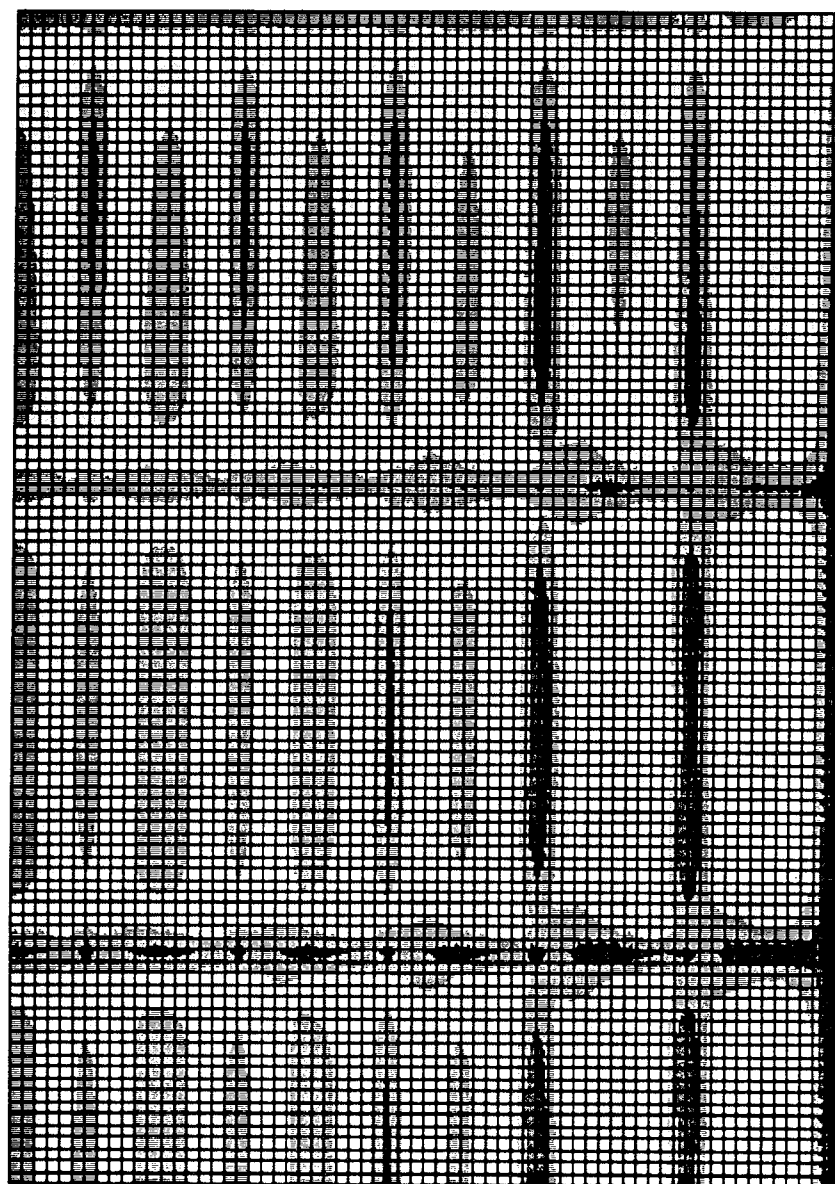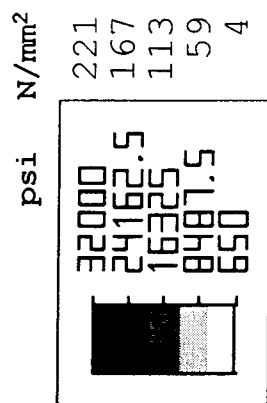
FIGURE 4.19 HSS BRICK MODEL 1; VON-MISES STRESS (VIEW FROM THE BOTTOM)

51

FIGURE 4.20 HSS BRICK MODEL 1; σ_{yy} STRESS (VIEW FROM THE BOTTOM)

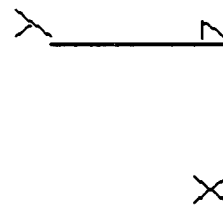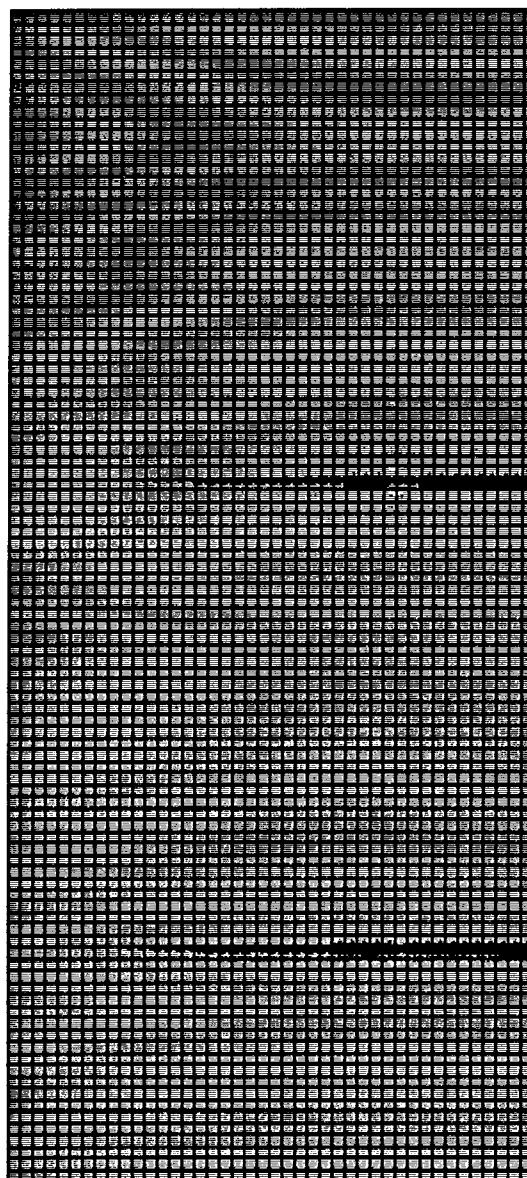FIGURE 4.21 HSS BRICK MODEL 1; τ_{yz} STRESS (VIEW FROM THE BOTTOM)

FIGURE 4.22 HSS BRICK MODEL 1; τ_{xz} STRESS (VIEW FROM THE BOTTOM)

FIGURE 4.23 OSS BRICK MODEL 2; VON-MISES STRESS (VIEW FROM THE BOTTOM)

psi	N/mm²
29667.5	205
16192.9	112
2718.29	19
-10756.	-74
-24230.	-167

FIGURE 4.24 OSS BRICK MODEL 2; σ_{yy} STRESS (VIEW FROM THE BOTTOM)

psi N/mm²

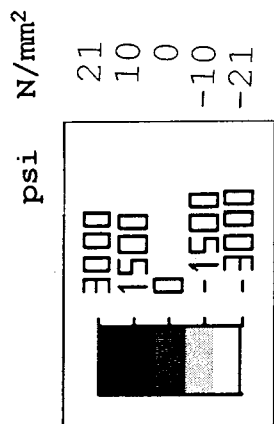3000 → 21
1500 → 10
0 → 0
-1500 → -10
-3000 → -21

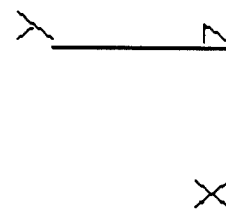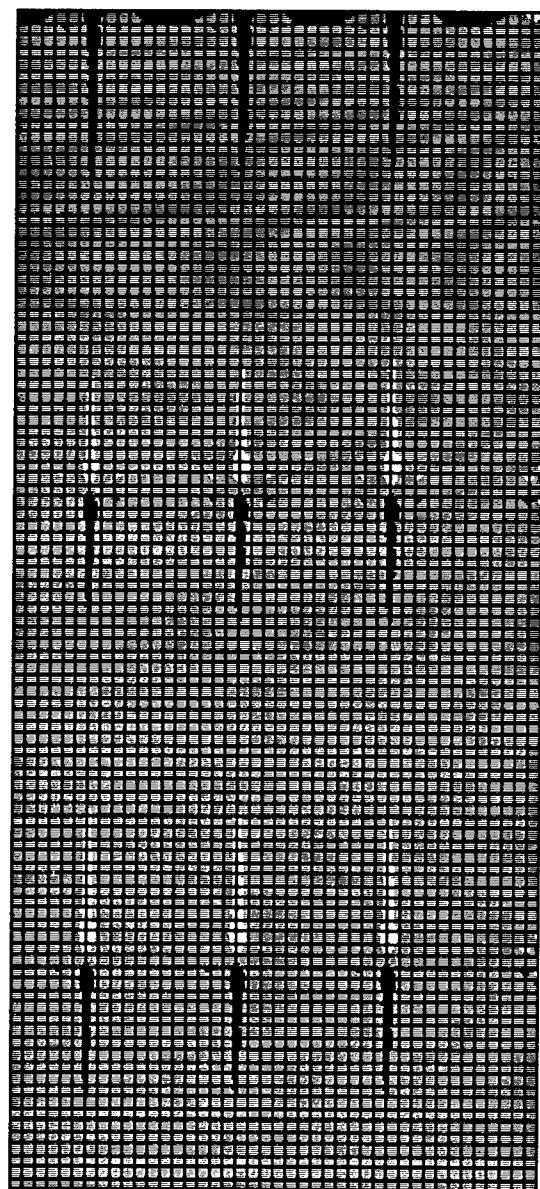FIGURE 4.25 OSS BRICK MODEL 2; τ_{yz} STRESS (VIEW FROM THE BOTTOM)

FIGURE 4.26 OSS BRICK MODEL 2; τ_{xz} STRESS (VIEW FROM THE BOTTOM)

psi   N/mm²
29000 200
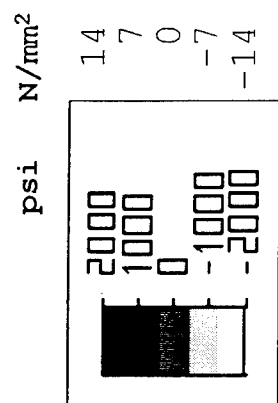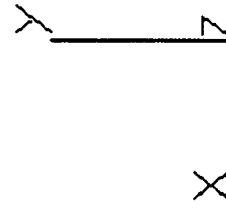21900 151
14800 102
7700   53
600   4
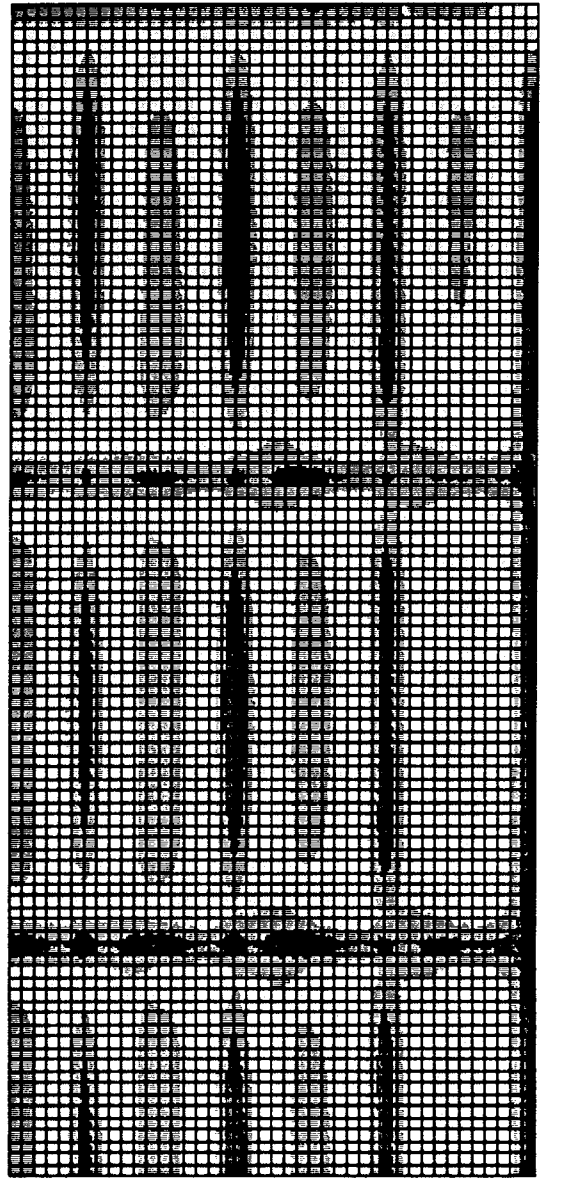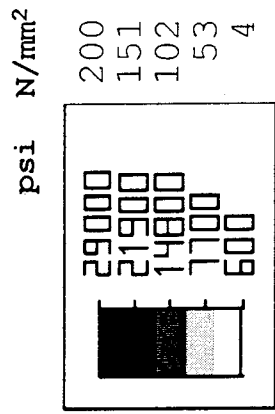
FIGURE 4.27 HSS BRICK MODEL 2; VON-MISES STRESS (VIEW FROM THE BOTTOM)

FIGURE 4.28 HSS BRICK MODEL 2; σ_{yy} STRESS (VIEW FROM THE BOTTOM)

psi	N/mm²
3000	21
1500	10
0	0
-1500	-10
-3000	-21

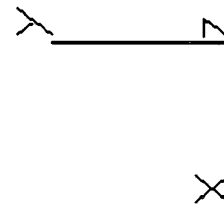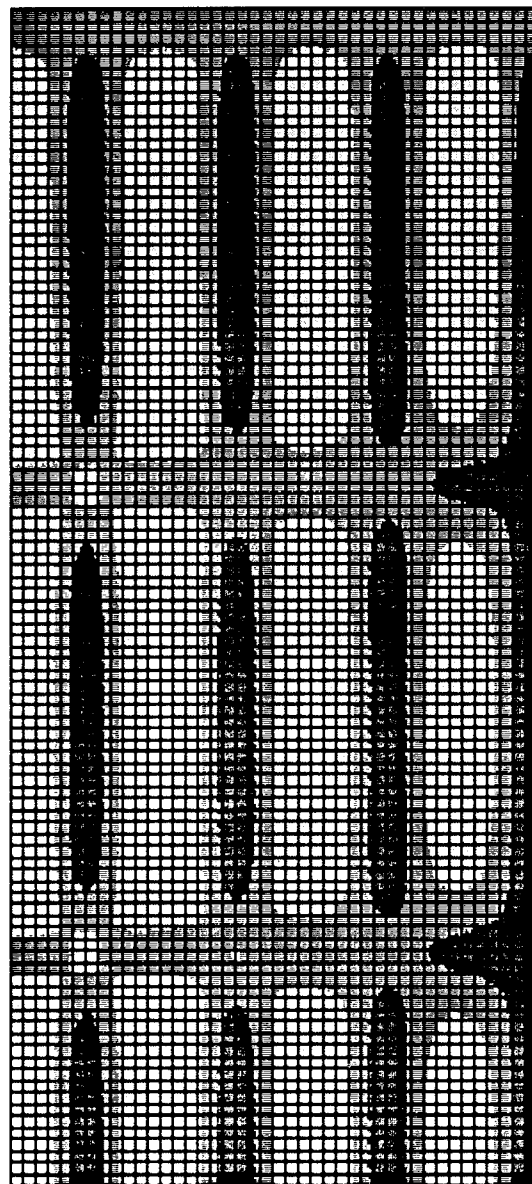FIGURE 4.29 HSS BRICK MODEL 2; τ_{yz} STRESS (VIEW FROM THE BOTTOM)

psi   N/mm²

2000 14
1000 7
0 0
−1000 −7
−2000 −14

FIGURE 4.30 HSS BRICK MODEL 2; τ_{xz} STRESS (VIEW FROM THE BOTTOM)
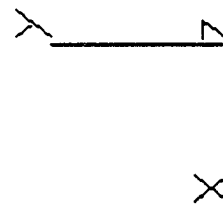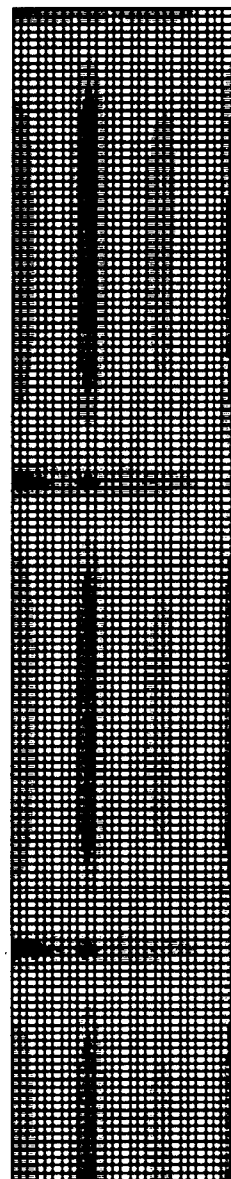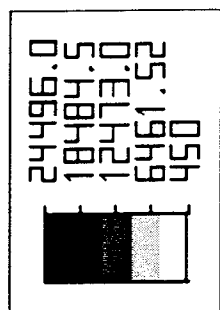
FIGURE 4.31 OSS BRICK MODEL 3; VON-MISES STRESS (VIEW FROM THE BOTTOM)

psi	N'/mm²
25873.1	178
12536.9	86
-799.33	-6
-14141.35	-97
-27474.77	-189

FIGURE 4.32 OSS BRICK MODEL 3; σ_{yy} STRESS (VIEW FROM THE BOTTOM)
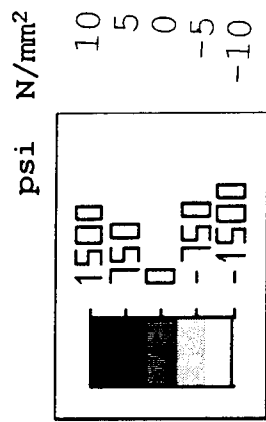
FIGURE 4.33 OSS BRICK MODEL 3; τ_{yz} STRESS (VIEW FROM THE BOTTOM)
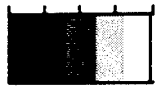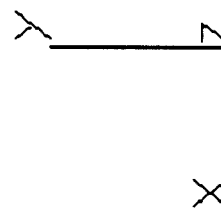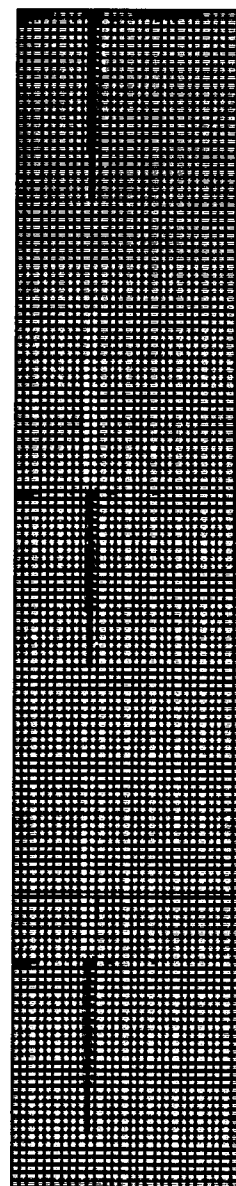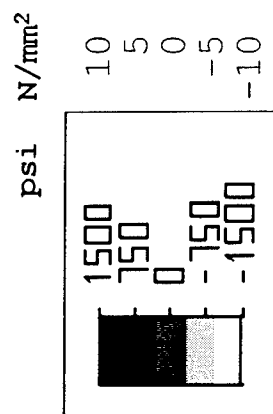
FIGURE 4.34 OSS BRICK MODEL 3; τ_{xz} STRESS (VIEW FROM THE BOTTOM)
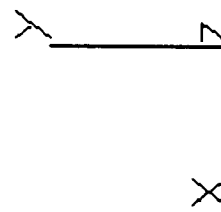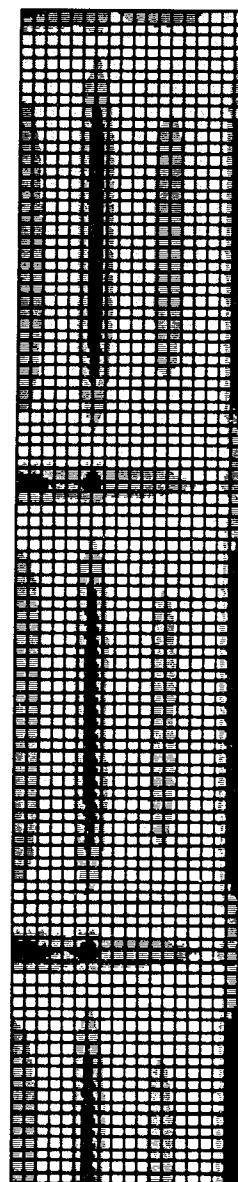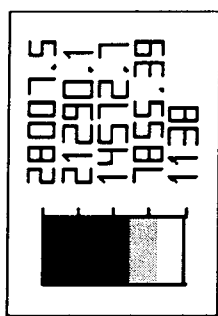
FIGURE 4.35 HSS BRICK MODEL 3; VON-MISES STRESS (VIEW FROM THE BOTTOM)

	psi	N/mm²
	29394.	203
	14194.	98
	-5.3	-7
	-16295.	-112
	-31495.	-217
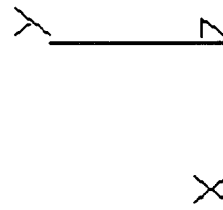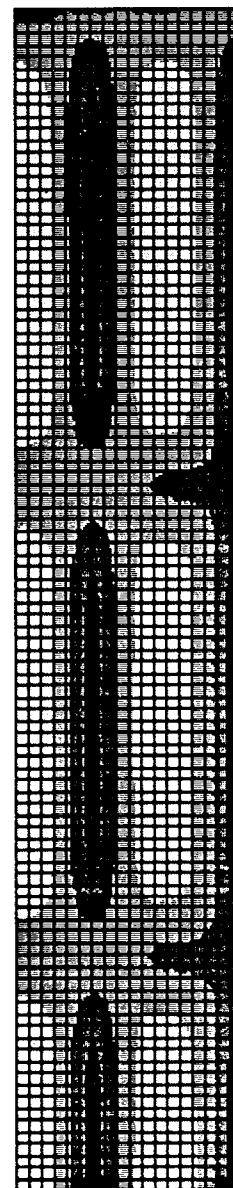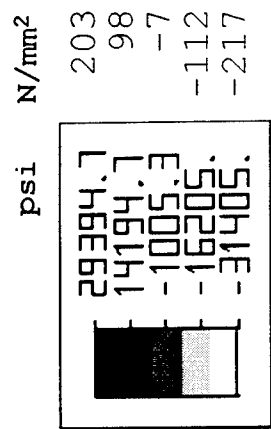
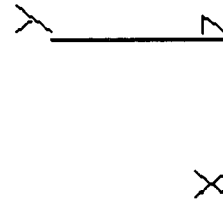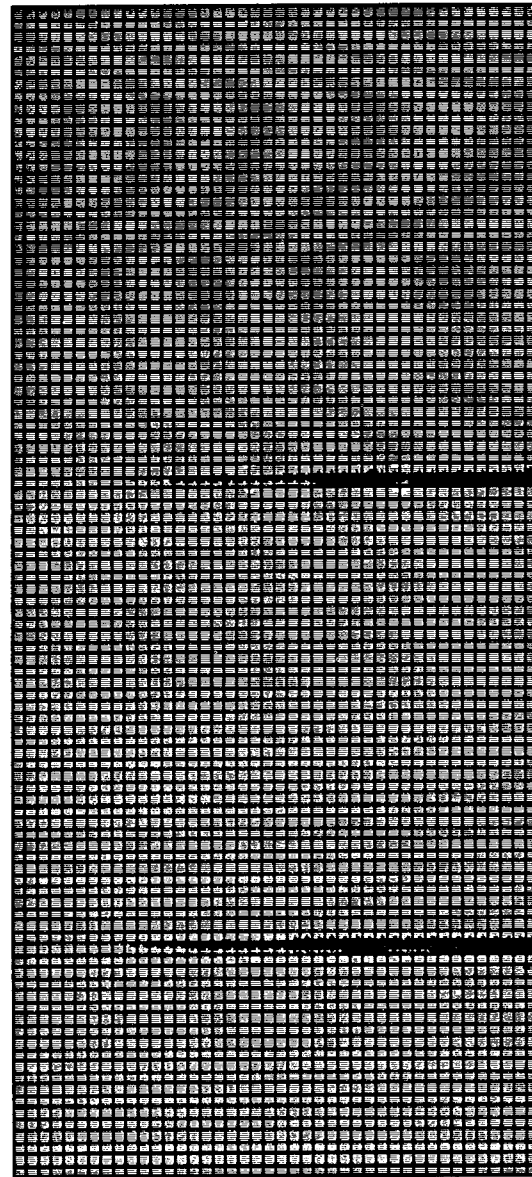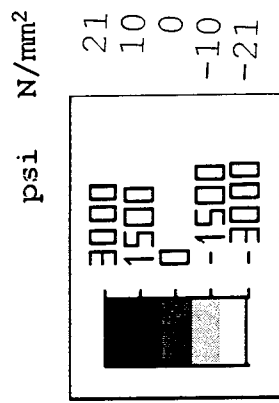FIGURE 4.36 HSS BRICK MODEL 3; σ_{yy} STRESS (VIEW FROM THE BOTTOM)
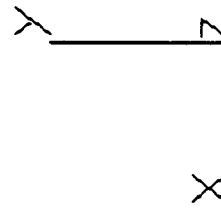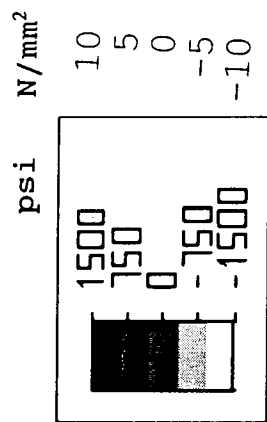
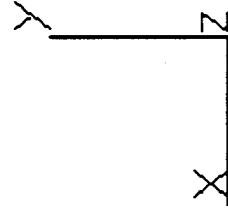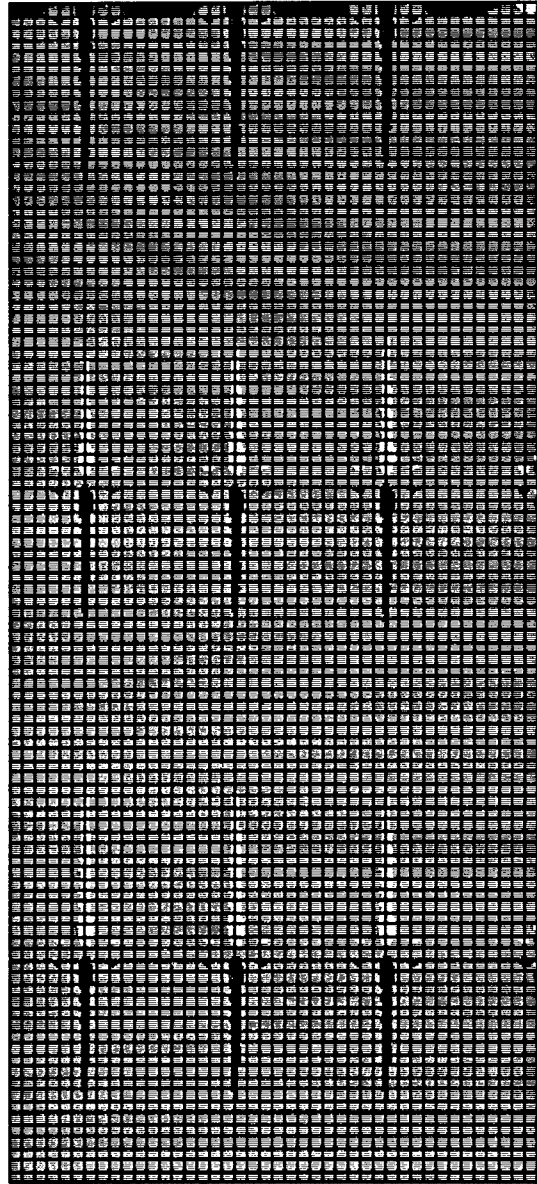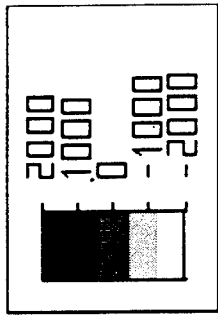FIGURE 4.37 HSS BRICK MODEL 3; τ_{yz} STRESS (VIEW FROM THE BOTTOM)

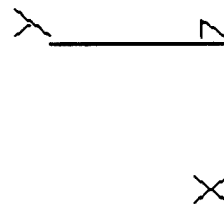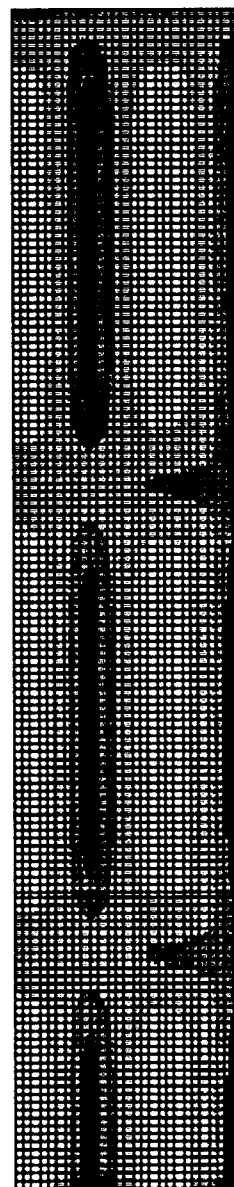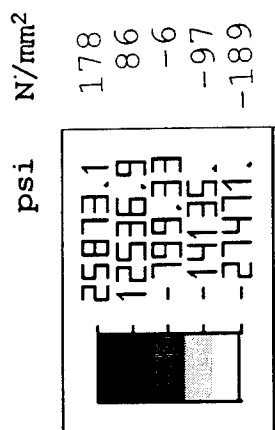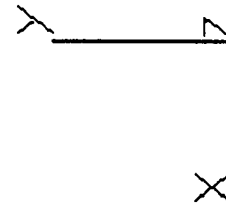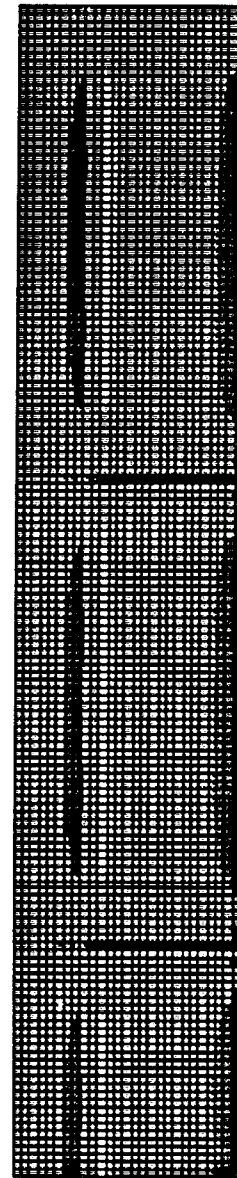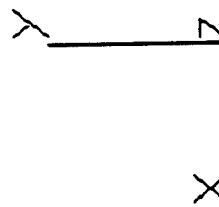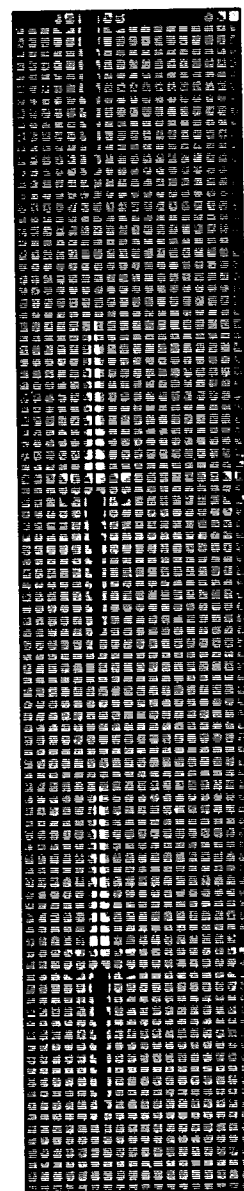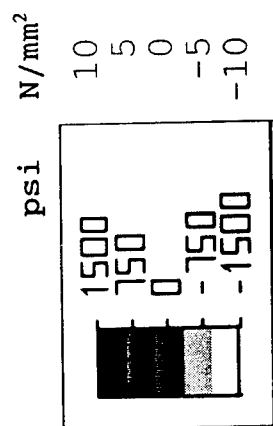FIGURE 4.38 HSS BRICK MODEL 3; τ_{xz} STRESS (VIEW FROM THE BOTTOM)
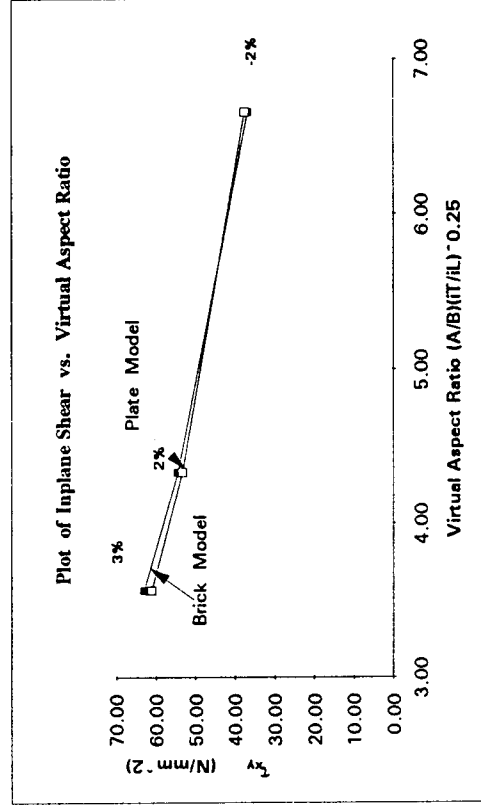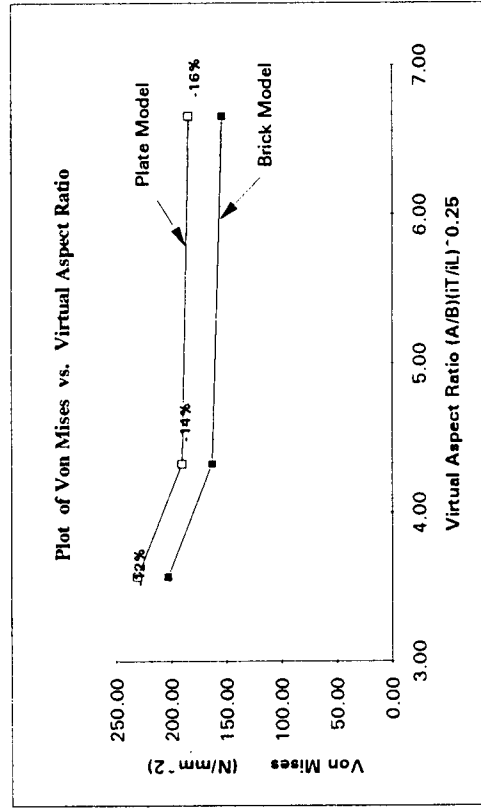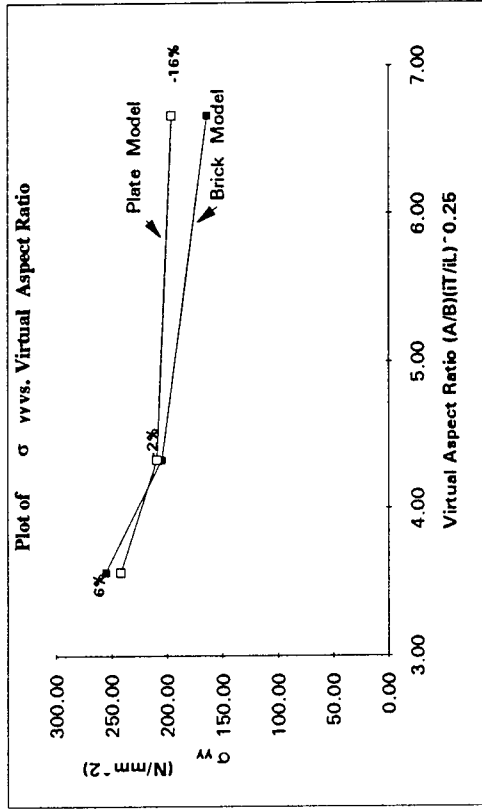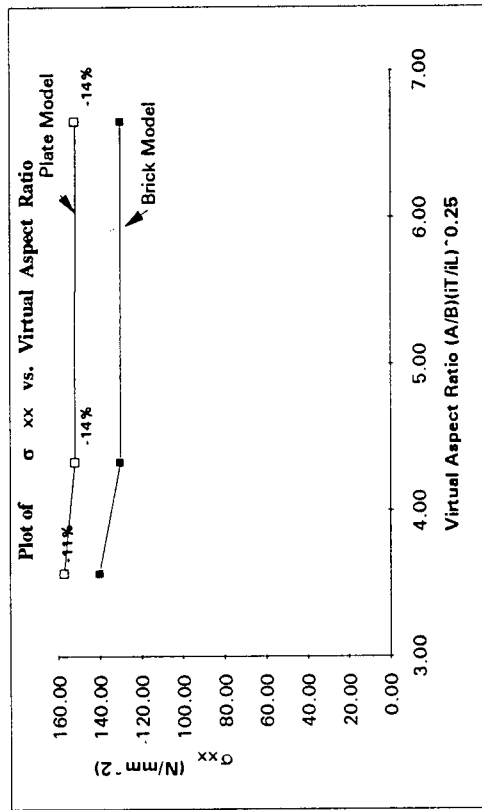
FIGURE 4.39 COMPARISON OF STRESSES IN OSS BRICK MODEL WITH OSS PLATE MODEL

71
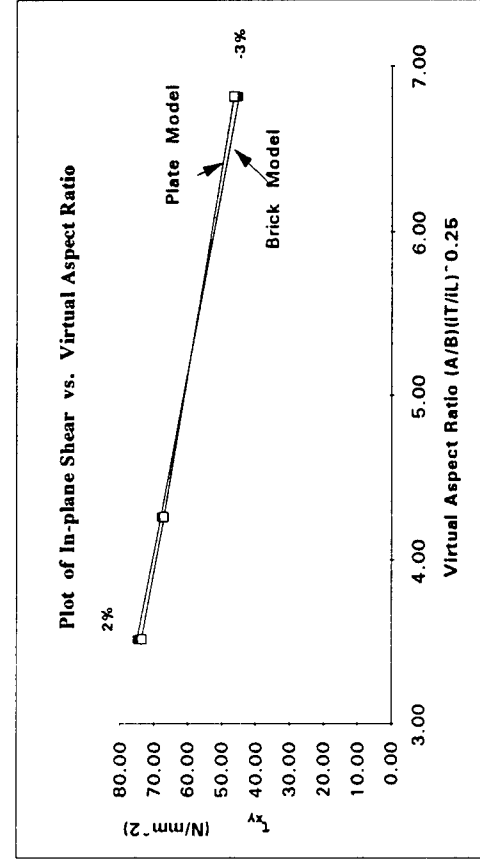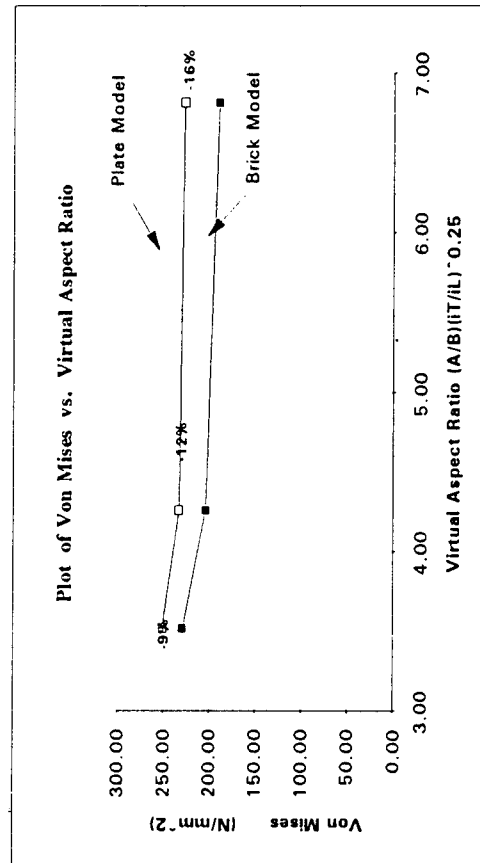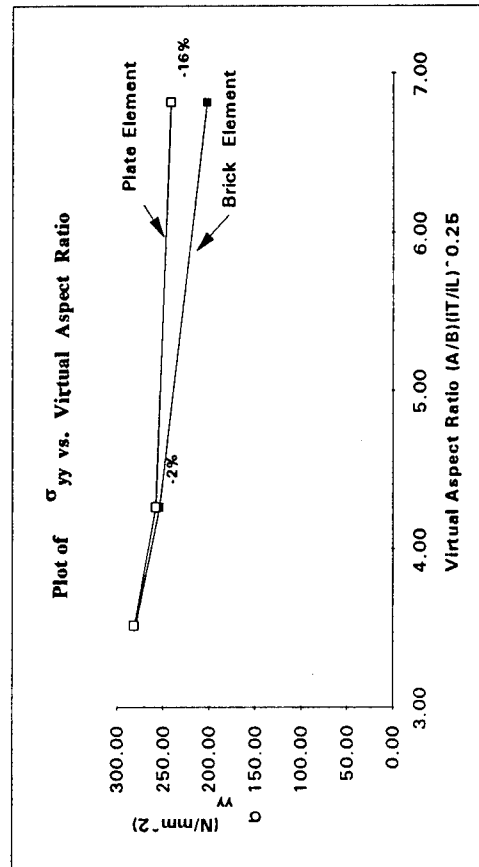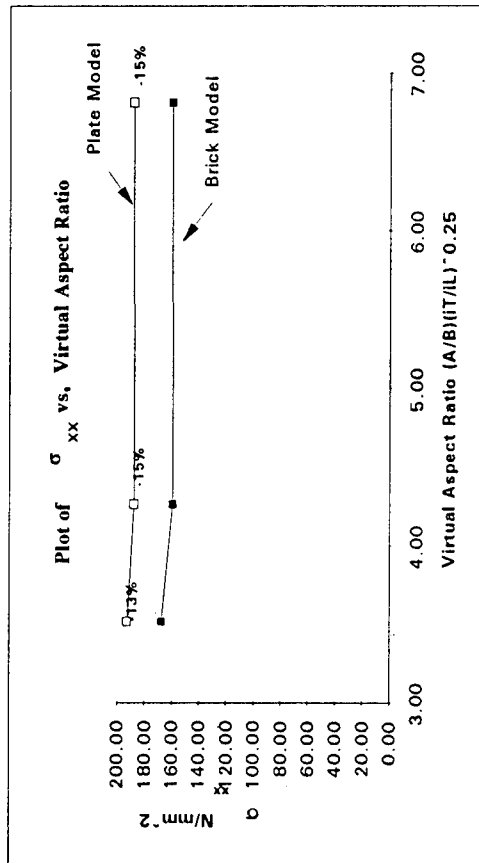
FIGURE 4.40 COMPARISON OF STRESSES IN HSS BRICK MODEL WITH HSS PLATE MODEL

72

virtual aspect ratio defined in section 2.0. For comparison, the values of these stresses obtained using plate elements have also been plotted. For each value of the virtual aspect ratio, the percentage differences in the stresses of the stiffened-plate structures using brick elements and plate elements are shown.

4.3 Comparison of Stresses with Initial Deflection in the Plating

Results of the finite element analyses of the third model, 15.24m x 2.74m (50'x9'), with initial deflection, are presented in Table 4.5. The same six stress components, σ_{xx}, σ_{yy}, σ_{zz}, τ_{xy}, τ_{xz}, τ_{yz} and von-mises have been considered. For comparison, another model without any initial deflection and having the same mesh size was also analysed for both the OSS and HSS materials. Results of which are also presented in the Table 4.5. In the table, the location of these maximum stress values are presented in parenthesis.

4.4 Discussion of Results

The results of the FEM analyses of the cross-stiffened plate panels, using plate elements, are shown in Tables 4.1 and 4.2 for OSS and HSS material respectively. It can be observed from Figures 4.13 and 4.14, that the plate bending, shear stresses and deflections are much higher in a grillage panel than in a single plate panel. The bending stresses, which are usually used to select plate thicknesses, can be as much as 50% higher. However, the difference decreases as the virtual aspect ratio,

73

TABLE 4.5. MAXIMUM STRESSES IN MODEL 3 WITH INITIAL DEFORMATION (OSS AND HSS)

(15.24 m. X 2.24 m)

STRESS	OSS (UNDEFORMED)	OSS (DEFORMED)	HSS (UNDEFORMED)	HSS (DEFORMED)
σ_{xx} (N/mm^2)	148.04	155.83	181.89	191.75
(cm, cm, cm)	(0,91,0.000)	(0,91,0.000)	(0,91,0.000)	(0,91,0.000)
σ_{yy} (N/mm^2)	185.75	160.86	229.40	196.65
(cm, cm, cm)	(457,0,0.000)	(610,0,0.000)	(457,0,0.000)	(610,0,0.000)
σ_{zz} (N/mm^2)	45.22	46.86	54.08	56.15
(cm, cm, cm)	(610,0,0.000)	(610,0,0.000)	(610,0,0.000)	(610,0,0.000)
τ_{xy} (N/mm^2)	37.40	33.74	45.98	41.34
(cm, cm, cm)	(587,103,1.588)	(591,95,1.628)	(587,103,1.430)	(591,95,1.466)
τ_{yz} (N/mm^2)	39.44	39.41	47.23	47.20
(cm, cm, cm)	(610,0,0.000)	(610,0,0.000)	(610,0,0.000)	(610,0,0.000)
τ_{xz} (N/mm^2)	34.41	34.08	39.58	39.16
(cm, cm, cm)	(0,91,0.000)	(0,91,0.000)	(0,91,0.000)	(0,91,0.000)
vm (N/mm^2)	173.13	176.31	213.88	216.09
(cm, cm, cm)	(457,0,1.588)	(610,91,0.0)	(457,0,1.430)	(610,91,0.0)

(A/B) $(i_T/i_L)^{1/4}$, decreases. Even at the higher virtual aspect ratios the significant bending stress is 17% and 19% higher than the single plate panel for the OSS and HSS gillages respectively. It can also be observed that the plate bending stress is greater than the yield stress for the OSS system and is approaching the yield stress for the HSS system as the virtual aspect ratio is approximately equal to 3. Hence, it is possible that ship structures will experience higher stresses than calculated using a first principals approach, resulting in failure and/or fractures. Therefore the stiffness of grillage supporting structure should be accounted for in the plate selection process. The results of the FEM analyses using brick elements are shown in Tables 4.3 and 4.4 for the OSS and HSS system respectively. Comparison of stress distributions (σ_{yy} and Von-Mises) produced by the plate element models and the brick element models reveal similarity in the location of the high stress regions although comparisons of the maximum values of the stresses in Figures 4.39 and Figure 4.40 show that the bending stresses from the brick models are lower than those of the plate by about 16% and the shear stresses are about 2%. This discrepancy can be attributed to the mesh size chosen for brick models. Table 4.6 presents results of two additional finite element analysis done on the smallest OSS model 15.24m x 2.74m (50'x9'), designed in section 2.0 with brick elements. These two models had mesh sizes of 50.8mm (2") and 38.1mm (1.5") square. Comparison of the results show that as the mesh size is made smaller, results. of the brick model approaches those of the plate model.

A comparison of the through the thickness shear stresses shows that the critical locations are at the intersection of the

TABLE 4.6.   EFFECT OF VARYING ELEMENT SIZE ON THE RESULTS OF BRICK MODEL 3
            (OSS MATERIAL)

Model	1	2	3	PLATE MODEL
Element Size (mm x mm)	76.2 x 76.2	50.8 x 50.8	38.1 x 38.1	76.2 x 76.2
Displ. (mm) (% Diff)	7.06 -3.24	7.09 -2.78	7.11 -2.61	7.30
σ_{xx} (N/mm^2) (% Diff)	130.15 -14.34	142.38 -6.29	148.63 -2.18	151.94
σ_{yy} (N/mm^2) (% Diff)	164.11 -16.24	178.39 -8.95	185.77 -5.18	195.92
τ_{xy} (N/mm^2) (% Diff)	36.70 -2.24	37.30 -0.64	37.72 0.46	37.54
vm (N/mm^2) (% Diff)	153.86 -16.40	166.55 -9.51	173.10 -5.95	184.05
time (min)	0.225	0.422	1.51	
memory (Mb)	0.024	0.095	1.001	

σ_{xx} = Normal Stress in 'x' direction

σ_{yy} = Normal Stress in 'y' direction

τ_{xy} = In-plane Shear Stress

v.mises   = von mises Stress

Note   :   %   Differences   are   with   respect   to   plate   model.

longitudinal and transverse stiffeners. However, these shear stresses are only 10% of the plate bending stresses. The use of sophisticated FEM analyses, using multi-noded elements, is not warranted because they will not significantly change the results for selecting the required plating thicknesses for ship structure subjected to normal loads.

The results of FEM analyses with initial deflection in the plating, using brick elements, are shown in Table 4.5 for both the OSS and HSS material systems. It is observed that the plate bending stresses in the x-x direction are only 5% higher than comparable stresses of the FEM analysis with no initial deflection in the plating, and that the plate bending stresses in the y-y direction are 13% less. Hence, the use of initial deflections, of the order of one plate thickness, in the analysis of plate bending stresses will not change the requirements for selecting plate thicknesses needed to resist normal loads.

5.0 CONCLUSIONS AND RECOMMENDATIONS FOR FUTURE WORKS

The primary objective of this task was to evaluate the effect of overall grillage behavior on the total stress of a stiffened-plate panel. Overall grillage behavior is defined as the deflection of the supporting structure (transverses and longitudinals) due to an applied loading. This deflection induces additional stresses on the plate panel which are not accounted for in the selection of the plating thickness. In order to quantify the impact of these additional stresses in a stiffened plate structure, finite element models were developed representing typical grillage structures designed to current industry recognized practice. The results of these finite element analyses are presented in section 4.0 and the following conclusions are based on those results.

1. As evident from Figure 4.13 and Figure 4.14, stresses induced in the plating of a stiffened panel due to the deflection of the stiffeners are significantly higher than those where the stiffeners are assumed to be fairly rigid and hence unyielding. The differences are as high as 50%. The differences in stresses depend on the virtual aspect ratio of the panel. The differences seem to attain a maximum at virtual aspect ratio of three. They then tend to decrease and become constant at higher values of virtual aspect ratio.

2. From Table 4.3 and 4.4, a comparison of the maximum values of the normal stresses σ_{xx} and σ_{yy} with the vertical shear stresses, τ_{xz} and τ_{yz} show that the vertical shear stresses are about 10% of the normal stresses and hence would not play a

significant part in selection of plating thicknesses based on static stress design.

3.   Figures 5.1 and 5.2 show the vertical shear stress distributions, τ_{xz} and τ_{yz} of a rectangular panel 3.05m x 0.91m (10'x3') fully fixed on all sides and under normal pressure load of 0.107 N/mm^2 (15.56 psi).   While these figures indicate that the maximum tends to occur at the middle of the boundaries of the panel, Tables 4.3 and 4.4 indicates that for a stiffened-plate structure, the location of maximum vertical shear stresses are at the intersection of the transverses and longitudinals. Therefore these regions in a stiffened-plate structure may be more prone to cracking.

4.   From the limited data produced in this study, it appears that initial plate deflection does not significantly affect the behavior of stiffened plate structures.   This could be due to the flexibility of the stiffening members (longitudinals and transverses) since they do not restrain the edges of the unsupported panel.

Based on the above conclusions, the following recommendations are being provided for future work:

1.   Figures 4.13 and 4.14 indicate that for virtual aspect ratio greater than 6.5, the maximum values of the normal and Von-Mises stresses seem to become constant.   But, for virtual aspect ratios less than 3.5, these values seem to increase. Therefore it is suggested that further finite element analysis be performed on models of aspect ratios less than 3.5 to ascertain the trend.

2. The design of a stiffened-plate panel is influenced by a number of factors including the loading, the overall dimensions of the panel, the scantlings of the plating and the stiffeners and the spacing of the stiffeners. Interaction of all these factors result in complex stress patterns for which there are no closed-form solutions. Hence, parametric studies should be performed taking into account these variables to develop methods to calculate stresses in terms of these variables.

3. Methods for selection of plate thickness subject to normal loads should be modified to take into account the deflection of the stiffeners and the orthotropic stiffeness of the grillage, i.e. $(A/B)(iT/iL)^{1/4}$. ABS rules in "Safe Hull" are currently doing this for in-plane loads.

4. The use of non-linear finite element methods should be persued as well as large scale testing of grillage structure to aid in verification of panel stress calculation methods described above. The analysis should account for geometrical and material non-linearity. Existing test data of structural grillages should be gathered and re-evaluated.
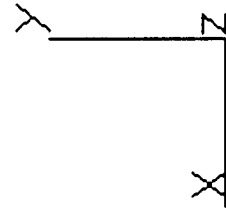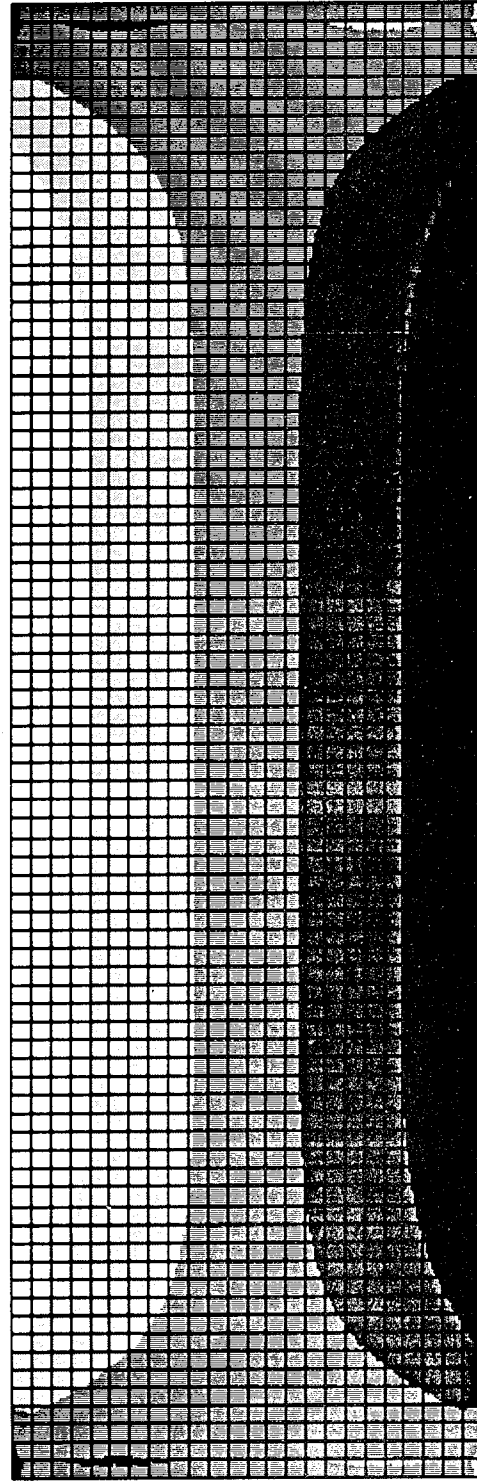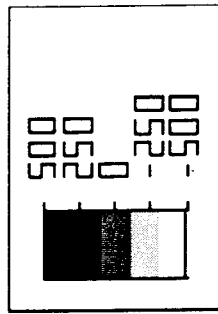
FIGURE 5.1   BRICK MODEL OF SINGLE PANEL; VERTICAL SHEAR STRESS, τ_{yz}

81
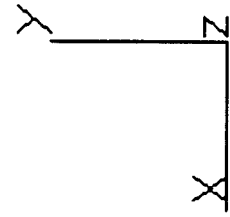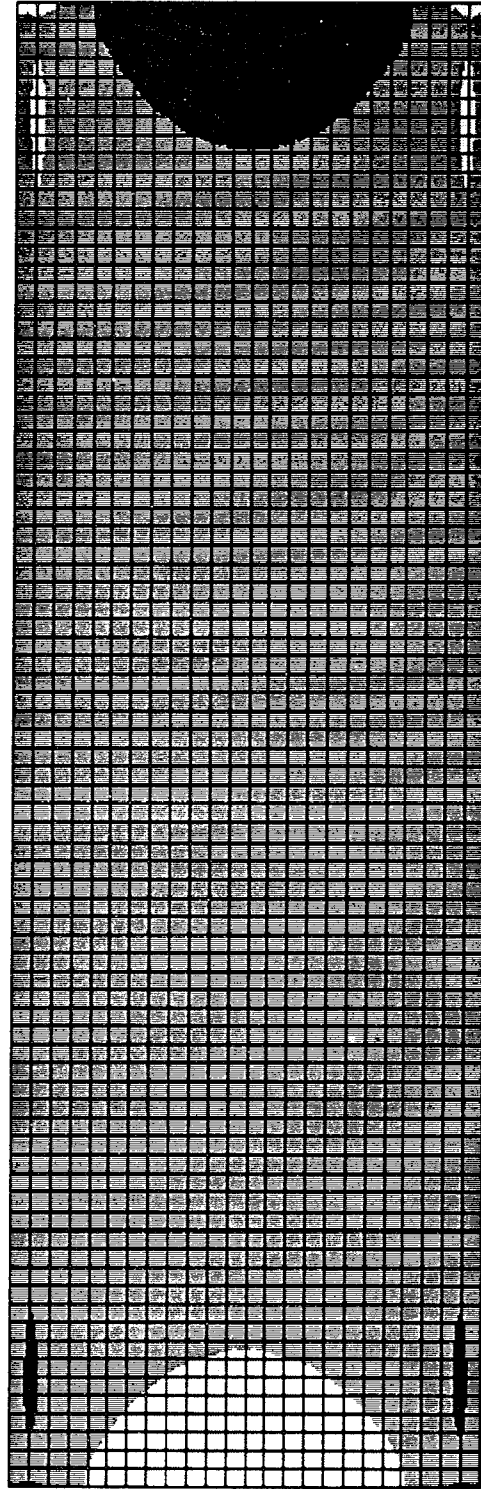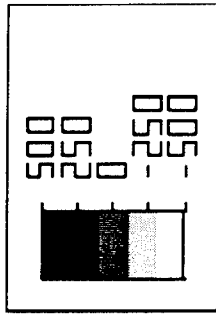
FIGURE 5.2   BRICK MODEL OF SINGLE PANEL; VERTICAL SHEAR STRESS, τ_{xz}

6.0 REFERENCES

1. Navy Sea Systems Command, "General Specifications for Ships of the United States Navy," Department of the Navy, NAVSEA S9AA0-AA-SPN-010/Gen. Spec. (1992 Edition).

2. Naval Ship Engineering Center, "Structural Design Manual foar Naval Surface Ships," NAVSEA 0900-LP-097-4010 (Dec. 1976).

3. Naval Ship Systems Command, "Design Data Book - Design Data Sheet, DDS100-4, 'Strength of Structural Members'," NAVSEA 09020LP-006-000 (Feb. 1983).

4. Hughes, O.F., "Ship Structural Design", SNAME, 1988.

APPENDIX 1

Following calculations illustrate the procedure used to design the OSS grillage having an overall dimension of 15.24m X 2.74m. The formulae and criterion used are those available in Structural Design Manual [2] and DDS-100-4 [3]. The same procedure is followed for the remaining five grillage structures designed in section 2.0.

(a) <u>Determination of Plate thickness</u>:

The minimum plate thickness required is determined using the following equation :

$$\frac{b}{t} \leq \frac{C}{K \cdot \sqrt{H}}$$

where for this study, C = 350 and the head of water, H = 35 ft. The panel dimensions are, a = 10' and b = 3'. Therefore K = 1. Substituting these values of C, H and K in the above equation, we get,

$$\frac{b}{t} \leq 59.16$$

or $t \geq 0.608$

The nearest available plate size is 0.625". Since the constants C and K and the variables b, t and H are in english units, therefore the thickness is derived in english units and converted to metric units to yield a thickness of 15.88mm.

84

(b) Determination of Transverse Girder:

The procedure mentioned in section 2.0 has been followed to determine the scantlings required for the transverse girder.

Given: Length of beam,   L =   2.74 m (9.0')
         Spacing of beam, s = 3050.0 mm (10.0')
         Uniform Pressure, p = 0.107 N/mm^2 (15.56 psi)
         Thickness of Plate, t = 15.88 mm (0.625")

         Beam Size: W-T 410 x 53.0 (16 x 7 1/8 x 50# I-T)
         Web depth, d_w =   397 mm (15.63")
         Web thickness, t_w = 9.65 mm (0.38")
         Flange width, b_f = 180.0 mm (7.07")
         Flange thickness t_f =   16.0 mm (0.63")

         Yield stress, σ_y =   235 N/mm^2 (34,000 psi)
         Allowable stress, σ_t =   195 N/mm^2 (28,000 psi)
         Proportional Limit, σ_{pl} =   176 N/mm^2 (25,000 psi)
         Young's Modulus,   E = 206,850 N/mm^2 (30 x 10^6 psi)
         Poissons' ratio, v = 0.3

Section Properties of Combined Plate-Beam Section:.
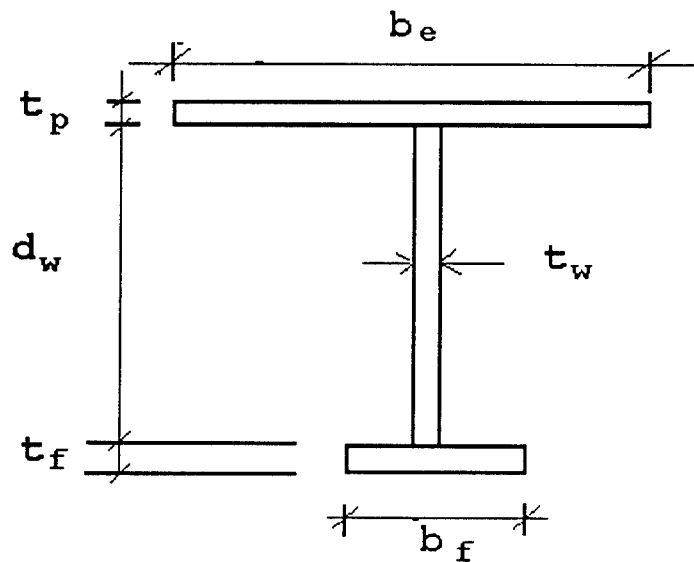
Effective Width of Plating, b_e:

Shear lag approach: $b_e = L/4 = 2740/4 = 685$ mm (27")

Post-buckling approach: $b_e = 60t = 60 \times 15.88 = 953$ mm (37.5")

Spacing of beam, $s = 3050$ mm (120")

The effective width of plating is the lesser of the above 3 values. Therefore,

$b_e = 685$ mm (27")

Computation of section properties:

Element	Area	y	A.y	A.y²	Io-o
Plate	10,878	7.94	86,371	685,788	228,596
Web	3,831	214.38	842727	180,663,982	50,316,673
Flange	2,880	420.88	1,212,134	510,163,126	61,440
Σ	17,589		2,141,232	691,512,896	50,606,709

$\Sigma A = 17,589$ mm²

$\Sigma A.y = 2,141,232 \text{ mm}^3$

$y_p = \Sigma A.Y/\Sigma A = 2,141,232/17,589 = 121.74 \text{ mm}$

$y_f = t_p + d_w + t_f - y_p = 15.88 + 397 + 16 - 121.74 = 307.14 \text{ mm}$

$Ix\text{-}x = \Sigma A.y2 + \Sigma Io\text{-}o = 691,512,896 + 50,606,709$

$\qquad\qquad\qquad = 742,119,605 \text{ mm}^4$

$CORR = y_p.\Sigma A.y = 121.74 \times 2,141,232 = 260,673,584 \text{ mm}^4$

Moment of Inertia, $I_{NA} = Ix\text{-}x - CORR$

$\qquad\qquad\qquad = 742,119,605 - 260,673,584$

$\qquad\qquad\qquad = 481,446,021 \text{ mm}^4$

Section Modulus, Plate, $SM_p = I_{NA}/y_p$

$\qquad\qquad\qquad = 481,446,021/121.74$

$\qquad\qquad\qquad = 3,954,707 \text{ mm}^3$

Section Modulus, Flange, $SM_f = I_{NA}/y_f$

$\qquad\qquad\qquad = 481,446,021/307.14$

$\qquad\qquad\qquad = 1,567,513 \text{ mmm}^3$

Shear Area, $A_{SH} = (t_p + d_w + t_f)t_w$

$\qquad\qquad\qquad = (15.88 + 397 + 16)9.65 = 4,139 \text{ mm}^2$

Radius of Gyration, $r = \sqrt{(I_{NA}/A)}$

$\qquad\qquad\qquad = \sqrt{481,446,021/17,589} = 165.4 \text{ mm}$

Secondary Bending Moments and Shear (Assuming Fixed Supports)

Bending Moment at middle span, $BM_m = wL^2/24$

Bending Moment at Support, $\qquad BM_s = wL^2/12$

where $w = b.p = (3050)(0.107) = 326.25 \text{ N-mm}$

Therefore, $BM_m = (326.25)(2740)^2/24 = 102,087,719 \text{ N-mm}$

$\qquad\qquad BM_s = (326.25)(2740)^2/12 = 204,175,438 \text{ N-mm}$

87

Shear Force, $V = wL/2 = (326.25)(2740)/2 = 447,099$ N

Secondary Bending and Shear Stresses

Bending Stresses;

Middle: Flange of Stiffener, $f_{BMS} = BM_m/SM_f$

$$= 102,087,719/1,567,513$$

$$= 65.1 \text{ N/mm}^2$$

              At the Plating, $f_{BMP} = BM_m/SM_p$

$$= 102,087,719/3,954,707$$

$$= 25.8 \text{ N/mm}^2$$

Support: Flange of Stiffener, $f_{BES} = BM_s/SM_f$

$$= 204,175,438/1,567,513$$

$$= 130.3 \text{ N/mm}^2$$

              At the Plating, $f_{BEP} = BM_s/SM_p$

$$= 204,175,438/3,954,707$$

$$= 51.6 \text{ N/mm}^2$$

Shear Stresses; $f_s = V/A_{SH} = 447,099/4,139$

$$= 108.0 \text{ N/mm}^2$$

Column Buckling Strength; F_c

$F_c = \sigma_y;$ $C \leq 1.4$

$F_c = \sigma_y(1.235 - 0.168C);$ $1.4 < C \leq 4.8$

$F_c = \sigma_y(9.87/C^2);$ $C > 4.8$

where $C = L/r \sqrt{(\sigma_y/E)} = 2740/162.5\sqrt{(235/206850)}$

$$= 0.57$$

Since C is less than 1.4,

Therefore, $F_c = \sigma_y = 235 \text{ N/mm}^2$

88

Ultimate Strength of Plating; F_u

$F_u = \sigma_y$ $\beta \leq 1.25$

$F_u = \sigma_y[\ 2.25/\beta - 1.25/\beta^2\ ]$ $\beta > 1.25$

where, $\beta = b/t\sqrt{(\sigma_y/E)}$.

Since b = s = 3050 mm, t = 15.88 mm, therefore

$\beta = b/t\sqrt{(\sigma_y/E)} = (3050/15.88)\sqrt{(235/206850)} = 6.47$

Since $\beta > 1.25$, $F_u = 235[\ 2.25/6.47 - 1.25/6.47^2\ ]$

                        $= 74.71\ N/mm^2$

Critrical Buckling Strength; Fp

$$F_{cr} = K \frac{\pi^2 E}{12\,(1-\mu^2)} \frac{1}{(a/t)^2}$$

where, $K = [\ 1 + (a/b)^2\ ]^2$.

Since a = L/3 = 913.33 mm and b = s = 3050 mm, therefore

$K = [\ 1 + (913/3050)^2\ ]^2 = 1.2$.

$F_p = F_{cr}$ $F_{cr} \leq \sigma_{PL}$

$$F_p = \frac{\sigma_Y}{1 + 0.1824\left(\dfrac{\sigma_Y}{F_{CR}}\right)^2} \qquad F_{CR} > \sigma_{PL}$$

Now a/t = 913/15.88 = 57.49. Therefore,

$$F_{CR} = 1.090 \frac{\pi^2(206850)}{12\,(1-0.3^2)} \frac{1}{(57.49)^2} = 61.6\,N/mm$$

<u>Maximum Tripping Length, L_T</u>

$$L_T = \frac{1.283 b_f}{\sqrt{\dfrac{\sigma_Y}{E}\left[1+\dfrac{1}{3}\left(\dfrac{d}{b_f}\right)\left(\dfrac{t_w}{t_f}\right)-0.128\left(\dfrac{t_f}{d}\right)^2 \dfrac{E}{\sigma_Y}\right]^{\frac{1}{2}}}}$$

$d = d_w + t_f = 397 + 16 = 413$ mm

$d/b_f = 413/180 = 2.2944$

$t_w/t_f = 9.65/16 = 0.6031$

$t_f/d = 16/413 = 0.0387$

$E/\sigma_Y = 206850/235 = 880.21$

$$L_T = \frac{(1.283)(180)}{\sqrt{\dfrac{1}{880.21}\left[1+.333(2.2944)(0.6031)-(0.128)(0.0387)^2(880.21)\right]^{\frac{1}{2}}}}$$

$= 6027.42$ mm ; $L_T \geq L$; $6027.4 > 3050$ O.K.

<u>Local Buckling of Flange and Web</u>

$b_f/t_f = 180/16 = 11.25 \leq 29.0$ O.K.

$d_w/t_w = 397/9.65 = 41.14 \leq 64.0$ O.K.

<u>Strength Assessment</u>

Tension:

     Stiffener Flange; $f_{BMS}/\sigma_b = 65.1/195 = 0.33 \leq 1.0$ O.K.

     Plate   ; $f_{BEP}/\_\sigma_b = 51.6/195 = 0.26 \leq 1.0$ O.K.

Compression:

     Ultimate Strength of Panel;

$$f_{BMP} \leq (0.8)(F_U)\frac{F_C}{F_Y}$$

     $25.8 \leq 0.8(74.7)(235)/(235)$

90

or $25.8 \leq 59.76$ O.K.

Buckling Strength of Panel; $f_{BMP} \leq F_{cr}$

$25.8 \leq 67.9$ O.K.

Stiffener; $f_{BES} \leq \sigma_b$

$130.3 \leq 195$ O.K.

(c) <u>Determination of Longitudinal Stiffeners:</u>

The procedure mentioned in section 2.0 has been followed to determine the scantlings required for the longitudinal stiffeners.

Given: Length of beam,   L =   3.05 m (10.0')
          Spacing of beam, s = 914.4 mm (3.0')
          Uniform Pressure,p = 0.107 N/mm^2 (15.56 psi)
          Thickness of Plate, t = 15.88 mm (0.625")

          Beam Size: WT 205 x 23.0 (8 x 5 1/2 x 15.5# I-T)
          Web depth, d_w =   190.5 mm (7.5")
          Web thickness, t_w =   7.0 mm (0.275")
          Flange width, b_f = 140.5 mm (5.53")
          Flange thickness t_f =   11.2 mm (0.44")

          Yield stress, σ_y =   235 N/mm^2 (34,000 psi)
          Allowable stress, σ_b =   195 N/mm^2 (28,000 psi)
          Proportional Limit, σ_{pl} =   176 N/mm^2 (25,000 psi)
          Young's Modulus,   E = 206,850 N/mm^2 (30 x 10^6 psi)
          Poissons' ratio, v = 0.3

Section Properties of Combined Plate-Beam Section:
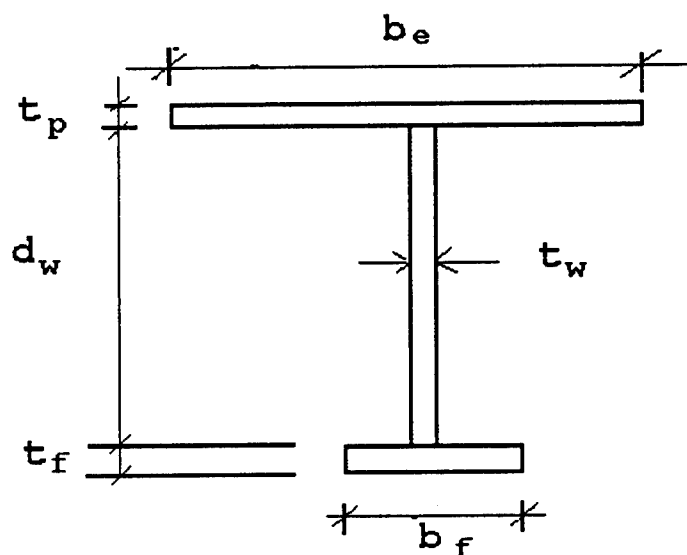
Effective Width of Plating, b_e:

Shear lag approach: $b_e = L/4 = 3050/4 = 762.5$ mm (30")

Post-buckling approach: $b_e = 60t = 60 \times 15.88 = 953$ mm (37.5")

Spacing of beam, $s = 914$ mm (36")

The effective width of plating is the lesser of the above 3 values. Therefore,

$b_e = 762.5$ mm (30")

Computation of section properties:

Element	Area	y	A.y	A.y⁻	Io-o
Plate	12,109	7.94	96,146	763,399	254,454
Web	1,334	111.13	148,247	16,474,689	4,032,754
Flange	1,574	211.98	333,657	70,728,611	16,449
Σ	15,017		578,050	87,966,700	4,303,657

$\Sigma A = 15,017$ mm^2

$\Sigma A.y = 578,050$ mm^3

92

$y_p = \Sigma A.Y/\Sigma A = 578,050/15,017 = 38.49$ mm

$y_f = t_p+d_w+t_f-y_p = 15.88+190.5+11.2-38.49 = 179.09$ mm

$I_{x-x} = \Sigma A.y2 + \Sigma Io-o = 87,966,700 + 4,303,657$
$= 92,270,357$ mm^4

CORR $= y_p.\Sigma A.y = 38.49 \times 578,050 = 22,249,145$ mm^4

Moment of Inertia, $I_{NA} = I_{x-x} - $ CORR
$= 92,270,357 - 22,249,145$
$= 70,021,212$ mm^4

Section Modulus, Plate, $SM_p = I_{NA}/y_p$
$= 70,021,212/38.49$
$= 1,819,205$ mm^3

Section Modulus, Flange, $SM_f = I_{NA}/y_f$
$= 70,021,212/179.09$
$= 390,983$ mm^3

Shear Area, $A_{SH} = (t_p+d_w+t_f)t_w$
$= (15.88+190.5+11.2)7.0 = 1,523$ mm^2

Radius of Gyration, $r = \sqrt{(I_{NA}/A)}$
$= \sqrt{70,021,212/15,017}$
$= 68.3$ mm

Secondary Bending Moments and Shear (Assuming Fixed Supports)

Bending Moment at middle span, $BM_m = wL^2/24$

Bending Moment at Support, $BM_s = wL^2/12$

where $w = s.p = (914)(0.107) = 97.8$ N-mm

Therefore, $BM_m = (97.8)(3050)^2/24 = 37,906,912$ N-mm

$BM_s = (97.8)(3050)^2/12 = 75,813,824$ N-mm

93

Shear Force, $V = wL/2 = (97.8)(3050)/2 = 149,145$ N

Secondary Bending and Shear Stresses

Bending Stresses;

Middle: Flange of Stiffener, $f_{BMS} = BM_m/SM_f$

$= 37,906,912/390,983$

$= 96.95$ N/mm^2

·At the Plating, $f_{BMP} = BM_m/SM_p$

$= 37,906,912/1,819,205$

$= 20.84$ N/mm^2

Support: Flange of Stiffener, $f_{BES} = BM_s/SM_f$

$= 75,813,824/390,983$

$= 193.91$ N/mm^2

At the Plating, $f_{BEP} = BM_s/SM_p$

$= 75,813.824/1,819,205$

$= 41.67$ N/mm^2

Shear Stresses; $f_s = V/A_{SH} = 149,145/1,523$

$= 97.93$ N/mm^2

Column Buckling Strength; F_c

$F_c = \sigma_y$; $C \leq 1.4$

$F_c = \sigma_y(1.235 - 0.168C)$; $1.4 < C \leq 4.8$

$F_c = \sigma_y(9.87/C^2)$; $C > 4.8$

where $C = L/r\sqrt{(\sigma_y/E)} = 3050/68.3\sqrt{(235/206850)}$

$= 1.51$

Since C is greater than 1.4 but less than 4.8,

94

Therefore, F_c = (1.235-0.168x1.51)235

$$= 230.6 \text{ N/mm}^2$$

Ultimate Strength of Plating; F_u

$F_u = \sigma_y$ $\qquad\qquad\qquad$ $\beta \le 1.25$

$F_u = \sigma_y[\ 2.25/\beta - 1.25/\beta^2\ ]$ $\quad$ $\beta > 1.25$

where, $\beta = b/t \sqrt{(\sigma_y/E)}$.

Since b = s = 914 mm, t = 15.88 mm, therefore

$\beta = b/t\sqrt{(\sigma_y /E)} = (914/15.88) \sqrt{(235/206850)} = 1.94$

Since β > 1.25, F_u = 235[2.25/1.94 - 1.25/1.96^2]
$$= 194.5 \text{ N/mm}^2$$

Critical Buckling Strength; Fp

$$F_{cr} = K \frac{\pi^2 E}{12 (1-\mu^2)} \frac{1}{(a/t)^2}$$

where, $K = [\ 1 + (a/b)^2\ ]^2$.

Since a = 3050 mm and b = s = 914 mm, therefore

a/b = 3050/914 = 3.34, then

K = 4.0.

$F_p = F_{cr}$ $\qquad\qquad\qquad$ $F_{cr} \le \sigma_{PL}$

$$F_p = \frac{\sigma_Y}{1 + 0.1824 \left(\dfrac{\sigma_Y}{F_{CR}}\right)^2} \qquad F_{CR} > \sigma_{PL}$$

Now a/t = 914/15.88 = 57.56. Therefore,

$$F_{CR} = 4 \frac{\pi^2 (206850)}{12 (1-0.3^2)} \frac{1}{(57.56)^2} = 225.7 \text{N/mm}^2$$

Since 225.7 > 176, therefore
95

$$F_{CRi} = \frac{235}{1 + 0.1824\left(\dfrac{235}{225.7}\right)^2} = 196.2 \text{N}/\text{mm}^2$$

Maximum Tripping Length, L_T

$$L_T = \frac{1.283\,b_f}{\sqrt{\dfrac{\sigma_Y}{E}\left[1 + \dfrac{1}{3}\left(\dfrac{d}{b_f}\right)\left(\dfrac{t_w}{t_f}\right) - 0.128\left(\dfrac{t_f}{d}\right)^2\dfrac{E}{\sigma_Y}\right]^{\frac{1}{2}}}}$$

$d = d_w + t_f = 190.5 + 11.2 = 201.7$ mm

$d/b_f = 201.7/140.5 = 1.44$

$t_w/t_f = 7.0/11.2 = 0.625$

$t_f/d = 11.2/201.7 = 0.0555$

$E/\sigma_Y = 206850/235 = 880.21$

$$L_T = \frac{(1.283)(140.5)}{\sqrt{\dfrac{1}{880.21}}\left[1 + .333(1.44)(0.625) - (0.128)(0.0555)^2(880.21)\right]^{\frac{1}{2}}}$$

$= 5479.33$ mm; $L_T \geq L$; $5479.3 > 3050$ O.K.

Local Buckling of Flange and Web

$b_f/t_f = 140.5/11.2 = 12.55 \leq 29.0$ O.K.

$d_w/t_w = 190.5/7.0 = 27.21 \leq 64.0$ O.K.

Srength Assessment

Tension:
    Stiffener Flange; $f_{BMS}/\sigma_b = 96.95/195 = 0.50 \leq 1.0$ O.K.

    Plate   ; $f_{BEP}/\_\sigma_b = 41.67/195 = 0.21 \leq 1.0$ O.K.

Compression:

Ultimate Strength of Panel; $f_{BMP} \leq (0.8)(\sigma_U)\dfrac{F_C}{\sigma_Y}$

$20.84 \leq 0.8(194.5)(235)/(235)$

or $20.84 \leq 147.6$ O.K.

Buckling Strength of Panel; $f_{BMP} \leq F_{cr}$

$20.84 \leq 196.2$ O.K.

Stiffener; $f_{BES} \leq \sigma_b$

$193.91 \leq 195$ O.K.

Project Technical Committee Members

The following persons were members of the committee that represented the Ship Structure Committee to the Contractor as resident subject matter experts. As such they performed technical review of the initial proposals to select the contractor, advised the contractor in cognizant matters pertaining to the contract of which the agencies were aware, and performed technical review of the work in progress and edited the final report.

Chairmen
Todd Ripley/Gary North   Maritime Administtio

Tom Ingram   American Bureau of Shipping

Stephen Yang   Director Ship Engineering, Canada

Alasdair Stirling   Director Ship Engineering, Canada

Thomas Hu   Defence Research Establishment Atlantic, Canada

Key Chang   U.S. Coast Guard

Hsien Y. Jan   MARTECH Inc.

William Siekierka   Naval Sea Systems Command,
                                                  Contracting Officer's
                                                  Technical Representative

Robert Sielski   National Academy of Science,
Alexander Stavovy   Marine Board Liaison

Steve Sharpe   U.S. Coast Guard, Executive Director
                                                  Ship Structure Committee

<u>COMMITTEE ON MARINE STRUCTURES</u>

Commission on Engineering and Technical Systems

National Academy of Sciences – National Research Council

The COMMITTEE ON MARINE STRUCTURES has technical cognizance over the interagency Ship Structure Committee's research program.

Peter M. Palermo Chairman, Alexandria, VA
Subrata K. Chakrabarti, Chicago Bridge and Iron, Plainfield, IL
John Landes, University of Tennessee, Knoxville, TN
Bruce G. Collipp, Marine Engineering Consultant, Houston, TX
Robert G. Kline, Marine Engineering Consultant, Winona, MN
Robert G. Loewy, NAE, Rensselaer Polytechnic Institute, Troy, NY
Robert Sielski, National Research Council, Washington, DC
Stephen E. Sharpe, Ship Structure Committee, Washington, DC

<u>LOADS WORK GROUP</u>
Subrata K. Chakrabarti Chairman, Chicago Bridge and Iron Company, Plainfield, IL
Howard M. Bunch, University of Michigan, Ann Arbor, MI
Peter A. Gale, John J. McMullen Associates, Arlington, VA
Hsien Yun Jan, Martech Incorporated, Neshanic Station, NJ
John Niedzwecki, Texas A&M University, College Station, TX
Solomon C. S. Yim, Oregon State University, Corvallis, OR
Maria Celia Ximenes, Chevron Shipping Co., San Francisco, CA

<u>MATERIALS WORK GROUP</u>
John Landes, Chairman, University of Tennessee, Knoxville, TN
William H Hartt, Florida Atlantic University, Boca Raton, FL
Horold S. Reemsnyder, Bethlehem Steel Corp., Bethlehem, PA
Barbara A. Shaw, Pennsylvania State University, University Park, PA
James M. Sawhill, Jr., Newport News Shipbuilding, Newport News, VA
Bruce R. Somers, Lehigh University, Bethlehem, PA
Jerry G. Williams, Conoco, Inc., Ponca City, OK

RECENT SHIP STRUCTURE COMMITTEE PUBLICATIONS

SSC–363   **Uncertainties in Stress Analysis on Marine Structures** by E. Nikolaidis and P. Kaplan 1991

SSC–364   **Inelastic Deformation of Plate Panels** by Eric Jennings, Kim Grubbs, Charles Zanis, and Louis Raymond 1991

SSC–365   **Marine Structural Integrity Programs (MSIP)** by Robert G. Bea 1992

SSC–366   **Threshold Corrosion Fatigue of Welded Shipbuilding Steels** by G. H. Reynolds and J. A. Todd 1992

SSC–367   **Fatigue Technology Assessment and Strategies for Fatigue Avoidance in Marine Structures** by C. C. Capanoglu 1993

SSC–368   **Probability Based Ship Design Procedures: A Demonstration** by A. Mansour, M. Lin, L. Hovem, A. Thayamballi 1993

SSC–369   **Reduction of S–N Curves for Ship Structural Details** by K. Stambaugh, D. Lesson, F. Lawrence, C–Y. Hou, and G. Banas 1993

SSC–370   **Underwater Repair Procedures for Ship Hulls (Fatigue and Ductility of Underwater Wet Welds)** by K. Grubbs and C. Zanis 1993

SSC–371   **Establishment of a Uniform Format for Data Reporting of Structural Material Properties for Reliability Analysis** by N. Pussegoda, L. Malik, and A. Dinovitzer 1993

SSC–372   **Maintenance of Marine Structures: A State of the Art Summary** by S. Hutchinson and R. Bea 1993

SSC–373   **Loads and Load Combinations** by A. Mansour and A. Thayamballi 1994

SSC–374   **Effect of High Strength Steels on Strength Consdierations of Design and Construction Details of Ships** by R. Heyburn and D. Riker 1994

SSC–375   **Uncertainty in Strength Models for Marine Structures** by O. Hughes, E. Nikolaidis, B. Ayyub, G. White, P. Hess 1994

SSC–377   **Hull Structural Concepts For Improved Producibility** by J. Daidola, J. Parente, and W. Robinson 1994

SSC–378   **The Role of Human Error in Design, Construction and Reliability of Marine Structures** by R. Bea 1994

SSC–379   **Improved Ship Hull Structural Details Relative to Fatigue** by K. Stambaugh, F. Lawrence and S. Dimitriakis 1994

SSC–380   **Ship Structural Integrity Information System** by R. Schulte–Strathaus, B. Bea 1995

SSC–381   **Residual Stregth of Damaged Marine Structures** by C. Wiernicki, D. Ghose, N. Nappi 1995

Ship Structure Committee Publications – A Special Bibliography